

Politecnico di Torino

Master of Science Program in

ENGINEERING AND MANAGEMENT

a.a. 2025/2026

Graduation Session September 2026

Coordinating Second-Life Allocation and the Timing of Recycling Capacity Expansion in the Italian Electric Vehicle Battery System: A System Dynamics Approach

CANDIDATE:

GOMEZ Sofía (s335205)

SUPERVISOR:

ZENEZINI Giovanni

ABSTRACT

As electric vehicle use grows in Italy, increasing amounts of battery mass will reach the end of automotive first life over the coming decades. Second-life use can delay when these batteries reach recycling, while their processing depends on the recycling capacity available when they return. This thesis develops a System Dynamics model to examine how second-life allocation and recycling-capacity timing interact in the Italian EV battery system over 2025–2050. Battery inflows and end-of-first-life flows are derived from Italian BEV and PHEV registration data using a cohort-based Weibull retirement model. The model represents collection, second-life allocation, delayed post-second-life returns, recycling backlog, capacity-constrained processing, and recovered-material availability.

Nine strategy scenarios combine low, reference, and high second-life allocation with anticipatory, reference, and delayed recycling-capacity expansion. Across these scenarios, recycling-capacity timing produces the largest differences in system performance. Anticipatory capacity substantially reduces backlog and processing delay and increases recovered-material availability, while delayed capacity leads to persistent congestion and limited recovery. Second-life allocation mainly changes when battery mass reaches recycling: lower allocation brings recycling demand forward, while higher allocation reduces earlier pressure but increases delayed returns. Among the evaluated configurations, the scenario combining anticipatory capacity with reference second-life allocation provides the most balanced operational and material-circularity outcomes.

Sensitivity analysis also shows that the timing of first-life retirement, represented by the Weibull scale parameter, has a strong influence on the magnitude of future recycling pressure. Overall, the results show that second-life allocation and recycling-capacity timing need to be planned together, with capacity availability aligned to future direct and post-second-life battery returns.

Acknowledgements

I would like to sincerely thank my supervisor, **Professor Giovanni Zenezini**, for his guidance, availability, and valuable feedback throughout the development of this thesis. His suggestions helped me transform an initial idea into a structured research project and encouraged me to approach the work with greater rigor and clarity. I am especially grateful for the trust he placed in my work and for his support throughout this process.

A **mi mamá, Laurina Elena**, por ser mi luz, mi apoyo incondicional y una de las personas que más ha creído en mí, incluso en los momentos en los que yo misma he dudado. Gracias por cada consejo, por cada palabra de ánimo, por escucharme, por todas las llamadas diarias, por hacerme reír y recordarme siempre que puedo salir adelante. Gracias por darme alas para venir a Italia, perseguir mis sueños y vivir una experiencia que cambió mi vida. Me siento infinitamente afortunada de tener una mamá tan amorosa y divertida. Gracias por ser mi compañera para todo y por hacerme sentir cerca de casa incluso estando a miles de kilómetros. Este logro también es tuyo, porque detrás de cada paso que he dado siempre ha estado tu amor dándome fuerzas para seguir.

A **mi papá, Laureano**, por ser el pilar de nuestra familia y uno de los mayores ejemplos de mi vida. Gracias por haberme dado siempre mucho más de lo que necesitaba, por recordarme siempre que soy suficiente y que tengo todo dentro de mí para salir adelante. Gracias por tus consejos, por levantarme cada vez que me he sentido triste, por creer en mi potencial y por hacer todo lo posible para ayudarme a cumplir mis sueños y estar presente en cada uno de ellos. Gracias por darme seguridad y por hacerme sentir, desde siempre, que puedo llegar tan lejos como me lo proponga. Eres mi guía, mi consejero y una de las personas a las que más admiro. Nada de esto habría sido posible sin ti, pa. Llegar hasta aquí sabiendo todo lo que hiciste para que yo pudiera cumplir este sueño hace que este logro también lleve una parte enorme de ti.

A **mi hermana, Andre**, por ser mi mejor amiga, mi mayor consejera y una de las personas que más me ayudó a atravesar esta etapa. Gracias por tener siempre las palabras correctas, por escucharme, ayudarme a ver las cosas desde otra perspectiva y estar presente incluso en la distancia. Gracias por acompañarme en cada momento, por celebrar conmigo lo bueno, sostenerme en lo difícil y hacerme sentir que siempre tenía a quién llamar. Gracias por ser esa voz que tantas veces me devolvió la calma y la confianza cuando yo no las

encontraba sola. Gracias por alegrar mis días y por hacerme sentir que, sin importar dónde esté, siempre tengo en ti un lugar seguro. Aunque hayamos tenido que vivir tantas cosas importantes desde ciudades distintas, nuestra relación sigue siendo una de las cosas más valiosas que tengo. Gracias por existir y por ser, además de mi hermana, una de mis personas favoritas en la vida.

Y a Andrés, mi cuñis, porque este título también tiene literalmente un pedacito tuyo. Gracias por todas las veces que te sentaste conmigo a explicarme materias, por las clases de economía, por tenerme paciencia y por ayudarme a superar momentos académicos en los que realmente necesitaba una mano. Hay materias que probablemente no habría logrado sacar adelante de la misma manera sin tu ayuda. Siempre he admirado muchísimo tu inteligencia y la facilidad que tienes para explicar incluso lo que a mí me parecía imposible de entender. Gracias por todos esos domingos en los que estuviste ahí apoyándome, por tu cariño, por tantas risas en los viajes y, sobre todo, gracias por ser parte de nuestra familia.

A ustedes cuatro, que son mi hogar sin importar en qué parte del mundo esté, gracias por hacer posible que llegara hasta aquí. Este título lleva mi nombre, pero detrás de él hay muchísimo de ustedes. Los amo más allá de las profundidades del mar, más que la infinidad del universo y más inconmensurable que el cielo.

A las personas que conocí en Turín y que terminaron convirtiéndose en mi familia durante esta etapa. Gran parte de lo que hizo especial mi vida en Italia fueron las personas con las que tuve la suerte de compartirla.

A **Chels**, por haber soñado conmigo esta aventura desde mucho antes de que comenzara. Qué bonito pensar que aquello de lo que hablábamos en 2022 terminó convirtiéndose en nuestra realidad. Gracias por acompañarme en cada etapa de esta chocoaventura, por todo el apoyo, los consejos, las risas, los estudios, la motivación, las clases de italiano juntas y por estar también en los momentos difíciles. Gracias por crecer conmigo durante estos años. La maestría no habría sido lo mismo sin ti, y siempre voy a recordar que uno de nuestros sueños más grandes se hizo realidad juntas. Sé que, sin importar en qué ciudad terminemos, nuestra amistad siempre tendrá un lugar especial en mi vida.

A **Nata Mojica**, mi reine, por ser parte de mi vida desde mucho antes de Italia y demostrarme que las amistades pueden cambiar de forma sin dejar de estar presentes. Gracias por acompañarme desde nuestros días en la Javeriana, por apoyarnos mutuamente en cada etapa, por hacerme reír demasiado, por tus ocurrencias y por siempre encontrar la forma de sacarme una sonrisa, incluso en medio de una crisis. Gracias también por escucharme, aconsejarme y estar siempre pendiente de mí. Me alegra muchísimo que nuestra amistad haya seguido creciendo con los años y saber que, aunque la vida nos lleve por caminos distintos, siempre podremos contar la una con la otra.

A **Manolo**, mi roomie favorito, gracias por escucharme, aguantarme, aconsejarme y estar siempre ahí. Gracias por cuidarme y llevarme a la casa en patineta cuando salíamos juntos. Gracias por las partidas de Mario Kart, los juegos de adivinar el personaje y por tus pensamientos random que siempre me hacen reír. Más allá de haber sido roomies, terminaste convirtiéndote en un gran amigo. No pude haber tenido mejor compañero durante estos años.

A **Gonza**, gracias por tu compañía, por los consejos, por tenerme siempre en cuenta, por ser tan buena gente y mega detodito, por recibirme siempre con algo rico en tu casa y por todos los momentos que terminamos compartiendo. Me hace muy feliz pensar en todo lo que nos acercamos durante esta etapa: los paseos, los viajes, las salidas de shopping y tantas conversaciones sobre la vida. Poco a poco te convertiste en uno de mis apoyos más grandes aquí y te agradezco mucho por eso.

A **Nata Pachón**, mi chica, gracias por una amistad que se fue haciendo cada vez más cercana con el paso del tiempo. Gracias por ser tan especial conmigo, por tu personalidad tan querida, por los planes, por estar pendiente de mí y por estar siempre presente. Contigo cualquier plan me encanta y siempre la paso increíble. Me alegra muchísimo que Italia nos haya dado la oportunidad de acercarnos tanto y de compartir tantos momentos juntas.

A **Majo**, gracias por tu generosidad, por tus consejos, por las risas y, especialmente, por todo el apoyo durante esas épocas de exámenes en las que necesitábamos apoyo moral más que nunca. Admiro mucho tu dedicación, tu nobleza y la manera en que siempre estás dispuesta a ayudar a quienes quieres.

A **Ema**, por formar junto con Majo una parte especial de mi familia turinense. Gracias por el apoyo, los consejos, los juegos (como el parques y geografía), por las risas viéndonos el desafio y apoyando al equipo Gamma Sin Límites, por ser el Paparrurru y por esa actitud que hace que en cualquier plan terminemos riéndonos demasiado.

A **Mapu**, por ser tan loca, auténtica y hermosa persona. Gracias por las pijamadas, que siempre terminaban siendo de los mejores planes, por contarnos todas tus chocoaventuras, tus storytimes y por recordarme que muchas veces lo mejor es simplemente vivir el presente y disfrutar lo que está pasando. Valencia siempre va a ser uno de los viajes que repetiría contigo mil veces.

A **mi estriper**, por una amistad incondicional que sobrevivió a la distancia hasta que finalmente pudimos compartir juntas el sueño italiano. Gracias por estar siempre pendiente de mí, por visitarme, por darme ánimos cuando los necesitaba y por ser esa amiga divertida e inteligente con la que sé que siempre puedo contar. Qué felicidad haber podido vivir una parte de esta etapa contigo más cerquita. Gracias por tantos años de amistad, por seguir estando y por hacerme sentir que, sin importar cuánto tiempo o distancia haya de por medio, seguimos siendo las mismas de siempre.

A **Maff**, por iluminar literalmente mis días cada vez que nos veíamos. Gracias por tu energía, por tu forma de ser y por convertirte en una amiga tan especial en tan poco tiempo. Gracias por el apoyo, por tantas risas y por esos momentos en los que vernos, aunque fuera un rato, ya hacía que el día se sintiera mejor. Me alegra muchísimo que nuestros caminos se hayan cruzado aquí.

A **Benja y Miguel**, gracias por recibirme siempre en Milán con la mejor actitud y por hacerme sentir bienvenida cada vez que llegaba. A **Osiris**, gracias por tenerme siempre en cuenta y por incluirme en los planes de chicas. A **Juanjo**, gracias por tu amistad, por los bailes en las rumbas, por las risas y por todos los buenos momentos que compartimos. Y a **Diego, Pablo, Vitor y Antonio**, gracias por estar siempre pendientes de mí, por incluirme en sus planes, por sacarme una sonrisa y por hacerme sentir acompañada y querida durante esta etapa.

Gracias a todos por los viajes, las salidas, las conversaciones, y sobre todo, gracias por haber convertido una ciudad que al principio era desconocida en un hogar. Gran parte de lo que me llevo de Italia está en todos los recuerdos que construí con ustedes.

A mis amigas en Colombia, por seguir tan presentes a pesar de la distancia. A **Vale Neira**, por crecer conmigo, por escribirme casi que todos los días y por tantos años de una amistad que sigue siendo una de las más importantes de mi vida. A **Pau**, por tu nobleza, tu corazón tan hermoso y ese cariño y apoyo incondicional que siempre me haces sentir. A **Adro**, por estar tan pendiente de mí, por llamarme todas las semanas y por hacerme sentir siempre tan querida. A **Vale Guz,** mi primera amiga caleña, por tus notas de voz, por hacerme reír tanto y por esa amistad que, aunque pase el tiempo y vivamos lejos, siempre se siente igual de cercana. A **Castroso**, por ser de esos amigos cactus que siguen teniendo un lugar especial en mi vida. Y a mis BDP, **Diany, Mandrusky y Andre P**, por las videollamadas de actualización, por los cumpleaños, las risas y por hacerme sentir acompañada incluso estando lejos de casa. Gracias a todas por demostrarme que, aunque cambien nuestras rutinas y vayamos por caminos diferentes, siempre encontramos la forma de seguir presentes en la vida de la otra.

Y finalmente, gracias a mí. Por seguir adelante cuando las cosas se pusieron difíciles, por confiar en mí incluso cuando dudaba y por no rendirme. Esta etapa me enseñó muchísimo y me recordó que soy capaz de mucho más de lo que a veces creo. Llegar hasta aquí hace que todo haya valido la pena.

TABLE OF CONTENTS

1. INTRODUCTION 16

1.1. Research Motivation 16

1.2. Research Purpose and Objective 17

1.3. Research Question 18

1.4. Research Hypotheses 18

1.5. Specific Objectives 19

2. LITERATURE REVIEW 19

2.1. End-of-Life EV Battery Management and Retirement Dynamics 20

2.2. Second-Life Allocation and Delayed Material Recovery 21

2.3. Recycling Capacity, Backlog, and Infrastructure Timing 23

2.4. Existing System Dynamics and Quantitative Models of EV Battery Circularity 25

2.4.1. System Dynamics Models of Recovery Pathways 25

2.4.2. Dynamic Material-Flow and Lifetime Models 26

2.4.3. Recycling-Capacity Planning and Inventory Models 27

2.5. Italian Context and Data Foundations 28

2.6. Research Gap and Contribution 30

3. RESEARCH METHODOLOGY 31

3.1. Research Approach 31

3.2. System Boundaries 32

3.2.1. Geographical Boundary 32

3.2.2. Lifecycle and Process Boundary 33

3.2.3. Level of Aggregation and Unit of Analysis 34

3.2.4. Temporal Boundary 35

3.2.5. Exogenous Conditions and Excluded Elements 35

3.3. Model Development Procedure 36
3.4. Data Sources, Parameterization, and Assumptions 37
3.4.1. Historical EV Registrations and Fleet Data 37
3.4.2. Conversion of Vehicle Registrations into Battery-Mass Inflows 39
3.4.3. Cohort-Based First-Life Retirement 40
3.4.4. Technical Parameters 42
3.4.5. Strategic Scenario Variables 43
3.4.6. Initial Conditions 44
3.4.7. Parameter Documentation and Treatment of Uncertainty 44
3.5. Simulation and Scenario Design 45
3.5.1. Scenario Structure 45
3.5.2. Baseline and Scenario Comparison 47
3.5.3. Sensitivity Analysis 48
3.6. Impact Dimensions and Performance Indicators 49
3.7. Model Design Specifications 50
4. MODEL DEVELOPMENT 51
4.1. Model Architecture and Variable Selection 52
4.2. Causal Loop Diagram (CLD) 55
4.3. Feedback Loop Analysis 56
4.4. Stock and Flow Diagram (SFD) 58
4.5. Implemented Inputs and Parameter Values 59
4.5.1. Vehicle Registration and Fleet Projection 59
4.5.2. Cohort-Based Vehicle Retirement and Fleet Balance 61
4.5.3. Battery-Mass Conversion 61
4.5.4. Mass-Based End-of-First-Life Flow 62
4.5.5. Reference Recycling-Capacity Trajectory 62
4.6. Model Equations 64

4.6.1. First-Life Battery Dynamics 64
4.6.2. Collection and Second-Life Allocation 65
4.6.3. Recycling Backlog and Processing 65
4.6.4. Accounting Stocks 67
4.6.5. Performance Indicators 67
4.6.6. Simulation Settings and Dimensional Consistency 69
4.7. Model Verification, Validation, and Testing 70
4.7.1. Mass-Balance and Non-Negativity Checks 70
4.7.2. Dimensional Consistency 70
4.7.3. External Plausibility Comparison 70
4.7.4. Extreme-Condition Testing 71
4.7.5. Integration-Error Testing 77
4.7.6. Sensitivity Analysis 78
4.7.7. Behavioral and External Validation 88
5. SIMULATION AND SCENARIO ANALYSIS 89
5.1. S1 – Baseline: Reference Capacity and Reference Second-Life Allocation ... 90
5.1.1. Scenario Configuration 90
5.1.2. Simulated Behavior 90
5.1.3. Interpretation 91
5.2. S2 – Reference Capacity and Low Second-Life Allocation 92
5.2.1. Scenario Configuration 92
5.2.2. Simulated Behavior 92
5.2.3. Interpretation 93
5.3. S3 – Reference Capacity and High Second-Life Allocation 94
5.3.1. Scenario Configuration 94
5.3.2. Simulated Behavior 94
5.3.3. Interpretation 95

5.4. S4 – Anticipatory Capacity and Reference Second-Life Allocation 98
5.4.1. Scenario Configuration 98
5.4.2. Simulated Behavior 98
5.4.3. Interpretation 99
5.5. S5 – Anticipatory Capacity and Low Second-Life Allocation 100
5.5.1. Scenario Configuration 100
5.5.2. Simulated Behavior 101
5.5.3. Interpretation 101
5.6. S6 – Anticipatory Capacity and High Second-Life Allocation 102
5.6.1. Scenario Configuration 102
5.6.2. Simulated Behavior 103
5.6.3. Interpretation 104
5.7. S7 – Delayed Capacity and Reference Second-Life Allocation 107
5.7.1. Scenario Configuration 107
5.7.2. Simulated Behavior 108
5.7.3. Interpretation 108
5.8. S8 – Delayed Capacity and Low Second-Life Allocation 109
5.8.1. Scenario Configuration 109
5.8.2. Simulated Behavior 110
5.8.3. Interpretation 110
5.9. S9 – Delayed Capacity and High Second-Life Allocation 111
5.9.1. Scenario Configuration 111
5.9.2. Simulated Behavior 112
5.9.3. Interpretation 112
5.10. Comparative Summary of Scenario Results 114
6. DISCUSSION 115
6.1. Effect of Second-Life Allocation – H1 115

6.2. Effect of Recycling Capacity Expansion Timing – H2 and H3 116
6.2.1. Interpretation of Capacity Utilization 117
6.3. Coordination of Second-Life Allocation and Recycling-Capacity Timing – H4 117
6.3.1. Comparison of the Anticipatory Scenarios 118
6.3.2. Evaluation of Hypothesis 4 118
6.4. Answer to the Research Question 119
6.5. Robustness and Sensitivity Implications 119
6.6. Engineering Design Implications 120
7. CONCLUSION 121
8. BIBLIOGRAPHY 124

LIST OF FIGURES

Figure 1: Causal Loop Diagram of the Italian EV battery system model. Source: Author's elaboration in Vensim..... 56
Figure 2: Stock and Flow Diagram of the Italian EV battery system model. Source: Author's elaboration in Vensim. 58
Figure 3: Recycling Backlog under the baseline and extreme recycling-capacity conditions. Source: Author's elaboration based on Vensim simulation results. 76
Figure 4: Recycling Backlog under Collection Rate Sensitivity. Source: Author's elaboration based on Vensim simulation results. 80
Figure 5: Post-Second-Life Return under Average Second-Life Duration Sensitivity. Source: Author's elaboration based on Vensim simulation results. 82
Figure 6: End-of-First-Life Flow under Weibull Scale Parameter Sensitivity. Source: Author's elaboration based on Vensim simulation results. 86
Figure 7: Recycling Backlog under Reference-Capacity Scenarios. Source: Author's elaboration based on Vensim simulation results. 96
Figure 8: Total Recycling Pathway Inflow under Reference-Capacity Scenarios. Source: Author's elaboration based on Vensim simulation results. 97
Figure 9: Cumulative Recovered Materials under Reference-Capacity Scenarios. Source: Author's elaboration based on Vensim simulation results. 97
Figure 10: Recycling Capacity Utilization under Anticipatory-Capacity Scenarios. Source: Author's elaboration based on Vensim simulation results. 105
Figure 11: Recycling Backlog under Anticipatory-Capacity Scenarios. Source: Author's elaboration based on Vensim simulation results. 106
Figure 12: Cumulative Recovered Materials under Anticipatory-Capacity Scenarios. Source: Author's elaboration based on Vensim simulation results. 107
Figure 13: Estimated Processing Delay under Delayed-Capacity Scenarios. Source: Author's elaboration based on Vensim simulation results. 113
Figure 14: Recycling Backlog under Delayed-Capacity Scenarios. Source: Author's elaboration based on Vensim simulation results. 113
Figure 15: Cumulative Recovered Materials under Delayed-Capacity Scenarios. Source: Author's elaboration based on Vensim simulation results. 114

LIST OF TABLES

Table 1: Projected annual end-of-life EV battery flows in Italy under selected national decarbonization scenarios. 29
Table 2: Reference Technical Parameters Implemented in the Model. 43
Table 3: Initial Conditions Implemented in the Model 44
Table 4: Second-Life Allocation Input Configurations 45
Table 5: Recycling-Capacity Input Configurations 46
Table 6: Scenario Matrix for Second-Life Allocation and Recycling-Capacity Timing. Source: Author's elaboration. 47
Table 7: Performance Indicators 50
Table 8: Variables Included in Module 1: First-Life Battery Accumulation and Retirement 52
Table 9: Variables Included in Module 2: Collection and Second-Life Allocation 53
Table 10: Variables Included in Module 3: Recycling and Backlog Management 54
Table 11: Variables Included in Module 4: Material Recovery and Performance Accounting 55
Table 12: Construction of the vehicle registration and fleet projection series. Source: Author's elaboration based on EAFO [42], Motus-E and Strategy& [36], and Motus-E et al. [33]. 60
Table 13: Battery-Mass Conversion Parameters Implemented in the Model 62
Table 14: Selected Values of the Mass-Based End-of-First-Life Flow. Source: Author's calculations based on the registration trajectories and battery-mass assumptions described in Sections 4.5.1–4.5.3 and the Weibull parameters adopted from Dei et al. [16]. 62
Table 15: Reference Recycling-Capacity Trajectory Implemented in the Model 63
Table 16: Simulation Settings 69
Table 17: Summary of Extreme-Condition Tests and Results. 73
Table 18: Integration-Error Test Results for Selected Performance Indicators 78
Table 19: Sensitivity Analysis Results for Collection Rate. Source: Author's elaboration based on Vensim simulation results. 79
Table 20: Sensitivity Analysis Results for Average Second-Life Duration. Source: Author's elaboration based on Vensim simulation results. 81
Table 21: Sensitivity Analysis Results for Material Recovery Efficiency. Source: Author's elaboration based on Vensim simulation results. 83

Table 22: Sensitivity Analysis Results for Minimum Processing Time. Source: Author's elaboration based on Vensim simulation results. 85
Table 23: Sensitivity Analysis Results for Weibull Scale Parameter. Source: Author's elaboration based on Vensim simulation results. 86
Table 24: Summary of Sensitivity Analysis Results for Selected Model Parameters. Source: Author's elaboration based on sensitivity-analysis results..... 87
Table 25: Summary of Model Verification and Validation Evidence. Source: Author's elaboration based on model tests and external comparisons. 89
Table 26: Baseline scenario configuration 90
Table 27: Baseline operational and material-circularity results. 91
Table 28: Reference and low second-life allocation trajectories. 92
Table 29: Performance comparison between S1 and S2. 94
Table 30: Reference and high second-life allocation trajectories. 94
Table 31: Performance comparison between the baseline and high second-life allocation scenarios 96
Table 32: Reference and anticipatory recycling-capacity trajectories..... 98
Table 33: Performance comparison between the baseline and anticipatory-capacity scenarios. 100
Table 34: Configuration of the anticipatory-capacity and low-allocation scenario 100
Table 35: Performance comparison of the low-allocation and anticipatory-capacity scenario with the relevant reference configurations. 102
Table 36: Configuration of the anticipatory-capacity and high-allocation scenario 103
Table 37: Performance comparison of the high-allocation and anticipatory-capacity scenario with the relevant reference configurations. 104
Table 38: Reference and delayed recycling-capacity trajectories 108
Table 39: Performance comparison between the baseline and delayed-capacity scenarios. 109
Table 40: Configuration of the delayed-capacity and low second-life allocation scenario. 110
Table 41: Performance comparison of S8 with the relevant low-allocation and delayed-capacity scenarios. 111
Table 42: Configuration of the delayed-capacity and high second-life allocation scenario. 112
Table 43: Comparative performance of the nine coordination scenarios 114

1. INTRODUCTION

The growing number of EV batteries reaching the end of their automotive life creates a long-term planning challenge. The issue is not only whether batteries are directed to second-life applications or recycling, but also when these flows occur and whether enough processing capacity is available. This study examines this coordination problem in the Italian EV battery system.

1.1. Research Motivation

The transition to electric mobility will increase the number of batteries leaving automotive use. These batteries must be collected, transported, assessed, disassembled, and assigned either to second-life applications or recycling. Since these activities depend on each other, delays or insufficient capacity at one stage can affect the performance of the entire end-of-life system [1]. Future battery volumes may therefore create operational problems if collection and processing systems do not develop at a similar pace.

Circular economy strategies offer different ways to retain battery value. Batteries that no longer meet automotive requirements may still be suitable for less demanding second-life applications [4], while recycling recovers materials such as lithium, nickel, cobalt, and manganese for possible use as secondary resources. Second life extends battery use but does not replace recycling, since repurposed batteries will also reach their end of life [5]. The main planning question is therefore how the allocation between these pathways changes recycling demand, capacity requirements, and the timing of material recovery.

Allocating batteries between second life and direct recycling creates a timing trade-off. A larger second-life share delays their arrival at recycling facilities and the recovery of embedded materials [3]. At the same time, sending more batteries directly to recycling increases short-term processing demand and may place pressure on the available infrastructure. The outcome depends on collection, battery lifetimes, allocation decisions, recycling capacity, and the timing of post-second-life returns [7].

These relationships are difficult to evaluate with a static approach because batteries accumulate in different lifecycle stages and move between them after long delays [2,7].

Recycling infrastructure may also need to expand before the corresponding end-of-life flows appear [1]. System Dynamics is therefore used to represent these stocks, delays, capacity constraints, and allocation decisions over time [2].

Italy is a relevant case because its EV fleet is expected to grow substantially over the coming decades. Globally, EV sales and fleet size have continued to expand rapidly in recent years [12], with the European fleet following a similar trajectory [11]. Existing projections estimate that annual vehicle-related end-of-life battery mass could increase from approximately 27.4 kt/year in 2030 to between 435 and 606 kt/year in 2050, depending on the national electrification scenario [16]. This growth creates both a waste-management challenge and an opportunity to recover secondary materials, increasing the need to plan second-life use and recycling capacity in advance. Beyond end-of-life material flows, this expansion also has implications for broader energy and grid planning in Italy [9].

To examine this problem, the study develops a System Dynamics model of the Italian EV battery system focused on second-life allocation and recycling-capacity timing. The model is used to compare long-term system behavior under different assumptions and scenarios; it is not intended as a precise forecast of future battery flows.

From an Industrial Engineering perspective, this is an operations and capacity-planning problem. The system must coordinate changing battery inflows, routing decisions, delayed returns, limited processing capacity, and accumulated unprocessed batteries.

1.2. Research Purpose and Objective

The purpose of this research is to examine how second-life allocation and recycling-capacity timing interact over time in the Italian EV battery system, and how this interaction affects backlog, processing delay, capacity utilization, and recovered-material availability.

The general objective is to design and evaluate a System Dynamics decision-support model that compares alternative combinations of second-life allocation and the timing of

recycling-capacity expansion to assess their effects on material circularity, recycling backlog, and material recovery delays.

Material circularity is evaluated through recovered-material availability and Battery Recovery Yield, while operational performance is assessed through the indicators related to recycling demand, backlog, processing delay, throughput, and capacity utilization.

1.3. Research Question

Under what combinations of second-life allocation and recycling-capacity timing can material circularity be improved while limiting recycling backlogs and material-recovery delays in the Italian electric vehicle battery system?

1.4. Research Hypotheses

The hypotheses translate the main mechanisms identified in the literature into relationships that can be evaluated with the model. The analysis compares the baseline with alternative combinations of second-life allocation and recycling-capacity timing. The aim is to evaluate the magnitude and timing of these effects in the Italian context.

H1. Compared with lower-allocation scenarios, higher second-life allocation will reduce short-term recycling inflows and delay recycling demand and the availability of recovered materials.

H2. Scenarios in which recycling capacity expands more slowly than recycling-pathway inflows will produce larger recycling backlogs and longer estimated processing delays than scenarios with anticipatory capacity expansion.

H3. Earlier recycling-capacity expansion will reduce recycling backlogs and processing delays but may result in lower capacity utilization during periods in which available capacity exceeds recycling demand.

H4. Scenario configurations in which recycling-capacity expansion is better aligned with direct and post-second-life battery returns will produce lower backlog burden and

processing delays than configurations in which capacity becomes available later than recycling demand.

1.5. Specific Objectives

To achieve the general objective, the study pursues the following specific objectives:

1. To define the system boundaries, lifecycle stages, key variables, causal relationships, data requirements, assumptions, and design constraints of the Italian electric vehicle battery system.

2. To develop a stock-and-flow System Dynamics model representing battery flows through first-life use, collection, second-life applications, recycling backlog, recycling processes, and recovered material outputs.

3. To parameterize, verify, and test the model using Italian data where available and literature-based assumptions where country-specific data are limited, including dimensional consistency checks.

4. To design and simulate alternative scenario combinations involving different levels of second-life allocation and different timings of recycling-capacity expansion.

5. To evaluate the operational and material-circularity effects of the simulated scenarios and identify the main trade-offs among the evaluated strategy configurations.

2. LITERATURE REVIEW

The literature reviewed in this chapter provides the basis for the model structure, parameter selection, and research contribution. It covers EV battery retirement, second-life use, recycling-capacity constraints, existing quantitative models, and the Italian context. These elements are then used to identify the research gap addressed by the study.

2.1. End-of-Life EV Battery Management and Retirement Dynamics

End-of-life management determines how retired EV batteries are collected, assessed, and assigned to an appropriate recovery pathway. Before entering second-life use or recycling, batteries may require transportation, storage, sorting, and disassembly [1,5]. These activities influence both the quantity of battery mass available for circular recovery and the timing with which it reaches each pathway.

Decisions made at one stage affect the flows reaching the next. Incomplete collection reduces the battery mass available for recovery, while second-life allocation delays its entry into recycling. Retirement timing and pathway allocation must therefore be considered when estimating future recycling demand and infrastructure requirements.
Automotive first-life duration is not the same for every battery. A commonly cited criterion considers a battery to have reached automotive end of life after losing approximately 20% of its original capacity, corresponding to a State of Health of around 80% [22]. Values between 70% and 80% are frequently used in end-of-life and second-life studies, although their continued applicability has been questioned as battery durability, vehicle range, warranties, and operating conditions have changed [23]. Since the present model does not simulate individual battery degradation, SoH is not used directly to calculate retirement.

Differences in battery chemistry, design, age, and State of Health also complicate testing, classification, and recovery operations [5]. Poor end-of-life management can create fire and leakage risks and may lead to the loss of materials that could otherwise be recovered as secondary resources [6].

End-of-life management also depends on collection, transportation, storage, labeling, and traceability. Fragmented networks and lithium-ion battery transport requirements can increase costs and complicate pathway allocation. Standardized labeling and traceability can instead reduce information gaps concerning battery chemistry, condition, and suitable recovery options [2,6].

EV battery end-of-life management in Italy operates within the broader European framework for producer responsibility, collection, treatment, material recovery, recycled content, and traceability [14,15].

Regulation (EU) 2023/1542 establishes collection targets of 63% by 2027 and 73% by 2030 for portable batteries, but it does not provide an equivalent percentage target for EV batteries [24]. Article 61 instead requires producers or producer responsibility organizations to take back waste EV batteries, ensure their separate collection, provide suitable infrastructure, and deliver them to permitted treatment facilities [24]. The regulation therefore supports a broad collection obligation but does not provide a numerical EV battery collection rate that can be transferred directly to the model. The implemented rate is therefore treated as a literature-based assumption and not as an observed Italian value.

Estimating future end-of-life flows requires linking annual battery inflows with retirement timing. Some studies apply a fixed lifetime, while others use probability distributions to represent variation among batteries. Dei et al. (2026), for example, combine Italian vehicle registrations with a Weibull lifetime distribution, allowing each annual cohort to retire gradually instead of after one fixed period [16].

Cobb et al. (2026) show that battery chemistry, vehicle-use intensity, and retirement conditions affect both first-life duration and battery condition at retirement [21]. These differences support representing retirement with a lifetime distribution instead of assuming one fixed retirement age.

2.2. Second-Life Allocation and Delayed Material Recovery

Retired EV batteries can follow different circular pathways, including reuse, remanufacturing, repurposing, and recycling. These pathways differ in the level of product value retained and in the processing required before the battery or its materials can be used again [1,3]. Since the present study examines the coordination between second-life allocation and recycling capacity, the analysis focuses specifically on repurposing and recycling. Repurposing involves assigning batteries that are no longer suitable for automotive use to alternative applications, particularly stationary energy storage, whereas recycling processes batteries to recover their constituent materials [25].

However, not every battery removed from an electric vehicle is suitable for second-life use. Eligibility depends on chemistry, operating history, remaining State of Health, safety condition, processing needs, and the intended application. Gu et al. (2024) show that batteries with similar remaining capacity may still have different remaining lifetimes because of their previous degradation history [26]. Cobb et al. (2026) also find that the preferred pathway varies across chemistries and operating conditions: repurposing is generally favored for LFP, recycling for NCA, and condition-based sorting for NMC batteries [21].

In the model, second-life allocation represents the share of collected batteries that pass assessment and are assigned to an additional-use application. It summarizes technical eligibility, battery condition, sorting outcomes, and the availability of suitable applications without assuming that second-life suitability is a fixed battery characteristic.

Second-life use delays recycling but does not remove the need for it. A battery may move directly from automotive use to recycling or pass through an additional-use stage before final treatment [25]. Tankou et al. (2023), for example, assign 50% of collected batteries to a ten-year second life and send the remaining share directly to recycling [19]. Although these percentages are scenario assumptions, they illustrate how second life introduces an additional stock and delay before material recovery.

In System Dynamics models, batteries allocated to second life remain in an intermediate stock and later return to recycling through a post-second-life flow [27]. Recycling demand therefore includes both direct end-of-first-life inflows and delayed returns from second life.

This delay creates a trade-off. Higher second-life allocation reduces immediate recycling inflows but keeps materials embedded in batteries for longer. Pratap et al. (2024) found that greater repurposing reduces short-term material recovery but increases the future supply of recyclable batteries when those units complete second life [7]. Second life therefore shifts recycling demand over time without eliminating it.

Policy and market conditions can also affect pathway allocation. Seika and Kubli (2024) find that recycled-content requirements may strengthen incentives for direct recycling

and weaken the relative attractiveness of repurposing [30]. Although this mechanism is outside the model boundary, it further shows that second-life allocation is not determined only by battery condition.

Post-second-life returns may overlap with direct end-of-first-life inflows and create greater recycling demand in later years. Expanding capacity before these returns occur may instead create temporary underutilization. Second-life allocation and recycling capacity must therefore be evaluated together. This timing also affects the interpretation of material recovery: within a fixed simulation horizon, higher allocation may produce lower cumulative recovery because more battery mass remains in second life, not because the material is permanently lost. Bobba et al. (2019) similarly show that second use temporarily retains embedded materials in active stocks and delays their availability for recycling [31].

2.3. Recycling Capacity, Backlog, and Infrastructure Timing

Recycling can make materials such as lithium, cobalt, nickel, and manganese available as secondary resources [1]. Actual recovery, however, depends on whether the system has enough capacity to process the batteries arriving for treatment. Recycling capacity is the maximum feedstock that can be processed during a period, while throughput is the amount actually processed. Throughput is therefore limited by both capacity and available battery feedstock [28].

Batteries that cannot be processed during the period accumulate in the Recycling Backlog. This stock increases when recycling-pathway inflows exceed throughput and decreases when the system processes more than the new inflow. Recycling demand and backlog are therefore different quantities: demand is an annual inflow, while backlog is the battery mass still awaiting treatment.

Battery mass waiting in the backlog cannot generate recovered materials until it is processed. A persistent backlog therefore delays material recovery. The model estimates processing delay from the relationship between backlog and throughput, while capacity utilization compares actual throughput with available capacity. High utilization means

that most of the installed capacity is in use; low utilization indicates spare processing capability.

Capacity and feedstock can become misaligned in either direction. If capacity grows more slowly than recycling inflows, the system becomes constrained and backlog accumulates. If facilities are installed before sufficient battery mass is available, they may remain underutilized. Li and Srai [18] identify this problem in EV battery supply networks, where formal recyclers may operate below their target capacity because they cannot secure enough feedstock. Their study includes informal repurposing channels, which are outside the present model, but still shows how utilization depends on the quantity and timing of available batteries.

Capacity expansion must often be decided before the corresponding battery flows are available. Kalchenko [17] suggests that European recycling systems may develop more slowly than EV adoption and identifies 2033–2035 as a possible period for the first major wave of end-of-life EV batteries. Delayed investment or collection development may therefore create bottlenecks even when suitable recycling technologies already exist. Infrastructure timing is consequently as important as the technology itself.

This issue is relevant in Italy, where annual lithium-ion battery waste from EVs and stationary storage systems is projected to rise from approximately 27 kt in 2030 to between 551 and 736 kt in 2050 [16]. Capacity that is sufficient during the early transition may become inadequate later, while infrastructure sized for future volumes may initially remain underutilized.

Second-life allocation further changes the timing of recycling feedstock. High allocation may make early capacity appear excessive because fewer batteries enter direct recycling. The same capacity may later become insufficient when post-second-life returns overlap with new end-of-first-life inflows.

Capacity planning therefore involves a timing trade-off. Late expansion may produce backlog, processing delays, and postponed material recovery, while early expansion may create periods of underutilization. Utilization also depends on the existing backlog, since spare capacity can process previously accumulated batteries. The model captures these

relationships by representing recycling capacity as a time-dependent constraint, backlog as a stock, and throughput as its capacity-constrained outflow.

2.4. Existing System Dynamics and Quantitative Models of EV Battery Circularity

The reviewed quantitative models are organized into three groups: System Dynamics models of recovery pathways and market behavior, dynamic material-flow models of battery stocks and retirement, and optimization models of recycling-capacity planning. Each group represents a different part of the circular battery system and provides mechanisms used in the present study.

2.4.1. System Dynamics Models of Recovery Pathways

Alamerew and Brissaud (2020) developed a System Dynamics model of end-of-life EV battery recovery from a reverse-supply-chain perspective. It connects recovery strategies with economic, regulatory, logistical, environmental, and managerial factors. Its focus is broad and mainly concerns the attractiveness of recovery alternatives, while battery accumulation across lifecycle stages is not the main focus of the model [2].

Kamath et al. (2023) modeled end-of-first-life battery availability in the United States and compared direct recycling with a sequential pathway that includes stationary second life. First- and second-life exits are represented through lifetime distributions, and the pathways are compared in terms of virgin-material demand, economic value, energy use, and carbon impacts [20]. The model captures the timing effect of an intermediate second-life stage, but it does not focus on recycling backlog or capacity-constrained processing.

Pratap et al. (2024) link battery collection, recycling, repurposing, chemistry, infrastructure development, and raw-material recovery in a System Dynamics model. Their results show that repurposing postpones recovery but later increases recyclable battery supply when repurposed units reach their second end of life [7]. The model also includes delays in collection and processing infrastructure. Its main outcomes, however, focus on material recovery and second-life availability, while backlog, processing delay, and capacity utilization are not the main indicators analyzed.

Seika and Kubli (2024) distinguish a one-loop pathway based on direct recycling from a two-loop pathway that includes repurposing before final recycling. Their model links battery flows and pathway allocation with regulation, profitability, market conditions, and investment in recycling capacity. It shows that recycled-content requirements may encourage recycling expansion while weakening the repurposing market [30].

Seika and Kubli (2025) extend this work to the commercial development of the second-use industry. Their model includes market entry and exit, repurposing capacity, demand, prices, profitability, and investment delays [27]. The analysis centers on second-use market development and does not address the coordination of recycling capacity with direct and delayed battery returns.

Vaz et al. (2026) model end-of-life battery management in São Paulo through landfill, direct-recycling, and second-life pathways. Batteries assigned to second life later return to recycling, allowing the model to compare business-as-usual, recycling-focused, and second-life-focused policies. In this model, recycling is treated as an allocation destination and not as a capacity-constrained process, so backlog formation and processing delays caused by insufficient capacity are not represented [29].

Overall, System Dynamics studies increasingly represent lifecycle stages, second-life stocks, delayed returns, infrastructure, and material recovery. Their main outcomes generally concern profitability, policy, environmental impacts, landfill diversion, or raw-material recovery. Less attention has been given to the combined behavior of second-life allocation, capacity-constrained throughput, recycling backlog, processing delay, and utilization.

2.4.2. Dynamic Material-Flow and Lifetime Models

Dynamic material-flow models provide detailed representations of battery cohorts, retirement timing, second-life stocks, and embedded materials. Bobba et al. (2019) model direct reuse, second use, and recycling for traction batteries in Europe. Their second-use stock delays the movement of batteries and embedded materials toward recycling, although all batteries are eventually treated after their first or second life. The results show

that second use retains cobalt and lithium in active stocks for longer and postpones their availability for recovery [31].

Kastanaki and Giannis (2023) combine projected battery inflows with Weibull lifetime distributions to estimate end-of-life flows in the EU-27. Their model distinguishes remanufacturing, second life, and recycling and estimates pathway availability, second-life storage capacity, and the recovery of lithium, cobalt, nickel, and copper [32]. It provides a useful basis for generating retirement flows from annual cohorts and converting recycled battery quantities into recovered-material outputs. Similar cohort-based material-flow approaches have been applied in other national contexts, including Catalonia [43] and the United States and China [44,45]. Recent work has also benchmarked different forecasting frameworks for end-of-life battery pack estimation [46].

These models support the representation of probabilistic retirement, lifecycle delays, second-life stocks, and recovered-material timing. Their main purpose is to estimate potential battery and material flows. Recycling capacity is generally not represented as a constraint on throughput, and batteries awaiting treatment do not accumulate in an explicit backlog.

2.4.3. Recycling-Capacity Planning and Inventory Models

Recycling-capacity planning models address infrastructure constraints through optimization. Brun and Sun developed BattOpt, a multistage stochastic model that separates strategic capacity-investment decisions from operational processing decisions. Throughput is limited by installed facility capacity, and unprocessed batteries remain in inventory for later periods [28].

BattOpt's retired-battery inventory provides the closest equivalent to the Recycling Backlog used in this thesis. It increases when newly available batteries exceed throughput and decreases when capacity is sufficient to process both current inflows and previous accumulation. The model also shows that capacity decisions must be made across multiple planning periods under uncertain battery supply. Its purpose, however, is to minimize facility, technology, and material-flow costs; second-life allocation and delayed returns are not central to its structure.

The three modeling families provide complementary elements. System Dynamics captures feedback, pathway interactions, and delays; material-flow models provide cohort-based retirement and second-life stock methods; and capacity-planning models connect installed infrastructure with throughput and accumulated inventory.

These mechanisms are generally examined separately. None of the reviewed models centers on the joint interaction among second-life allocation, delayed returns, capacity-constrained throughput, backlog, processing delay, utilization, and recovered-material availability. This separation provides the basis for the research gap presented in Section 2.6.

2.5. Italian Context and Data Foundations

Italy combines a large and highly motorized passenger-car fleet with an EV market that is still at an early stage of development. In 2024, the country recorded approximately 701 passenger cars per 1,000 inhabitants, one of the highest motorization rates in the European Union [10]. At the end of 2025, the national fleet included approximately 41.09 million passenger cars, including about 363,000 BEVs and 375,000 PHEVs. Together, plug-in vehicles represented around 1.8% of the circulating fleet, although BEVs accounted for 6.2% of new registrations during 2025 [35]. Most Italian EV battery retirements have therefore yet to occur, and future end-of-life flows will depend strongly on the pace of adoption.

Future projections vary considerably. Motus-E and Strategy& estimate an Italian EV fleet of 3.7–4.6 million vehicles in 2030 and 9.8–11.4 million in 2035, depending on market and policy conditions [36]. These ranges show that future battery inflows cannot be treated as a single certain trajectory.

Dei et al. (2026) provide an Italy-specific sales-stock-lifespan model based on historical registrations, future vehicle scenarios, and a Weibull lifetime distribution with a scale parameter of 12 years and a shape parameter of 3.5 [16]. Their results estimate approximately 27.4 kt/year of vehicle-related end-of-life battery mass in 2030 and between 435 and 606 kt/year in 2050, depending on the scenario. These values provide

external comparison points for the retirement series developed in this thesis, while the detailed differences in scope and calculation are discussed in Chapter 4. Table 1 summarizes the BEV and PHEV end-of-life flows reported for selected Italian scenarios.

Scenario and year	BEV batteries (kt/year)	PHEV batteries (kt/year)	Total EV batteries (kt/year)
INECP, 2030	23.2	4.2	27.4
GA-IT, 2050	412	23	435
DE-IT, 2050	581	25	606

Table 1: Projected annual end-of-life EV battery flows in Italy under selected national decarbonization scenarios.

Source: Author's elaboration based on Dei et al. (2026) [16].

Italian studies also provide assumptions for second-life development. Dei et al. represent no significant reuse before 2030, a 10% allocation rate in 2030, gradual growth to 50% by 2050, and an average second-life duration of ten years [16]. An industry assessment uses a similar duration and estimates that available second-life battery capacity could reach approximately 77 GWh by 2050 [33]. The same source estimates almost 0.4 million tonnes of batteries directed toward recycling, although its boundary also includes damaged batteries and manufacturing scrap.

Available evidence indicates that Italian end-of-life battery flows may grow faster than domestic recycling infrastructure. A 2023 assessment reported that Italy did not yet have facilities specifically suited to EV battery recycling at the required industrial scale [33]. A later study described the lithium-ion recycling chain as being at an early stage, with several actors transitioning from other recycling sectors and second-life activity still concentrated in pilots and case studies [34]. Estimates of European recycling capacity also vary according to the facilities and treatment stages included. The Joint Research Centre reported approximately 116 kt/year in 2023 and announced growth toward 400 kt/year by 2030 [37], while a narrower inventory identified 14 operating facilities with a combined capacity of 55.81 kt/year [38]. These differences show the uncertainty surrounding accessible processing-capacity data.

A comparative policy analysis also found that Italy lacks detailed targets and monitoring mechanisms for battery reuse, recovery, and critical-material reintegration, despite having broader waste-management and sustainable-development strategies [40].

Battery throughput and recovered-material output are not equivalent. An Italian assessment estimates that a hydrometallurgical chain including disassembly, pretreatment, and treatment can recover approximately 60% of incoming battery mass [33]. European studies report higher recovery rates for some individual materials, including copper, cobalt, nickel, and manganese, while lithium recovery may be lower depending on the process [38,39].

Overall, the Italian literature provides useful data for vehicle adoption, battery retirement, second-life development, and treatment requirements, but important gaps remain for collection performance, installed recycling capacity, and operational processing conditions. The model therefore combines Italian data with clearly identified literature-based and modeling assumptions, as described in Chapter 3.

2.6. Research Gap and Contribution

The mechanisms required to analyze EV battery circularity are well established but are generally studied separately. System Dynamics models often focus on profitability, policy, environmental performance, or material recovery; material-flow models estimate lifecycle stocks and flows without constraining recycling throughput by installed capacity; and capacity-planning models do not usually place second-life allocation and delayed returns at the center of the analysis.

This separation is relevant in Italy, where EV battery retirements are expected to increase while the timing and scale of recycling infrastructure remain uncertain [33,34,37]. Second-life allocation can reduce immediate recycling inflows but increase delayed returns, while insufficient capacity can turn these flows into backlog and postpone material recovery. The reviewed models do not examine this coordination problem as their main analytical focus within the Italian EV battery system.

This thesis addresses the gap through a stock-and-flow System Dynamics model that connects first-life retirement, second-life allocation, delayed returns, recycling backlog,

capacity-constrained throughput, and recovered-material availability. The model is used to compare the trade-offs among different combinations of second-life allocation and capacity timing in terms of backlog, processing delay, capacity utilization, and recovered-material availability.

3. RESEARCH METHODOLOGY

3.1. Research Approach

This thesis uses a quantitative, simulation-based System Dynamics approach to examine the long-term interaction between second-life allocation and recycling-capacity strategies in the Italian EV battery system. System Dynamics is suitable for this purpose because batteries accumulate in different lifecycle stages, move between them after substantial delays, and may remain unprocessed when recycling inflows exceed available capacity [2,7]. Similar approaches have also been applied to capacity-planning problems in circular-economy and waste-management systems [8].

The model structure was developed from peer-reviewed literature and institutional evidence without relying on interviews or stakeholder workshops. Direct access to Italian recyclers, vehicle manufacturers, and second-life operators was not available within the scope and timeframe of the study. Each main relationship represented in the model was therefore derived from the reviewed literature or documented explicitly as a modeling assumption.

The identified relationships were first organized in a Causal Loop Diagram and subsequently translated into a quantitative Stock and Flow Diagram in Vensim. The model represents battery inflow and retirement, collection, allocation between direct recycling and second life, delayed post-second-life returns, recycling backlog, capacity-constrained throughput, and recovered-material availability.

Physical accumulations are represented as explicit stocks with defined inflows and outflows. These include Batteries in First Life, Batteries in Second Life, and Recycling Backlog. Accounting stocks are used separately to record cumulative processed batteries, recovered materials, recycling-pathway inflow, and backlog burden. Exogenous inputs are identified as external trajectories and are not generated internally within the model.

Battery mass is the main unit of analysis. Stocks are expressed in kilotonnes, annual flows and recycling capacity in kilotonnes per year, time-related indicators in years, and rates and shares as dimensionless fractions. Dimensional consistency is checked in Vensim and must result from physically meaningful equations, without introducing artificial variables solely to correct unit errors.

Italian observed and projected data are used where available and are complemented by European evidence and literature-based assumptions when compatible national values cannot be identified. The completed model is then evaluated through the verification, testing, sensitivity, and validation procedures presented in Chapter 4.

The model is intended to compare strategy configurations under consistent assumptions. It does not produce a precise forecast or determine a mathematically optimal infrastructure plan. Its outputs are interpreted as conditional results for the scenarios and assumptions evaluated.

3.2. System Boundaries

This section defines the geographical, lifecycle, aggregation, and temporal boundaries of the model. The modeled system begins when battery mass enters automotive first life in Italy and ends when batteries are processed and recovered materials become available. Mechanisms that do not directly support the research question are excluded.

3.2.1. Geographical Boundary

The geographical boundary is Italy. The model includes traction batteries entering automotive first life through newly registered BEV and PHEV passenger cars and the end-of-life flows subsequently generated by these batteries. Italy is represented as one aggregated national system and does not distinguish between separate regions, facilities, or local markets.

Within this boundary, Recycling Capacity refers to the effective processing capability available to manage Italian EV battery flows. The model does not distinguish whether

this capability is located domestically or accessed through the wider European recycling system. Facility location, ownership, regional distribution, and cross-border movements are not represented explicitly.

The European regulatory framework is treated as an external institutional condition; regional implementation and individual compliance decisions are not modeled.

Italian data are used where sufficiently compatible information is available. European or international values are used only when country-specific evidence cannot be identified and are documented as proxy values or assumptions in Section 3.4.

3.2.2. Lifecycle and Process Boundary

The lifecycle boundary begins when battery mass enters automotive first-life use and ends when recovered materials become available after recycling. Raw-material extraction, cell manufacturing, battery-pack production, and vehicle production are outside the model. Battery inflow is therefore introduced as an external annual series.

Battery mass entering newly registered BEV and PHEV passenger cars accumulates in Batteries in First Life. Its outflow, End-of-First-Life Flow, is derived externally through a cohort-based Weibull calculation and imported into Vensim as an exogenous annual trajectory. The stock remains explicitly represented to preserve and verify the first-life battery-mass balance.

The Collection Rate determines the share of retiring battery mass entering the modeled circular system. Uncollected batteries leave the model boundary. Collected batteries are divided between Direct Recycling Inflow and Second Life Inflow according to the Second-Life Allocation Rate. Battery-level assessment, sorting, and State-of-Health evaluation are represented through the aggregated allocation rate and are not modeled as separate processes.

Batteries allocated to second life remain in the Batteries in Second Life stock before returning to recycling through Post-Second-Life Return. Second-life applications are

represented as one aggregated pathway. Losses, exports, and a separate post-second-life collection stage are not included.

Direct Recycling Inflow and Post-Second-Life Return enter the Recycling Backlog. Battery mass remains in this stock when it cannot be processed immediately and leaves through Recycling Throughput, which is constrained by available capacity and feedstock.

Recovered Material Flow is calculated from Recycling Throughput and the aggregated Material Recovery Efficiency. The model ends when these recovered materials become available; their reintegration into cathode, cell, or battery production is outside the system boundary.

3.2.3. Level of Aggregation and Unit of Analysis

The model is developed at an aggregated national level and represents battery mass instead of individual vehicles, battery packs, firms, transactions, or recycling facilities. This level of aggregation is consistent with the long-term planning purpose of the study and with the national scale of the available data.

BEV and PHEV registrations are processed separately during the external calculation because their battery packs differ substantially in mass. Their battery-mass inflows and retirement flows are then aggregated before being imported into Vensim. The System Dynamics model therefore does not maintain separate BEV and PHEV stocks or recycling pathways.

Battery chemistries, pack designs, individual materials, operating conditions, and retirement states are not represented separately. Recovered-material availability is calculated as an aggregated mass output. Battery stocks are expressed in kt, annual flows and recycling capacity in kt/year, time-related variables in years, and rates and shares as dimensionless fractions or percentages.

Accordingly, material-recovery indicators are evaluated at the aggregated battery-system level and are not calculated separately for lithium, nickel, cobalt, or other individual materials.

3.2.4. Temporal Boundary

The simulation covers 2025–2050. The year 2025 defines the initial state, while the 2050 endpoint provides sufficient time to observe first-life retirement, second-life returns, capacity expansion, backlog accumulation, and material recovery.

Historical BEV and PHEV battery cohorts preceding 2025 are included in the external calculation because part of this battery mass remains in use at the beginning of the simulation and may retire during the modeled period. These cohorts are also used to calculate the initial Batteries in First Life stock.

Time is represented in years. Inputs and reported results use an annual resolution, while the internal simulation uses a smaller time step tested for integration error. Battery mass may remain in second life or in the recycling backlog in 2050; these terminal stocks are reported when interpreting the results.

3.2.5. Exogenous Conditions and Excluded Elements

The main exogenous inputs are the BEV and PHEV registration trajectories, powertrain-specific battery-mass assumptions, battery-mass inflow and retirement series, Collection Rate, Second-Life Allocation Rate, Recycling Capacity, Average Second-Life Duration, Minimum Processing Time, and Material Recovery Efficiency. These variables influence the modeled stocks and flows but are not generated by feedback from backlog, throughput, utilization, or recovered materials.

Second-life allocation and recycling capacity are treated as externally specified strategic variables. EV adoption is also external; the model does not simulate vehicle demand, consumer decisions, charging infrastructure, energy prices, or adoption incentives.

The model excludes upstream battery and vehicle manufacturing; manufacturing scrap and batteries produced directly for stationary storage; non-plug-in and non-passenger vehicle categories; battery-level chemistry, degradation, and State-of-Health assessment; separate reuse, refurbishment, and remanufacturing pathways; facility-level recycling technologies and locations; transportation, storage, logistics, and cross-border flows;

prices, costs, revenues, investment optimization, and firm behavior; detailed policy responses; and the reintegration of recovered materials into new battery production.

Some excluded mechanisms are reflected indirectly through aggregated parameters. Battery condition and technical eligibility influence the Second-Life Allocation Rate, chemistry and recycling technology influence Material Recovery Efficiency, and BEV–PHEV size differences are included in the external battery-mass conversion.

3.3. Model Development Procedure

Model development followed four main stages. First, the mechanisms relevant to battery retirement, collection, second-life allocation, recycling capacity, backlog formation, and material recovery were identified from the literature reviewed in Chapter 2. Relationships required to complete the quantitative structure but not directly specified in the evidence were documented as modeling assumptions.

Second, these mechanisms were organized in a Causal Loop Diagram to identify the direction of the relationships, the main delays, and the balancing feedback associated with recycling-backlog adjustment. Economic, investment, market, and policy feedbacks were excluded according to the boundaries defined in Section 3.2.

Third, the conceptual relationships were translated into a Stock and Flow Diagram. Physical stocks represent batteries in first life, batteries in second life, and batteries awaiting recycling. Accounting stocks record cumulative inflows, processed batteries, recovered materials, and backlog burden. The first-life battery inflow and retirement trajectories were prepared externally through registration, battery-mass, and cohort calculations before being imported into Vensim.

Finally, the equations, parameters, initial values, and time-dependent trajectories were implemented in Vensim. The completed model was then evaluated through equation and unit checks, mass-balance and non-negativity tests, extreme-condition testing, integration-error testing, sensitivity analysis, and behavioral and external comparisons. Chapter 4 presents the model implementation and these evaluation results.

3.4. Data Sources, Parameterization, and Assumptions

Model inputs were selected according to their compatibility with the geographical, vehicle-category, lifecycle, and temporal boundaries. Italian observed data were preferred, followed by Italian projections, European evidence, broader literature, and explicit modeling assumptions when no compatible value was available.

Each input was classified according to both its source and its role in the model. The main categories are observed data, projected data, derived values, proxy values, literature-based assumptions, modeling assumptions, initial conditions, strategic scenario variables, and external comparison values. No single source defines the complete parameterization; different sources are used according to the variable they report and the method they support.

3.4.1. Historical EV Registrations and Fleet Data

Historical annual BEV and PHEV registrations for Italian M1 passenger cars were obtained from the EAFO AF New Registrations dataset [42]. Observations from 2008 to 2025 were retained as separate powertrain cohorts because BEV and PHEV registrations are later converted using different battery-mass assumptions.

The 2026 EAFO observations covered January–June. Full-year registrations were estimated separately for each powertrain using the relationship between first-half and full-year registrations observed in 2025:

$$\widehat{R_{v_{2026}}} = R_{v,Jan-Jun\ 2026}\left(\frac{R_{v,full\ year\ 2025}}{R_{v,Jan-Jun\ 2025}}\right)$$

where R denotes vehicle registrations and v identifies the powertrain category, either BEV or PHEV. The calculation produced estimates of 167,944.78 BEVs and 183,466.45 PHEVs for 2026. These values are classified as author-derived estimates based on EAFO observations and not as complete observed annual data [42].

The EAFO fleet dataset provided end-of-2025 stocks of 372,693 BEVs and 383,258 PHEVs. For 2027–2035, fleet values were constructed using the conservative passenger-car scenario reported by Motus-E and Strategy& [36]: 2.3 million BEVs and 1.2 million

PHEVs in 2030, and 7.7 million BEVs and 1.2 million PHEVs in 2035. Annual values between these points were estimated through geometric interpolation:

$$Fleet_{v,t} = Fleet_{v,a} \left(\frac{Fleet_{v,b}}{Fleet_{v,a}}\right)^{\frac{t-a}{b-a}}$$

where v denotes the powertrain category, either BEV or PHEV; t is the year being estimated; a is the initial year of the period; and b is the final year of the period. $Fleet_{v,a}$ and $Fleet_{v,b}$ represent the published or calculated fleet values for powertrain v at the beginning and end of the period, respectively.

Annual registrations for 2027–2035 were then derived from the fleet-balance identity after calculating cohort-based retirements. This prevents the annual change in fleet stock from being incorrectly interpreted as gross new registrations.

$$Registrations_{v,t} = Fleet_{v,t} - Fleet_{v,t-1} + Retirements_{v,t}$$

Since no directly compatible annual M1 BEV–PHEV projection was available after 2035, the broader electric-vehicle sales trajectory reported by Motus-E et al. [33] was used only to transfer relative growth. The combined BEV and PHEV registration level calculated for 2035 was used as the starting point:

$$R_{BEV,2040} = \left(R_{BEV,2035} + R_{PHEV,2035}\right) \left(\frac{2.044}{1.817}\right)$$

The 2045 value was subsequently calculated using the 2040–2045 growth factor:

$$R_{BEV,2045} = R_{BEV,2040} \left(\frac{2.080}{2.044}\right)$$

Annual values between 2035–2040 and 2040–2045 were distributed evenly. New PHEV registrations were set to zero from 2036, while the existing PHEV fleet declined gradually through retirements. BEV registrations were held at the 2045 value from 2046 to 2050. These choices are modeling assumptions introduced to complete the external driver, since no published M1 forecasts were available for these years.

Vehicle fleets were updated through:

$$Fleet_{v,t} = Fleet_{v,t-1} + Registrations_{v,t} - Retirements_{v,t}$$

3.4.2. Conversion of Vehicle Registrations into Battery-Mass Inflows

Annual registrations were converted into battery-mass inflows separately for BEVs and PHEVs:

$$Battery\ Inflow\ into\ First\ Life = (\{BEV\ Registrations\}_t \times Average\ BEV\ Battery\ Mass + \{PHEV\ Registrations\}_t \times Average\ PHEV\ Battery\ Mass) / 10^6$$

The factor 10^6 converts kilograms into kilotonnes.

Average pack masses were calculated from reference capacities of 60 kWh for BEVs and 15 kWh for PHEVs [16], together with a pack-level specific energy of 165 Wh/kg

$$Average\ BEV\ Battery\ Mass = \frac{60{,}000\ Wh}{165\ Wh/kg} = 363.6\ kg/vehicle$$

$$Average\ PHEV\ Battery\ Mass = \frac{15{,}000\ Wh}{165\ Wh/kg} = 90.9\ kg/vehicle$$

These values were kept constant across cohorts as aggregated assumptions for the modeled fleet and do not represent observed averages for every vehicle registered in Italy. No additional cell-to-pack correction was applied because the specific-energy value was interpreted at pack level.

BEV and PHEV inflows were calculated separately and subsequently aggregated:

$$BEV\ Battery\ Mass\ Inflow_t = \frac{BEV\ Registrations_t \times 363.6}{10^6}$$

$$PHEV\ Battery\ Mass\ Inflow_t = \frac{PHEV\ Registrations_t \times 90.9}{10^6}$$

$$Battery\ Inflow\ into\ First\ Life_t = BEV\ Battery\ Mass\ Inflow_t + PHEV\ Battery\ Mass\ Inflow_t$$

Using constant average pack masses simplifies the representation and may overestimate or underestimate particular historical or future cohorts. This limitation is acknowledged in the interpretation of the model.

3.4.3. Cohort-Based First-Life Retirement

End-of-First-Life Flow was derived externally through a cohort-based Weibull calculation. The method was first applied at vehicle level to connect registrations, retirements, and fleet targets and was then applied to the corresponding battery-mass cohorts.

For a cohort of age a, the cumulative probability of reaching the end of automotive first life is represented by a two-parameter Weibull distribution:

$$F(a) = 1 - exp[-\left(\frac{a^k}{\lambda}\right)]$$

Where a is the age of the battery cohort in years, λ is the Weibull scale parameter, and k is the Weibull shape parameter.

For vehicles registered in cohort year y, the probability of retiring during calendar year t is calculated as the difference between the cumulative probabilities at the end and beginning of the corresponding age interval:

$$p_{y,t} = F(t-y) - F(t-1-y)$$

$F(t-y)$is the cumulative retirement probability at the end of year t; and $F(t-y\ -1)$ is the cumulative retirement probability at the beginning of that year.

Annual vehicle retirements are obtained by multiplying each cohort by its annual retirement probability and summing across all previous cohorts:

$$Retirements_{v,t} = \sum_{y<t} Registrations_{v,y} \times p_{y,t}$$

The reference parameterization is:

$$\lambda = 12 \text{ years}$$

$$k = 3.5$$

The scale parameter follows the Italy-specific application of Dei et al. [16], while the same shape parameter is used in several EV battery end-of-life studies [43–46]. The parameters are applied initially to both BEV and PHEV cohorts because no sufficiently consistent Italian evidence supporting separate powertrain-specific lifetime distributions was identified.

The spreadsheet implementation was verified manually for the 2026, 2027, and 2028 retirement years. Separate cohort tables show the age interval, Weibull cumulative probability at the beginning and end of the year, annual retirement probability, and expected BEV and PHEV retirements for every historical cohort. The resulting totals were then reproduced through a consolidated cohort formula for the remaining projection years. This two-stage implementation was used to make the calculation auditable before automating the full 2029–2050 series.

The vehicle-level retirement results feed the fleet-balance calculation described in Section 3.4.1. Using the finalized reference masses of 363.6 kg per BEV and 90.9 kg per PHEV, the same annual cohort probabilities are then applied to the corresponding battery-mass inflows. BEV and PHEV mass retirements are calculated separately and subsequently summed to obtain the total End-of-First-Life Flow in kilotonnes per year.

$$End\ of\ First\ Life_{v,t} = \sum_{y<t} Battery\ Inflow\ into\ First\ Life_{v,y} \times p_{y,t}$$

$$End\ of\ First\ Life\ Flow_t = End\ of\ First\ Life\ Flow_{BEV,t} + End\ of\ First\ Life\ Flow_{PHEV,t}$$

The resulting annual retirement series covers the complete 2025–2050 simulation period. The total End-of-First-Life Flow increases from approximately 1.58 kt/year in 2025 to 12.90 kt/year in 2030, 60.86 kt/year in 2035, 211.17 kt/year in 2040, 484.53 kt/year in 2045, and 709.55 kt/year in 2050. These values were derived through the external cohort calculation and imported into Vensim as an exogenous annual time series. They should not be interpreted as imposed retirement targets, since they result from the historical and projected battery-mass cohorts and the adopted Weibull lifetime distribution.

Historical cohorts preceding the 2025 simulation start are retained because part of the battery mass already operating in Italy may retire during the modeled period. The initial

Batteries in First Life stock was calculated using the finalized powertrain-specific battery masses and the Weibull survival function $S(a) = 1 - F(a)$ applied to the historical battery-mass cohorts.

$$Initial\ First\ Life\ Stock = \sum_{y < 2025} Battery\ Inflow\ into\ First\ Life_{v,y} \times S(2024 - y)$$

where $S(2024 - y)$ is the probability that the cohort remains in automotive first life at the beginning of 2025. The surviving BEV and PHEV battery-mass cohorts are summed to obtain the initial first-life stock.

This calculation produced an initial first-life battery stock of 136.81 kt. The retirement trajectory was subsequently compared with compatible Italian values reported by Dei et al. [16] to assess external consistency. This comparison was not intended as independent empirical validation.

3.4.4. Technical Parameters

Technical parameters describe operational assumptions that remain constant during the main scenario comparison. Their reference values and bases are summarized in Table 2.

Parameter	Implemented Value	Unit	Basis
Weibull scale parameter	12	year	Dei et al. [16]
Weibull shape parameter	3.5	dmnl	EV battery lifetime studies [43–46]
Average BEV battery mass	363.6	kg/vehicle	Capacity from [16]; specific-energy assumption
Average PHEV battery mass	90.9	kg/vehicle	Capacity from [16]; specific-energy assumption
Collection Rate	0.95	dmnl	Literature-based assumption [43]
Average Second-Life Duration	10	year	Italy-specific literature [16,33]
Material Recovery Efficiency	0.60	dmnl	Aggregated recovery estimate [33]

Minimum Processing Time	1	year	Modeling assumption

Table 2: Reference Technical Parameters Implemented in the Model.

Source: Author's elaboration based on [16], [33], and [43], together with the modeling assumptions described in this section.

The collection rate is not an observed Italian value, since Regulation (EU) 2023/1542 does not establish an equivalent percentage target for EV batteries. The second-life duration and recovery efficiency are aggregated assumptions and do not represent every battery application, chemistry, or recycling process. Minimum Processing Time was introduced to convert available recycling backlog into an annual processing rate. All values remain constant across the main strategy scenarios.

3.4.5. Strategic Scenario Variables

Second-Life Allocation Rate and Recycling Capacity are the two strategic variables evaluated in the scenario analysis.

Second-Life Allocation Rate determines how collected battery mass is divided between second-life applications and direct recycling. The reference trajectory follows the Italian cascade-use assumptions reported by Dei et al. [16], while lower and higher trajectories represent alternative scenario configurations supported by the ranges examined in [43] and [45].

Recycling Capacity represents the effective processing capability available to Italian EV battery flows. Because a complete time series of installed Italian capacity was unavailable, the reference trajectory uses the treatment requirements reported by Motus-E, Strategy&, and Politecnico di Milano [33,13] as a proxy. The published points are 5 kt/year in 2025, 17 in 2030, 48 in 2035, 111 in 2040, 235 in 2045, and 367 in 2050.

Intermediate values of 10 kt/year during 2026–2028 and 12 kt/year in 2029 were added as modeling assumptions to represent gradual early development. These values were not reported directly in [33]. The reference trajectory is therefore a combination of published treatment-requirement points and explicitly documented intermediate assumptions.

Alternative capacity scenarios modify primarily the timing of the main expansion steps. Together, the second-life and capacity configurations form the scenario matrix defined in Section 3.5.

3.4.6. Initial Conditions

Initial conditions correspond to the beginning of 2025. Batteries in First Life was calculated from the surviving historical BEV and PHEV battery-mass cohorts, producing an initial value of 136.81 kt.

Batteries in Second Life was initialized at zero because the reference cascade-use trajectory assumes no significant allocation before 2030 [16]. Recycling Backlog was also initialized at zero because no compatible national estimate of battery mass awaiting treatment in 2025 was available. These are analytical initial conditions and do not imply that no pilot second-life projects or unprocessed batteries existed in Italy.

Cumulative Recovered Materials was initialized at zero because it records only recovery occurring during the simulation period.

Initial Condition	Implemented Value
Initial Batteries in First Life	136.81 kt
Initial Batteries in Second Life	0 kt
Initial Recycling Backlog	0 kt
Initial Cumulative Recovered Materials	0 kt

Table 3: Initial Conditions Implemented in the Model

All initial conditions are checked for non-negativity, dimensional consistency, and compatibility with the external battery-inflow and retirement series.

3.4.7. Parameter Documentation and Treatment of Uncertainty

All derived inputs and modeling assumptions were documented in the external calculation workbook, including their original sources, formulas, intermediate calculations, units, and final trajectories imported into Vensim. Where several values were available, the reference assumption was selected based on geographical compatibility and methodological consistency; no unsupported average was calculated. Comparisons with

studies sharing some of the same source assumptions are used as consistency checks and do not constitute independent validation.

Uncertainty in technical assumptions is addressed separately through sensitivity analysis. This allows the effect of parameter variation to be distinguished from the strategic changes evaluated through the main scenario matrix.

The external calculation workbook is organized into dedicated worksheets for the main data sources and calculation stages, allowing the registration, fleet, battery-mass, retirement, and sensitivity calculations to be traced back to their corresponding inputs and formulas.

3.5. Simulation and Scenario Design

The model is simulated from 2025 to 2050. The main scenario analysis varies the Second-Life Allocation Rate and the timing of Recycling Capacity expansion while maintaining the remaining technical parameters and external battery-flow trajectories constant.

3.5.1. Scenario Structure

The scenario design follows a three-by-three matrix containing three second-life allocation configurations and three recycling-capacity timing configurations. This produces nine main strategy combinations, including the baseline scenario.
The second-life allocation configurations are defined as follows:

Year	Low allocation	Reference allocation	High allocation
2025–2029	0% (0.00)	0% (0.00)	0% (0.00)
2030	5% (0.05)	10% (0.10)	25% (0.25)
2035	10% (0.10)	20% (0.20)	37.5% (0.375)
2040	15% (0.15)	30% (0.30)	50% (0.50)
2045	20% (0.20)	40% (0.40)	50% (0.50)
2050	25% (0.25)	50% (0.50)	50% (0.50)

Table 4: Second-Life Allocation Input Configurations

How each trajectory is defined:

- Low second-life allocation: 0% before 2030, 5% in 2030, followed by an increase of one percentage point per year until reaching 25% in 2050.
- Reference second-life allocation: 0% before 2030, 10% in 2030, followed by an increase of two percentage points per year until reaching 50% in 2050 [16].

- High second-life allocation: 0% before 2030, 25% in 2030, followed by an increase of 2.5 percentage points per year to 50% in 2040, remaining constant afterward.

These configurations are selected within the ranges supported by the reviewed literature and are not interpreted as forecasts of actual Italian second-life adoption.

The recycling-capacity configurations are defined as follows:

Period	Anticipatory capacity (kt/year)	Reference capacity (kt/year)	Delayed capacity(kt/year)
2025	5	5	5
2026–2028	10	10	10
2029	12	12	12
2030–2034	48	17	12
2035–2039	111	48	17
2040–2044	235	111	48
2045–2049	367	235	111
2050	367	367	235
2055	—	—	367

Table 5: Recycling-Capacity Input Configurations

How each trajectory is defined:

- **Anticipatory capacity:** the major reference additions are introduced five years earlier from the 2035 expansion onward.
- **Reference capacity:** expansion follows the trajectory defined in Section 3.4.5.
- **Delayed capacity:** the major reference additions are introduced five years later, placing the final 367 kt/year level outside the simulation horizon.

Where possible, the anticipatory and delayed configurations retain the same capacity-addition magnitudes as the reference configuration and modify primarily their timing. This allows the consequences of capacity timing to be evaluated without simultaneously changing every characteristic of the capacity pathway. Any differences in expansion magnitude required by the final capacity assumptions are stated explicitly in Chapter 5.

The resulting scenario structure is:

Second Life Allocation	Reference Capacity	Anticipatory Capacity	Delayed capacity

Reference	**S1. Baseline:** Reference Capacity + Reference Second-Life Allocation	S4. Anticipatory Capacity + Reference Second-Life Allocation	S7. Delayed Capacity + Reference Second-Life Allocation
Low	S2. Reference Capacity + Low Second-Life Allocation	S5. Anticipatory Capacity + Low Second-Life Allocation	S8. Delayed Capacity + Low Second-Life Allocation
High	S3. Reference Capacity + High Second-Life Allocation	S6. Anticipatory Capacity + High Second-Life Allocation	S9. Delayed Capacity + High Second-Life Allocation

Table 6: Scenario Matrix for Second-Life Allocation and Recycling-Capacity Timing. Source: Author's elaboration.

Each scenario combines one Second-Life Allocation Rate trajectory with one Recycling Capacity trajectory. All remaining technical parameters, initial conditions, and external battery-flow inputs are held constant across the nine main scenarios. The nine combinations constitute the main strategy matrix evaluated under the reference battery-inflow trajectory. They allow the interaction between second-life allocation and recycling-capacity timing to be compared while keeping the remaining model assumptions constant.

3.5.2. Baseline and Scenario Comparison

The reference second-life allocation and reference-capacity combination, S1, is used as the baseline. The remaining eight scenarios combine the low, reference, and high second-life allocation trajectories with the reference, anticipatory, and delayed recycling-capacity configurations.

Comparisons within the same capacity pathway show how second-life allocation changes recycling demand, delayed returns, terminal second-life stock, backlog, and recovered-material availability. Comparisons across capacity pathways show how the timing of infrastructure expansion affects backlog, processing delay, throughput, utilization, and material recovery.

All nine scenarios use the same battery-inflow and retirement series, Collection Rate, Average Second-Life Duration, Material Recovery Efficiency, Minimum Processing Time, and initial conditions. This allows differences in the main comparison to be attributed to the two strategic variables.

3.5.3. Sensitivity Analysis

Sensitivity analysis is used to assess how uncertainty in the model parameters affects the main outputs and whether the behavior observed in the scenario analysis remains stable under changes in the main assumptions. It is kept separate from the strategic scenario comparison because the two analyses serve different purposes: scenario analysis evaluates alternative strategy configurations, while sensitivity analysis evaluates the influence of uncertain model parameters.

The analysis uses the baseline configuration (S1) as the common reference case. Collection Rate, Average Second-Life Duration, Material Recovery Efficiency, and Minimum Processing Time are varied one at a time while the remaining parameters, strategic variables, initial conditions, and external battery-flow inputs are kept unchanged. The resulting operational and material-circularity indicators are compared with the baseline results to identify which assumptions have the greatest influence on model behavior.

The Weibull scale parameter was evaluated separately because changing it requires recalculating the external vehicle-retirement and battery-flow series before running the System Dynamics model. Initial Batteries in First Life was also recalculated for each Weibull scale case. The Weibull shape parameter was maintained at its reference value of 3.5, which is commonly used in EV battery end-of-life studies [43–46]. Sensitivity testing focused on the scale parameter because it directly changes the characteristic timing

of battery retirement and was selected as the more relevant lifetime assumption for this analysis.

3.6. Impact Dimensions and Performance Indicators

The model evaluates two impact dimensions: operational performance and material circularity. These dimensions correspond directly to the research objective of improving material circularity while limiting recycling backlog and material-recovery delays. Their mathematical formulation and implementation in Vensim are presented in Section 4.6.

Operational performance refers to the ability of the system to process batteries entering the recycling pathway without generating persistent accumulation, excessive processing delay, or prolonged underutilization of available capacity. Material circularity refers to the extent and timing with which battery-derived material is recovered and becomes available as a secondary resource. It does not measure the actual reintegration of recovered material into new battery production.

Dimension	Indicator	Meaning	Unit
Operational	Recycling Backlog	Battery mass that has entered recycling but remains unprocessed	kt
Operational	Backlog Burden	Cumulative recycling backlog over time.	kt·year
Operational	Estimated Processing Delay	Approximate time required to process the current backlog at the current throughput	year
Operational	Recycling Throughput	Battery mass processed during the year	kt/year
Operational	Recycling Capacity Utilization	Share of available capacity used	%
Operational	Peak Recycling Demand	Maximum annual Total Recycling Pathway Inflow	kt/year
Operational	Demand-Capacity Gap	Difference between annual recycling-pathway inflow and available recycling capacity; positive values indicate that inflow exceeds capacity	kt/year
Material circularity	Annual Recovered Material Availability	Battery-derived material recovered during the year	kt/year
Material circularity	Cumulative Recovered Materials	Total material recovered since 2025	kt
Material circularity	Battery Recovery Yield	Cumulative recovered-material mass relative to cumulative battery mass entering the recycling pathway	%

Contextual	Terminal Second-Life Stock	Battery mass remaining in second-life applications in 2050	kt

Table 7: Performance Indicators

Battery Recovery Yield is included as an aggregated material-circularity indicator. Its formulation is adapted from recovery-yield indicators used in the battery-recycling literature [49]. Vaccari et al. (2024) evaluate recycling performance through indicators related to material recovery and yield. In the present model, however, individual materials and battery chemistries are not represented separately. Battery Recovery Yield is therefore calculated for the total recovered battery-derived material and does not distinguish between lithium, nickel, cobalt, or other individual materials.

At the system level, the indicator compares Cumulative Recovered Materials with Cumulative Recycling Pathway Inflow. It therefore reflects both the amount of battery mass processed within the simulation horizon and the assumed Material Recovery Efficiency. For this reason, Battery Recovery Yield is not interpreted as the technical efficiency of the recycling process. It is used together with Cumulative Recovered Materials to evaluate how much of the battery mass entering the recycling pathway has become available as recovered material by a given time.

The indicators are interpreted together and are not combined into a weighted score. A low backlog may be accompanied by low capacity utilization, while greater second-life allocation may reduce recycling pressure but delay material recovery beyond 2050. Battery Recovery Yield is also interpreted together with absolute recovered-material availability because a higher yield may result from a smaller amount of battery mass entering the recycling pathway. Scenario performance is therefore assessed by considering these trade-offs across multiple indicators, without assigning a single universal ranking.

3.7. Model Design Specifications

The engineering design developed in this thesis is a System Dynamics-based decision-support prototype implemented in Vensim. It represents the movement and accumulation of EV battery mass through automotive first life, collection, direct recycling, second-life

applications, post-second-life return, recycling backlog, capacity-constrained processing, and material recovery.

Its engineering contribution lies in translating the long-term coordination problem identified in the literature into a functional simulation environment. The model allows alternative second-life allocation and recycling-capacity trajectories to be tested before their potential implementation and makes their operational and material-circularity consequences observable over time.

Design statement

The proposed design is a System Dynamics decision-support model that evaluates how second-life allocation and the timing of recycling-capacity expansion affect recycling backlog, processing delay, capacity utilization, and recovered-material availability in the Italian EV battery system.

Design requirements

The model must preserve battery-mass balance, represent first and second life as explicit stocks, accumulate unprocessed battery mass in a recycling backlog, constrain throughput according to feedstock and capacity, allow the two strategic trajectories to be modified independently, and generate the indicators defined in Section 3.6.

Design constraints

The prototype is limited to an aggregated Italian system and relies on exogenous battery-inflow, retirement, allocation, and capacity trajectories. It does not provide facility-level, spatial, economic, chemistry-specific, or investment optimization. It is designed to support strategic scenario comparison and does not address the design of individual recycling facilities.

4. MODEL DEVELOPMENT

The System Dynamics model was implemented in Vensim using the system boundaries, parameters, and scenario variables defined in Chapter 3. The final structure links battery retirement, second-life allocation, recycling backlog, capacity-constrained processing, and material recovery over the 2025–2050 simulation horizon.

4.1. Model Architecture and Variable Selection

Model variables were selected according to the research question, system boundaries, and design requirements defined in Chapter 3. The final structure contains only the stocks, flows, parameters, strategic variables, and indicators required to represent battery lifecycle transitions, second-life delays, recycling-capacity constraints, backlog formation, and material recovery.

The model contains four connected modules:

1. First-life battery accumulation and retirement.
2. Collection and allocation between direct recycling and second life.
3. Capacity-constrained recycling and backlog management.
4. Material recovery and performance accounting.

The model distinguishes physical stocks from accounting stocks. Batteries in First Life, Batteries in Second Life, and Recycling Backlog represent battery mass located at a lifecycle stage. Cumulative Recycling Pathway Inflow, Cumulative Processed Batteries, Cumulative Recovered Materials, and Backlog Burden record cumulative performance without representing additional physical locations.

All lifecycle quantities are represented in terms of battery mass, with battery counts excluded from the model. Recovered Material Flow and Cumulative Recovered Materials represent the aggregated material mass obtained after recycling.

Module 1: First-Life Battery Accumulation and Retirement

Variable	Type	Unit	Function
Initial Batteries in First Life	Initial value	kt	Battery mass in automotive first-life use at the start of the simulation.
Battery Inflow into First Life	Flow	kt/year	Battery mass entering automotive use through new BEV and PHEV registrations.
Batteries in First Life	Physical Stock	kt	Battery mass currently in use in BEV and PHEV passenger cars
End-of-First-Life Flow	Flow	kt/year	Battery mass retiring from automotive first life

Table 8: Variables Included in Module 1: First-Life Battery Accumulation and Retirement

Module 2: Collection and Allocation Between Direct Recycling and Second Life

Variable	Type	Unit	Function
Collection Rate	Technical parameter	dmnl	Share of batteries leaving first life that enters the modeled collection system
Collected Batteries Flow	Flow	kt/year	Collected proportion of the End-of-First-Life Flow
Second-Life Allocation Rate	Strategic variable	dmnl	Share of collected batteries allocated to second-life applications
Second Life Inflow	Flow	kt/year	Collected battery mass allocated to second-life applications
Direct Recycling Inflow	Flow	kt/year	Collected battery mass sent directly to recycling
Initial Batteries in Second Life	Initial value	kt	Battery mass in second-life applications at the start of the simulation
Batteries in Second Life	Physical stock	kt	Battery mass retained in additional-use applications
Average Second-Life Duration	Technical parameter	year	Average period during which allocated batteries remain in second-life applications
Post-Second-Life Return	Flow	kt/year	Battery mass returning to recycling after completing second life

Table 9: Variables Included in Module 2: Collection and Second-Life Allocation

Module 3: Capacity-Constrained Recycling and Backlog Management

Variable	Type	Unit	Function
Total Recycling Pathway Inflow	Auxiliary variable	kt/year	Sum of direct recycling inflow and post-second-life returns
Initial Recycling Backlog	Initial value	kt	Unprocessed battery mass in the recycling pathway at the start of the simulation

Recycling Backlog	Physical stock	kt	Battery mass that has entered the recycling pathway but has not yet been processed
Recycling Capacity	Strategic variable	kt/year	Maximum battery mass that can be processed during each year
Minimum Processing Time	Technical parameter	year	Minimum time required to process available recycling feedstock
Recycling Throughput	Flow	kt/year	Battery mass processed according to available feedstock and recycling capacity
Recycling Capacity Utilization	Performance indicator	dmnl	Share of available recycling capacity used during each period
Estimated Processing Delay	Performance indicator	year	Approximate time required to process the existing recycling backlog

Table 10: Variables Included in Module 3: Recycling and Backlog Management

Module 4: Material Recovery and Performance Accounting

Variable	Type	Unit	Function
Material Recovery Efficiency	Technical parameter	dmnl	Share of processed battery mass converted into recovered-material availability
Recovered Material Flow	Flow	kt/year	Aggregated material mass recovered from recycling throughput
Initial Cumulative Recovered Materials	Initial value	kt	Recovered materials accounted for at the start of the simulation (set to zero)
Cumulative Recovered Materials	Accounting stock	kt	Total material recovered through recycling since the beginning of the simulation

Recycling Pathway Inflow Accumulation	Flow	kt/year	Records total battery mass entering the recycling pathway
Cumulative Recycling Pathway Inflow	Accounting stock	kt	Total battery mass entering recycling directly or after second life
Cumulative Processed Batteries	Accounting stock	kt	Total battery mass processed through recycling
Backlog Burden Accumulation	Flow	kt	Accumulates Recycling Backlog over time
Backlog Burden	Accounting stock	kt·year	Cumulative recycling backlog over time
Battery Recovery Yield	Performance indicator	dmnl	Cumulative recovered-material mass relative to cumulative recycling-pathway inflow

Table 11: Variables Included in Module 4: Material Recovery and Performance Accounting

End-of-First-Life Flow is calculated externally through the cohort-based Weibull procedure and imported as an annual time series. Second-Life Allocation Rate and Recycling Capacity can be modified independently across scenarios, while Collection Rate, Average Second-Life Duration, Minimum Processing Time, and Material Recovery Efficiency remain constant in the main scenario comparison.

4.2. Causal Loop Diagram (CLD)

Figure 1 presents the Causal Loop Diagram used to organize the main relationships represented in the quantitative model. Positive links indicate that the connected variables move in the same direction, all else being equal, while negative links indicate movement in opposite directions [41].

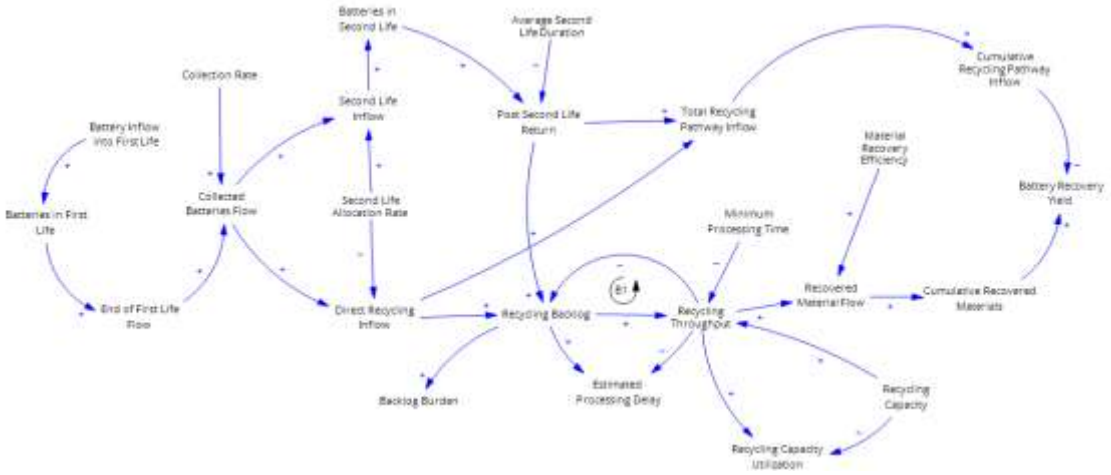


Figure 1: Causal Loop Diagram of the Italian EV battery system model. Source: Author's elaboration in Vensim

The first part of the diagram represents battery movement from automotive use to collection. Battery Inflow into First Life increases the first-life stock, while End-of-First-Life Flow makes battery mass available for collection and pathway allocation. Retirement timing is implemented quantitatively through the externally calculated Weibull series.

Collected Batteries Flow is divided between direct recycling and second life. A higher Second-Life Allocation Rate increases Second Life Inflow and reduces Direct Recycling Inflow. Batteries retained in second life later return through Post-Second-Life Return.

Direct Recycling Inflow and Post-Second-Life Return increase the battery mass reaching recycling. Recycling Throughput removes mass from the Recycling Backlog and is limited by available feedstock and Recycling Capacity. Throughput then determines recovered-material availability and the main recycling-performance indicators.

Battery Inflow into First Life, Second-Life Allocation Rate, and Recycling Capacity are specified externally. Market, price, investment, and policy responses are outside the model boundary. The main endogenous feedback is the Recycling Backlog Adjustment loop, B1, described in Section 4.3.

4.3. Feedback Loop Analysis

The model contains one principal endogenous feedback loop: B1 – Recycling Backlog Adjustment.

$$Recycling\ Backlog \rightarrow Recycling\ Throughput \rightarrow Recycling\ Backlog$$

When available capacity is not fully used, a larger Recycling Backlog provides more feedstock for processing and allows Recycling Throughput to increase. Higher throughput removes battery mass from the backlog, creating a balancing response [41]. The response is limited by Recycling Capacity and Minimum Processing Time.

$$Recycling\ throughput\ = min(Recycling\ capacity, \frac{Recycling\ Backlog}{Minimum\ Processing\ Time})$$

If throughput exceeds the new recycling inflow, previously accumulated backlog is reduced. If throughput remains below the inflow, backlog continues to grow. When capacity exceeds available feedstock, the system operates below full utilization.

Once Recycling Capacity is fully used, additional backlog cannot increase throughput further. Direct and post-second-life inflows may continue adding battery mass, causing backlog and processing delay to increase even while the system operates at maximum capacity.

Second-life allocation changes the timing of the inflows acting on B1 but does not form a separate closed feedback loop. Similarly, Recycling Capacity does not increase automatically in response to congestion; alternative expansion trajectories are introduced through the scenario analysis. The behavior of B1 therefore depends on whether processing capability becomes available before or after direct and post-second-life battery returns.

4.4. Stock and Flow Diagram (SFD)

Figure 2 presents the final stock-and-flow model developed in Vensim.

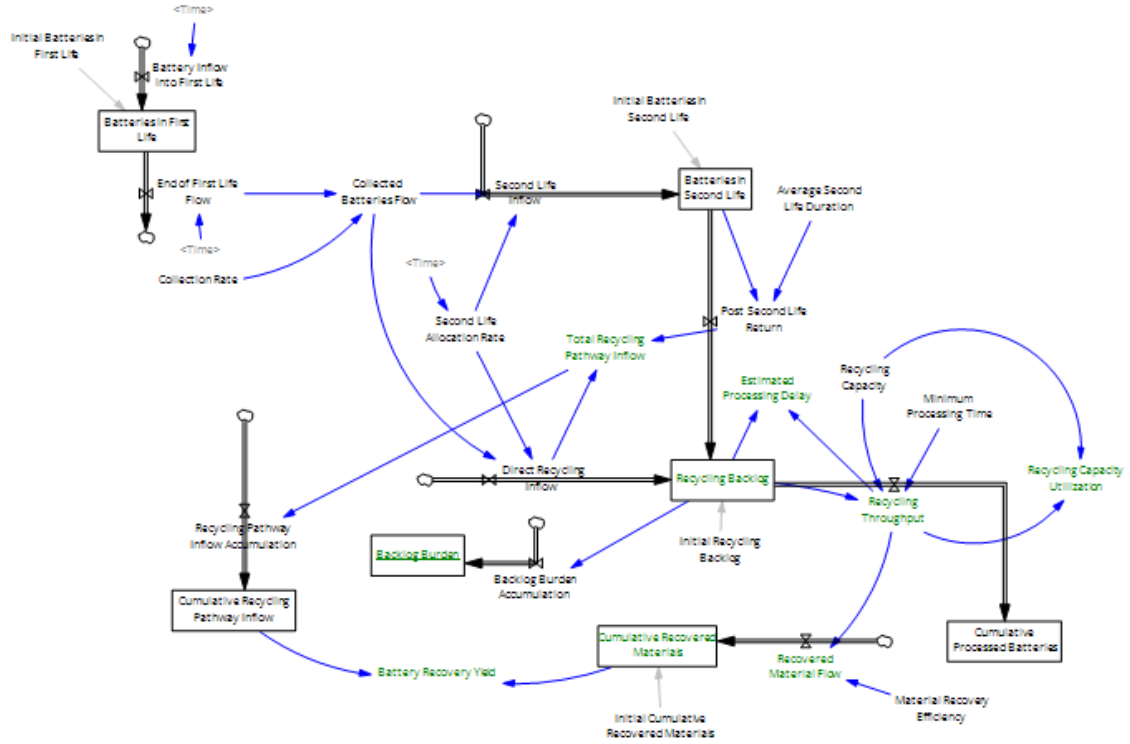


Figure 2: Stock and Flow Diagram of the Italian EV battery system model. Source: Author's elaboration in Vensim.

Note: Green variables represent performance indicators. Time-dependent external inputs and initial-value variables are also shown.

The physical lifecycle is represented through three stocks. Batteries in First Life receives Battery Inflow into First Life and is reduced by End-of-First-Life Flow. Collected batteries are divided between direct recycling and second life. Batteries in Second Life retains allocated battery mass before it returns through Post-Second-Life Return.

Direct Recycling Inflow and Post-Second-Life Return enter the Recycling Backlog. Recycling Throughput removes battery mass from this stock and is constrained by available feedstock, Recycling Capacity, and Minimum Processing Time.

Four accounting stocks record cumulative system behavior. Cumulative Recycling Pathway Inflow records all battery mass entering recycling, Cumulative Processed Batteries integrates Recycling Throughput directly, Cumulative Recovered Materials

records recovered-material output, and Backlog Burden accumulates recycling congestion over time.

The green indicators are calculated from these structures. Estimated Processing Delay compares backlog to current throughput, Recycling Capacity Utilization compares throughput with available capacity, and Battery Recovery Yield compares cumulative recovered material with cumulative battery mass entering the recycling pathway. Their equations are presented in Section 4.6.

4.5. Implemented Inputs and Parameter Values

This section summarizes the external vehicle projection, cohort calculation, battery-mass conversion, retirement series, and recycling-capacity trajectory implemented in the model. The corresponding data sources and calculation methods were introduced in Section 3.4.

4.5.1. Vehicle Registration and Fleet Projection

The implemented vehicle dataset contains direct historical BEV and PHEV M1 registrations from 2008 to 2025, a seasonal annualization for 2026, and a constructed external projection for 2027–2050. Table 12 summarizes the treatment assigned to each period and distinguishes observed data, source-based endpoints, and modeling assumptions.

Period	Implemented treatment	Principal source	Evidence classification
2008 – 2025	Direct annual BEV and PHEV M1 registrations.	EAFO [42]	Italian observed data
2026	Annualized separately from January–June observations using the 2025 first-half seasonal share.	EAFO [42]; author calculation	Derived estimate
2027 – 2030	Geometric fleet interpolation from the calculated 2026 fleet to 2.3 million BEVs and 1.2 million PHEVs in 2030;	Motus-E and Strategy& [36]	Italian projected endpoints + modeling assumption

	registrations derived through fleet balance.		
2031 – 2035	Geometric fleet interpolation to 7.7 million BEVs and 1.2 million PHEVs in 2035; PHEV fleet held at the identical 2030 and 2035 endpoint.	Motus-E and Strategy& [36]	Italian projected endpoints + modeling assumption
2036 - 2040	BEV registration growth based on the 2035–2040 ratio in the broader Motus-E sales trajectory; annual values linearly interpolated. PHEV registrations set to zero.	Motus-E et al. [33]; author calculation	Scaled proxy + reference-scenario assumption
2041 - 2045	BEV registration growth based on the 2040–2045 Motus-E ratio; annual values linearly interpolated.	Motus-E et al. [33]; author calculation	Scaled proxy + modeling assumption
2046 - 2050	BEV registrations held at the 2045 level; PHEV registrations remain zero; fleets evolve through annual retirements.	Motus-E stabilization pattern [33] Terna and Snam [47]	Modeling assumption

Table 12: Construction of the vehicle registration and fleet projection series. Source: Author's elaboration based on EAFO [42], Motus-E and Strategy& [36], and Motus-E et al. [33].

The 2026 annualization produced approximately 167,945 BEV registrations and 183,466 PHEV registrations. Together with the 2025 EAFO fleet values and calculated retirements, these flows produced end-of-2026 fleet estimates of approximately 534,768 BEVs and 561,274 PHEVs.

For 2027–2035, gross registrations were calculated by adding annual retirements to the change in fleet stock. This prevents net fleet growth from being interpreted directly as new registrations.

After 2035, only the relative growth reported in the broader Motus-E sales trajectory was transferred to the M1 passenger-car series [33]. This produced approximately 2.122 million BEV registrations in 2040 and 2.159 million in 2045. The resulting combined BEV and PHEV fleet reaches 16.69 million vehicles in 2040, within the 15–17 million range reported by Terna and Snam [47].

4.5.2. Cohort-Based Vehicle Retirement and Fleet Balance

The Weibull cohort procedure was first implemented manually for the 2026–2028 retirement years to verify cohort ages and annual retirement probabilities. The same results were then reproduced through the consolidated spreadsheet calculation used for the remaining years.

Only cohorts registered before the retirement year were included. Calculated retirements were combined with the fleet trajectory through the annual balance:

$$Fleet_{v,t} = Fleet_{v,t-1} + Registrations_{v,t} - Retirements_{v,t}$$

The calculation maintains a clear distinction among registrations as annual inflows, fleets as vehicle stocks, and retirements as annual outflows. This prevents double counting and preserves the vehicle-level balance used to construct future cohorts.

4.5.3. Battery-Mass Conversion

Annual BEV and PHEV registration cohorts were converted into battery mass using the parameters defined in Section 3.4.2. Reference capacities of 60 kWh for BEVs and 15 kWh for PHEVs were combined with the adopted pack-level specific energy of 165 Wh/kg.

Powertrain	Reference capacity	Pack-level specific energy	Derived pack mass	Basis
BEV	60 kWh/vehicle	165 Wh/kg	363.6 kg/vehicle	Capacity from Dei et al. [16]; specific energy as modeling assumption supported by [48]

PHEV	15 kWh/vehicle	165 Wh/kg	90.9 kg/vehicle	Capacity from Dei et al. [16]; specific energy as modeling assumption supported by [48]

Table 13: Battery-Mass Conversion Parameters Implemented in the Model

The resulting pack masses of 363.6 kg/BEV and 90.9 kg/PHEV were multiplied by annual registrations and converted from kilograms to kilotonnes. The two series were then aggregated to obtain Battery Inflow into First Life.

4.5.4. Mass-Based End-of-First-Life Flow

The Weibull retirement probabilities were applied separately to BEV and PHEV battery-mass cohorts. Only cohorts entering first life before the retirement year were included. The two resulting series were then summed and imported into Vensim as End-of-First-Life Flow.

Year	BEV battery retirement (kt/year)	PHEV battery retirement (kt/year)	End-of-First-Life Flow (kt/year)
2025	1.30	0.28	1.58
2030	10.36	2.54	12.90
2035	52.86	8.00	60.86
2040	200.21	10.96	211.17
2045	478.46	6.08	484.53
2050	708.27	1.28	709.55

Table 14: Selected Values of the Mass-Based End-of-First-Life Flow. Source: Author's calculations based on the registration trajectories and battery-mass assumptions described in Sections 4.5.1–4.5.3 and the Weibull parameters adopted from Dei et al. [16].

4.5.5. Reference Recycling-Capacity Trajectory

In the model, Recycling Capacity changes at predefined expansion years and remains constant between these points. Because a complete time series of observed Italian recycling capacity was not available, the reference configuration uses the projected treatment requirements reported by Motus-E, Strategy&, and Politecnico di Milano [33] as a proxy for effective processing capacity. The published values are 5 kt/year in 2025, 17 in 2030, 48 in 2035, 111 in 2040, 235 in 2045, and 367 in 2050.

Intermediate levels of 10 kt/year from 2026 to 2028 and 12 kt/year in 2029 were introduced as modeling assumptions to represent gradual early development. These values are not reported directly in [33].

Year	Reference capacity (kt/year)	Capacity addition (kt/year)	Basis
2025	5	5	Published reference point [33]
2026-2028	10	5	Modeling assumption
2029	12	2	Modeling assumption
2030	17	5	Published reference point [33]
2035	48	31	Published reference point [33]
2040	111	63	Published reference point [33]
2045	235	124	Published reference point [33]
2050	367	132	Published reference point [33]

Table 15: Reference Recycling-Capacity Trajectory Implemented in the Model

Capacity remains constant between expansion points. Anticipatory and delayed scenarios modify the timing of the main capacity additions, as defined in Section 3.5. The implemented reference equation is:

$$Recycling\ Capacity = 5 + STEP(5, 2026) + STEP(2, 2029) + STEP(5, 2030) + STEP(31, 2035) + STEP(63, 2040) + STEP(124, 2045) + STEP(132, 2050)$$

4.6. Model Equations

The model equations translate the Stock and Flow Diagram into a quantitative simulation structure. Physical and accounting stocks are calculated through integration, while auxiliary variables define allocation, processing, and performance relationships. Battery stocks are expressed in kt and annual flows in kt/year unless otherwise stated.

4.6.1. First-Life Battery Dynamics

The annual battery mass entering automotive first life was calculated externally from the projected BEV and PHEV registrations and their respective average battery-pack masses:

$$Battery\ \text{Inflow}\ into\ First\ Life = (\{BEV\ Registrations\}_t \times Average\ BEV\ Battey\ Mass + \{PHEV\ Registrations\}_t \times Average\ PHEV\ Battey\ Mass) / 10^6$$

The resulting annual trajectory was imported into Vensim as a time-dependent lookup:

$$Battery\ Inflow\ into\ First\ Life = Battery\ Inflow\ with\ Lookup\ (Time)$$

The first-life battery stock is calculated as:

$$Battery\ in\ First\ Life = INTEG\ (Battery\ Inflow\ into\ First\ Life - End\ of\ First\ Life\ Flow, Initial\ Batteries\ in\ First\ Life)$$

End-of-First-Life Flow was imported as a WITH LOOKUP (Time, …) series derived from the cohort calculation. The complete 2025–2050 series is reported in the external calculation workbook.

This approach preserves the mass balance of the aggregate first-life stock while representing retirement timing according to the age distribution of individual registration cohorts.

4.6.2. Collection and Second-Life Allocation

The quantity of retired batteries entering the modeled collection system is calculated as:

$$Collected\ Batteries\ Flow = End\ of\ First\ Life\ Flow \times Collection\ Rate$$

Collected batteries are divided between second-life applications and direct recycling. The Second-Life Allocation Rate is introduced as a scenario-dependent lookup function:

$$Second\ Life\ Allocation\ Rate = Scenario\ Allocation\ with\ Lookup\ (Time)$$

The battery mass entering second life is:

$$Second\ Life\ Inflow = Collected\ Batteries\ Flow \times Second\ Life\ Allocation\ Rate$$

The complementary fraction enters the recycling pathway directly:

$$Direct\ Recycling\ Inflow = Collected\ Batteries\ Flow \times (1 - Second\ Life\ Allocation\ Rate)$$

These equations ensure that the complete collected flow is allocated between the two pathways:

$$Collected\ Batteries\ Flow = Second\ Life\ Inflow + Direct\ Recycling\ Inflow$$

The second-life battery stock is represented as:

$$Batteries\ in\ Second\ Life = INTEG\ (Second\ Life\ Inflow - Post\ Second\ Life\ Return, Initial\ Batteries\ in\ Second\ Life)$$

The return flow is calculated using a first-order delay structure:

$$Post\ Second\ Life\ Return = \frac{Batteries\ in\ Second\ Life}{Average\ Second\ Life\ Duration}$$

4.6.3. Recycling Backlog and Processing

The total annual flow entering the recycling pathway combines direct recycling and batteries returning from second life:

$$Total\ Recycling\ Pathway\ Inflow = Direct\ Recycling\ Inflow\ +\ Post\ Second\ Life\ Return$$

Recycling Capacity is introduced as an externally defined, scenario-dependent trajectory:

$$Recycling\ Capacity =\ Scenario\ Capacity\ Function\ (Time)$$

A STEP function is used to introduce each capacity addition at the specified year. Capacity remains unchanged between expansion points. Anticipatory and delayed scenarios use the same structure with the main additions shifted according to the timing defined in Section 3.5. The exact allocation and capacity trajectories used in each scenario are presented in Chapter 5.

The recycling backlog accumulates battery mass entering the recycling pathway and removes the battery mass processed through Recycling Throughput.

$$Recycling\ Backlog = INTEG(Direct\ Recycling\ Inflow\ +\ Post\ Second\ Life\ Return - Recycling\ Throughput, Initial\ Recycling\ Backlog)$$

Recycling Throughput is constrained by both the installed capacity and the amount of feedstock available for processing:

$$Recycling\ Throughput = MIN(Recycling\ capacity, \frac{Recycling\ Backlog}{Minimum\ Processing\ Time})$$

The equation prevents throughput from exceeding installed capacity or processing more battery mass than is available in the backlog.

The annual recovered-material flow is calculated as:

$$Recovered\ Material\ Flow =\ Recycling\ Throughput \times\ Material\ Recovery\ Efficiency$$

Recovered Material Flow represents the total recovered battery-derived mass and does not distinguish between individual metals.

4.6.4. Accounting Stocks

Four accounting stocks record cumulative system behavior without representing additional physical locations.

Cumulative Recycling Pathway Inflow is calculated as:

$$Recycling\ Pathway\ Inflow\ Accumulation\ =\ Total\ Recycling\ Pathway\ Inflow$$

$$Cumulative\ Recycling\ Pathway\ Inflow = INTEG(Recycling\ Pathway\ Inflow\ Accumulation, Initial\ Cumulative\ Recycling\ Pathway\ Inflow)$$

Cumulative Processed Batteries directly integrates Recycling Throughput:

$$Cumulative\ Processed\ Batteries = INTEG(Recycling\ Throughput, Initial\ Cumulative\ Processed\ Batteries)$$

Cumulative Recovered Materials is calculated as:

$$Cumulative\ Recovered\ Materials = INTEG(Recovered\ Material\ Flow, Initial\ Cumulative\ Recovered\ Materials)$$

Backlog Burden accumulates Recycling Backlog over time:

$$Backlog\ Burden\ Accumulation\ =\ Recycling\ Backlog$$

$$Backlog\ Burden = INTEG(Backlog\ Burden\ Accumulation, Initial\ Backlog\ Burden)$$

Backlog Burden is expressed in kt·year because a backlog measured in kt is integrated over time. It captures both the amount of battery mass awaiting treatment and the duration of its accumulation.

4.6.5. Performance Indicators

Estimated Processing Delay is calculated by dividing Recycling Backlog by the current Recycling Throughput:

$$Estimated\ Processing\ Delay\ =\ IF\ THEN\ ELSE(Recycling\ Throughput > 0, \frac{Recycling\ Backlog}{Recycling\ Throughput}, 0)$$

The zero condition prevents division by zero. When throughput is positive, the indicator approximates the time required to process the existing backlog at the current processing rate.

Recycling Capacity Utilization is calculated as:

$$Recycling\ Capacity\ Utilization\ =\ IF\ THEN\ ELSE(Recycling\ Capacity > 0, \frac{Recycling\ Throughput}{Recycling\ Capacity}, 0)$$

A value of one represents full utilization. Values below one indicate available processing capacity that is not currently being used.

Demand-Capacity Gap is calculated as the difference between Total Recycling Pathway Inflow and Recycling Capacity:

$$Demand - Capacity\ Gap = Total\ Recycling\ Pathway\ Inflow\ -\ Recycling\ Capacity$$

Positive values indicate that annual recycling inflow exceeds available processing capacity, while negative values indicate that available capacity is greater than the annual inflow. The indicator is mainly reported for 2050 to assess whether the recycling system is still facing a capacity shortfall at the end of the simulation horizon. A negative gap does not necessarily imply that previously accumulated backlog has been cleared.

Battery Recovery Yield is calculated as:

$$Share\ of\ Recycling\ Pathway\ Batteries\ Successfully\ Processed = IF\ THEN\ ELSE(Cumulative\ Recycling\ Pathway\ Inflow > 0, \frac{Cumulative\ Recovered\ Materials}{Cumulative\ Recycling\ Pathway\ Inflow}, 0)$$

As described in Section 3.6, the indicator adapts the literature-based recovery-yield concept [49] to the aggregated system boundary used in this model. It is calculated for total recovered battery-derived material and does not distinguish between individual materials.

Battery Recovery Yield is different from Material Recovery Efficiency. Material Recovery Efficiency is a fixed technical parameter applied to processed battery mass,

while Battery Recovery Yield is a system-level result that also reflects whether battery mass entering the recycling pathway is processed within the simulation horizon.

Peak Recycling Demand is obtained as the maximum Total Recycling Pathway Inflow. Terminal, cumulative, peak, and average indicators reported in Chapter 5 were extracted from the Vensim simulation outputs in Excel.

4.6.6. Simulation Settings and Dimensional Consistency

The model was simulated using the following settings:

Simulation Setting	Value
Initial Time	2025
Final Time	2050
Time Step	0.25 years
SAVEPER	1 year
Integration method	Euler

Table 16: Simulation Settings

The model was simulated from 2025 to 2050 using Euler integration with a time step of 0.25 years. Results were saved annually using SAVEPER = 1 year. The principal dimensional relationships are:

$$kt = \frac{kt}{year} \times year$$

$$year = \frac{kt}{kt/year} \times year$$

$$dmnl = \frac{kt/year}{kt/year}$$

$$kt/year = kt/year \times dmnl$$

$$dmnl = \frac{kt}{kt}$$

$$kt \times year = kt \times year$$

These relationships correspond to stock integration, Estimated Processing Delay, Recycling Capacity Utilization, Recovered Material Flow, Battery Recovery Yield, and Backlog Burden, respectively.

4.7. Model Verification, Validation, and Testing

4.7.1. Mass-Balance and Non-Negativity Checks

Mass balance was checked across the nine simulated scenarios. Collected Batteries Flow was fully divided between Second Life Inflow and Direct Recycling Inflow. With Initial Recycling Backlog equal to zero, Cumulative Recycling Pathway Inflow remained equal to Cumulative Processed Batteries plus Recycling Backlog. Cumulative Recovered Materials also remained equal to Cumulative Processed Batteries multiplied by the constant Material Recovery Efficiency.

Physical stocks and flows were also checked for non-negativity. No negative values were observed for Batteries in First Life, Batteries in Second Life, Recycling Backlog, or their associated flows across the nine scenarios. Recycling Throughput is constrained by the available feedstock and Recycling Capacity, preventing the model from processing more battery mass than is available.

4.7.2. Dimensional Consistency

The model was reviewed using Vensim's Check Model and Units Check functions. The stock-and-flow equations are dimensionally consistent.

Vensim reports warnings for the time-dependent lookup functions used for Battery Inflow into First Life, End-of-First-Life Flow, and Second-Life Allocation Rate. These warnings occur because Time, measured in years, is used as the lookup argument while the lookup outputs retain their assigned units. The warnings are specific to the lookup functions and do not indicate dimensional inconsistencies in the resulting stock-and-flow equations.

The warnings were documented as part of the model implementation, and no dummy variable was introduced just to suppress the Units Check warning.

4.7.3. External Plausibility Comparison

The reconstructed End-of-First-Life Flow was compared with the Italian estimates reported by Dei et al. [16]. The model produces 12.90 kt/year in 2030, below their estimate of 27.4 kt/year, and 709.55 kt/year in 2050, above their reported vehicle-related range of 435–606 kt/year.

These differences are consistent with differences in registration trajectories, cohort coverage, battery-mass assumptions, and system boundaries. The projected combined BEV and PHEV fleet reaches 16.69 million vehicles in 2040, within the 15–17 million range reported by Terna and Snam [47]. Because some lifetime assumptions are shared with [16], the comparison provides supporting evidence of plausibility but cannot be considered independent empirical validation.

4.7.4. Extreme-Condition Testing

Extreme-condition tests were performed to assess whether the model preserves logically and physically consistent behavior when selected inputs are assigned values outside their reference operating conditions. Each test was based on the baseline configuration (S1), with only one input changed at a time while all other parameters and exogenous trajectories were kept unchanged. This approach allows the structural response associated with each tested mechanism to be evaluated separately.

The following six extreme-condition tests were conducted to verify the model behavior under limiting values of the main variables controlling collection, pathway allocation, recycling capacity, and material recovery:

E1: Collection Rate = 0

E2: Second-Life Allocation Rate = 0

E3: Second-Life Allocation Rate = 1

E4: Recycling Capacity = 0

E5: Recycling Capacity = 10,000 kt/year (effectively non-binding capacity)

E6: Material Recovery Efficiency = 0

The tested variables were selected because they control distinct stages of the modeled battery pathway:

- Collection Rate determines whether retired batteries enter the modeled circular system.
- Second-Life Allocation Rate determines their routing between second life and direct recycling.
- Recycling Capacity constrains the processing of batteries entering the recycling pathway.

- Material Recovery Efficiency determines the amount of recovered material generated from processed battery mass.

The purpose of these tests is not to represent realistic future scenarios, but to verify that the model produces the expected directional and boundary behavior under extreme assumptions.

Test	Extreme condition	Structural mechanism tested	Expected behavior	Observed behavior	Result
E1	Collection Rate = 0	Entry of retired batteries into the modeled circular system	No battery mass enters second life or recycling; downstream circular-system flows, stocks, and material-recovery outputs remain zero	All downstream circular-system flows, stocks, and recovery outputs remained at zero throughout 2025–2050	**PASS**
E2	Second-Life Allocation Rate = 0	Routing between second life and direct recycling	No mass enters second life and all collected batteries are directed to recycling	Second-life stock and flows remained zero; Direct Recycling Inflow and Total Recycling Pathway Inflow exactly matched Collected Batteries Flow.	**PASS**
E3	Second-Life Allocation Rate = 1	Routing through second life	All collected battery mass enters second life; direct recycling remains zero; recycling inflow occurs only through post-second-life returns.	Second Life Inflow matched Collected Batteries Flow, Direct Recycling Inflow remained zero, and Total Recycling Pathway Inflow matched Post-Second-Life Return	**PASS**
E4	Recycling Capacity = 0	Capacity constraint on recycling processing	Throughput and recovered-material generation remain zero; all recycling inflow	Throughput and recovered materials remained zero; Recycling Backlog exactly matched	**PASS**

			accumulates in backlog.	Cumulative Recycling Pathway Inflow.	
E5	Recycling Capacity = 10,000 kt/year	Throughput behavior when recycling capacity is non-binding	Throughput is limited by available feedstock and Minimum Processing Time, with capacity remaining non-binding; utilization stays low and no capacity-induced backlog develops.	Throughput remained below available capacity, average utilization fell to 1.41%, terminal backlog decreased to 452.77 kt, and processing delay remained at the 1-year minimum once recycling began	**PASS**
E6	Material Recovery Efficiency = 0	Relationship between battery processing and material recovery	Recycling operations remain unchanged, while recovered-material generation and Battery Recovery Yield remain zero	Recycling dynamics remained identical to S1; 2,060.93 kt were processed by 2050, while Recovered Material Flow, Cumulative Recovered Materials, and Battery Recovery Yield remained zero	**PASS**

Table 17: Summary of Extreme-Condition Tests and Results.

E1: Zero Collection Rate

The Collection Rate was reduced from its baseline value of 0.95 to zero. As expected, Collected Batteries Flow and all downstream second-life, recycling, backlog, throughput, and recovered-material variables remained at zero throughout the simulation. Estimated Processing Delay, Recycling Capacity Utilization, and Battery Recovery Yield also remained at zero, confirming that the IF THEN ELSE conditions used in their definitions (Section 4.6.5) correctly return zero when the corresponding denominators are zero. Battery Inflow into First Life, End-of-First-Life Flow, and Recycling Capacity remained unchanged from the baseline. The test therefore confirmed that battery mass enters the

modeled circular pathway only through the collection mechanism and that the downstream equations behave consistently when collection is zero.

E2: Zero Second-Life Allocation

The Second-Life Allocation Rate was set to zero throughout the simulation. As expected, Second Life Inflow, Batteries in Second Life, and Post-Second-Life Return remained at zero. Direct Recycling Inflow and Total Recycling Pathway Inflow were equal to Collected Batteries Flow throughout the simulation, confirming that the allocation equations (Section 4.6.2) correctly route the complete collected flow to direct recycling when the Second-Life Allocation Rate is zero. Battery Inflow into First Life, End-of-First-Life Flow, Collection Rate, and Recycling Capacity remained unchanged from the baseline.

E3: Full Second-Life Allocation

The Second-Life Allocation Rate was set to one throughout the simulation. As expected, Second Life Inflow was equal to Collected Batteries Flow, while Direct Recycling Inflow remained at zero. Batteries accumulated in the second-life stock and gradually returned through Post-Second-Life Return. Total Recycling Pathway Inflow was therefore equal to Post-Second-Life Return throughout the simulation, confirming that the allocation equations (Section 4.6.2) correctly route the complete collected flow through second life when the Second-Life Allocation Rate is one. Battery Inflow into First Life, End-of-First-Life Flow, Collection Rate, and Recycling Capacity remained unchanged from the baseline.

E4: Zero Recycling Capacity

The Recycling Capacity was set to zero throughout the simulation. As expected, Recycling Throughput, Cumulative Processed Batteries, Recovered Material Flow, and Cumulative Recovered Materials remained at zero. All battery mass entering the recycling pathway therefore accumulated in the Recycling Backlog, which remained equal to Cumulative Recycling Pathway Inflow throughout the simulation and reached 3,823.97 kt by 2050. Estimated Processing Delay and Recycling Capacity Utilization also remained at zero, confirming that their respective IF THEN ELSE conditions (Recycling Throughput > 0 and Recycling Capacity > 0) correctly return zero instead of producing an undefined value when their denominators are zero. In this boundary case, these zero

values do not represent meaningful values of zero delay or zero utilization; the indicators cannot be calculated because no recycling throughput or capacity is available. Battery Recovery Yield also remained at zero. Once Cumulative Recycling Pathway Inflow became positive, the ratio was simply zero because Cumulative Recovered Materials remained at zero. The remaining upstream and allocation variables remained unchanged from the baseline.

E5: Very High Recycling Capacity

Recycling Capacity was set to 10,000 kt/year throughout the simulation to represent a condition in which processing capacity does not constrain the system. Recycling Throughput remained well below the available capacity, and average Recycling Capacity Utilization decreased to 1.41%. Estimated Processing Delay remained at exactly 1 year once recycling began, confirming that Recycling Throughput reduces to Recycling Backlog divided by Minimum Processing Time (Section 4.6.3) when Recycling Capacity is not binding. Terminal Recycling Backlog decreased from 1,763.04 kt in the baseline to 452.77 kt, with the remaining backlog resulting from the Minimum Processing Time of 1 year and not from insufficient recycling capacity. Cumulative Recovered Materials increased to 2,022.72 kt by 2050, while the upstream and allocation variables remained unchanged from the baseline. The test therefore confirmed that, when capacity is effectively unconstrained, Recycling Throughput is determined by available feedstock and Minimum Processing Time.

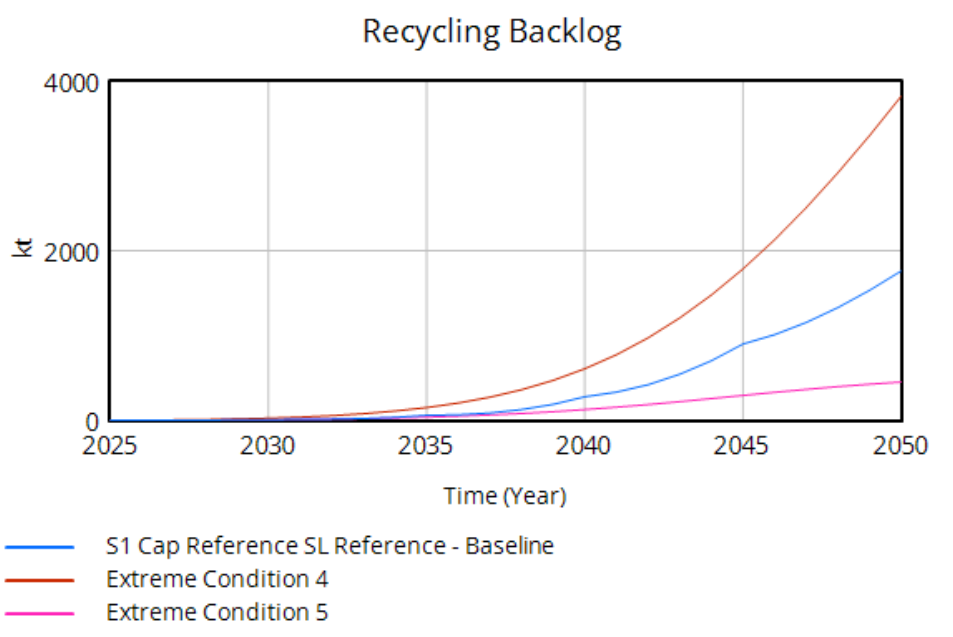


Figure 3: Recycling Backlog under the baseline and extreme recycling-capacity conditions. Source: Author's elaboration based on Vensim simulation results.

Figure 3 compares Recycling Backlog under the baseline with the two extreme recycling-capacity tests. With zero Recycling Capacity (E4), all battery mass entering the recycling pathway accumulates in the backlog, which reaches 3,823.97 kt by 2050. Under near-unconstrained capacity (E5), terminal backlog decreases to 452.77 kt. The remaining backlog is explained by the implemented Minimum Processing Time and is not caused by insufficient processing capacity. The baseline remains between these two boundary conditions, with a terminal backlog of 1,763.04 kt.

E6: Zero Material Recovery Efficiency

Material Recovery Efficiency was set to zero throughout the simulation. As expected, Recovered Material Flow, Cumulative Recovered Materials, and Battery Recovery Yield remained at zero, consistent with the recovery relationships defined in Sections 4.6.3–4.6.5. Recycling Throughput and Cumulative Processed Batteries remained unchanged from the baseline, with 2,060.93 kt of battery mass still processed by 2050 despite no recovered material being generated. Recycling Backlog, Estimated Processing Delay, Recycling Capacity Utilization, and all upstream and allocation variables also remained unchanged. The test therefore confirmed that Material Recovery Efficiency affects recovered-material generation without altering battery processing or the physical dynamics of the recycling pathway.

4.7.5. Integration-Error Testing

Integration-error testing was performed by progressively reducing the simulation time step while maintaining the baseline configuration (S1), Euler integration method, and all model parameters unchanged. The reference time step of 0.25 years was compared with simulations using 0.125 and 0.0625 years. As the time step was reduced, the differences between successive simulations also decreased. For example, terminal Recycling Backlog changed by 1.94% between 0.25 and 0.125 years and by only 0.95% between 0.125 and 0.0625 years. Peak Estimated Processing Delay changed by 2.10% and 1.03%, respectively, while Cumulative Recovered Materials changed by less than 0.1% in both comparisons. Backlog Burden showed the largest variation, but the difference decreased from 3.71% in the first comparison to 1.81% in the second. All other evaluated indicators showed the same convergence pattern, and the main behavioral results and timing of the baseline simulation remained unchanged. This pattern of progressively halving the time step is consistent with the expected first-order convergence behavior of the Euler integration method. The test therefore indicates that the model results converge as the time step is reduced and that the reference time step of 0.25 years is sufficiently small for the scenario analysis.

KPI	Time STEP: 0.25	Time STEP: 0.125	Time STEP: 0.0625	Change 0.25→0.125	Change 0.125→0.0625
Peak processing delay (year)	6.534	6.671	6.740	+2.10%	**+1.03%**
Peak recycling backlog (kt)	1,763.04	1,797.23	1,814.34	+1.94%	**+0.95%**
Avg. capacity utilization	82.500%	82.546%	82.568%	+0.06%	**+0.03%**
Cumulative recovered materials (kt)	1,236.56	1,237.30	1,237.68	+0.06%	**+0.03%**
Battery Recovery Yield	32.337%	32.059%	31.923%	−0.86%	**−0.43%**

Backlog burden (kt·year)	9,483.89	9,835.52	10,013.50	+3.71%	**+1.81%**

Table 18: Integration-Error Test Results for Selected Performance Indicators

4.7.6. Sensitivity Analysis

Sensitivity testing was performed using the baseline configuration (S1), changing one parameter at a time. For the parameters implemented directly in the System Dynamics model, the remaining assumptions and external inputs were kept unchanged. The Weibull scale parameter was assessed separately by recalculating the corresponding retirement and battery-flow inputs.

Collection Rate

Collection Rate was tested under three values: 0.90 for the low case, 0.95 for the baseline, and 1.00 for the high case. The baseline follows the literature-based assumption adopted in [43], while the lower and upper values were used as analytical variations around the reference assumption.

The results show that Collection Rate mainly affects recycling congestion. When the rate was reduced to 0.90, peak Recycling Backlog decreased from 1,763.04 kt to 1,564.33 kt, peak Estimated Processing Delay decreased from 6.53 to 5.79 years, and Backlog Burden decreased from 9,483.89 to 8,429.95 kt·year. When Collection Rate was increased to 1.00, the same indicators increased to 1,961.98 kt, 7.28 years, and 10,541.60 kt·year, respectively.

Cumulative Recovered Materials changed very little across the three runs, reaching 1,235.03 kt with a Collection Rate of 0.90, 1,236.56 kt in the baseline, and 1,237.95 kt with a Collection Rate of 1.00. This indicates that collecting more battery mass does not produce a similar increase in recovered materials when recycling capacity is already constrained. Most of the additional mass instead remains in the Recycling Backlog.

Battery Recovery Yield decreased from 34.09% under the lower Collection Rate to 30.75% under full collection, compared with 32.34% in the baseline. This does not indicate lower technical recycling efficiency. The change occurs because more battery

mass enters the recycling pathway while recovered-material output remains almost unchanged.

Peak Recycling Demand and terminal second-life stock both changed by ±5.26%. The demand-capacity gap showed a stronger response, ranging from 83.67 to 133.74 kt/year across the tested values.

KPI	Low 0.90	Baseline 0.95	High 1.00	Low vs Baseline	High vs Baseline
Peak recycling demand (kt/year)	450.67	475.70	500.74	**−5.26%**	**+5.26%**
Peak recycling backlog (kt)	1,564.33	1,763.04	1,961.98	**−11.27%**	**+11.28%**
Peak processing delay (year)	5.792	6.534	7.277	**−11.36%**	**+11.37%**
Avg. capacity utilization	81.80%	82.50%	83.20%	−0.70 pp	+0.70 pp
Cumulative recovered materials (kt)	1,235.03	1,236.56	1,237.95	**−0.12%**	**+0.11%**
Battery Recovery Yield	34.09%	32.34%	30.75%	+1.75 pp	−1.58 pp
Terminal second-life stock (kt)	1,313.69	1,386.67	1,459.65	**−5.26%**	**+5.26%**
Backlog burden (kt·year)	8,429.95	9,483.89	10,541.60	**−11.11%**	**+11.15%**
Demand-capacity gap in 2050 (kt/year)	83.67	108.70	133.74	**−23.03%**	**+23.03%**

Table 19: Sensitivity Analysis Results for Collection Rate. Source: Author's elaboration based on Vensim simulation results.

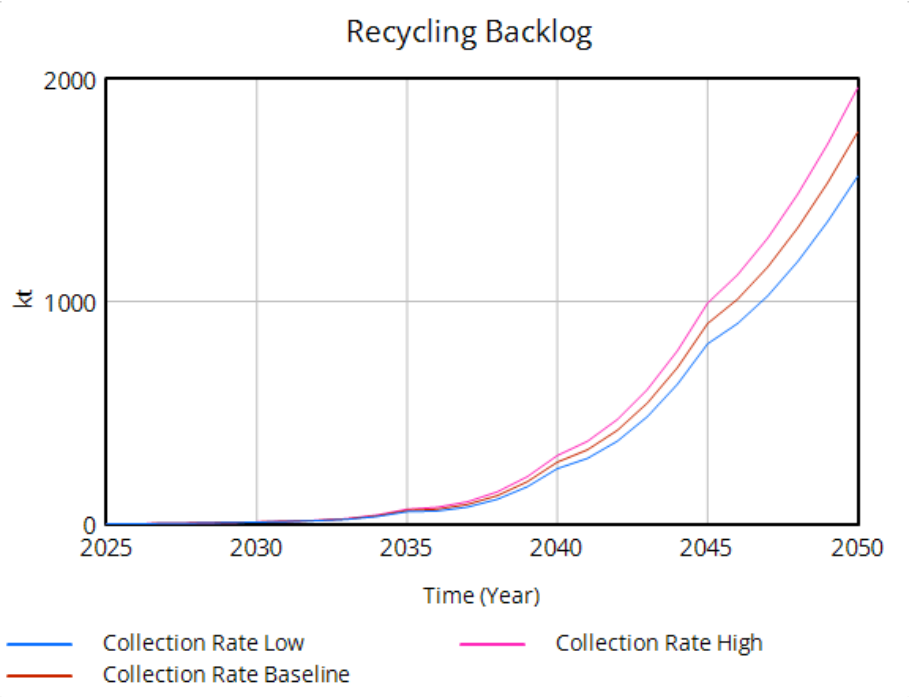


Figure 4: Recycling Backlog under Collection Rate Sensitivity. Source: Author's elaboration based on Vensim simulation results.

Figure 4 shows that the differences among the three Collection Rate assumptions become larger toward the end of the simulation, when the recycling system is already capacity-constrained. A higher Collection Rate therefore increases the amount of battery mass accumulating in the Recycling Backlog.

Average Second-Life Duration

Average Second-Life Duration was tested under three values: 5 years for the low case, 10 years for the baseline, and 12 years for the high case. The baseline follows the Italian assumptions adopted in [16] and [33], while the lower and upper values represent alternative durations within the range considered in the reviewed literature [43,45].

Reducing the duration to 5 years increased peak Recycling Backlog from 1,763.04 to 2,121.45 kt and peak Estimated Processing Delay from 6.53 to 7.79 years. Backlog Burden also increased to 10,904.20 kt·year, and peak Recycling Demand reached 542.65 kt/year. With a 12-year duration, peak backlog decreased to 1,681.71 kt and peak delay to 6.25 years.

A shorter duration causes more battery mass to return to recycling within the simulation horizon, while a longer duration keeps more mass in second-life applications. This effect

is visible in the terminal second-life stock, which falls to 1,028.09 kt in the 5-year case and rises to 1,468.04 kt in the 12-year case.

Cumulative Recovered Materials remained almost unchanged across the three runs, ranging from 1,236.54 to 1,236.66 kt. Under the baseline capacity trajectory, the additional mass returning earlier did not lead to greater material recovery by 2050. Battery Recovery Yield varied from 29.57% in the 5-year case to 33.04% in the 12-year case, mainly because the amount of battery mass entering the recycling pathway changed while recovered-material output remained nearly constant.

KPI	Low 5 years	Baseline 10 years	High 12 years	Low vs Baseline	High vs Baseline
Peak recycling demand (kt/year)	542.65	475.70	459.37	**+14.07%**	**−3.43%**
Peak recycling backlog (kt)	2,121.45	1,763.04	1,681.71	**+20.33%**	**−4.61%**
Peak processing delay (year)	7.79	6.53	6.25	**+19.25%**	**−4.31%**
Avg. capacity utilization	82.56%	82.50%	82.49%	**+0.06 pp**	**−0.01 pp**
Cumulative recovered materials (kt)	1,236.66	1,236.56	1,236.54	**+0.01%**	**≈0.00%**
Battery Recovery Yield	29.57%	32.34%	33.04%	**−2.77 pp**	**+0.70 pp**
Terminal second-life stock (kt)	1,028.09	1,386.67	1,468.04	**−25.86%**	**+5.87%**
Backlog burden (kt·year)	10,904.20	9,483.89	9,174.41	**+14.98%**	**−3.26%**
Demand-capacity gap in 2050 (kt/year)	175.65	108.70	92.37	**+61.59%**	**−15.02%**

Table 20: Sensitivity Analysis Results for Average Second-Life Duration. Source: Author's elaboration based on Vensim simulation results.

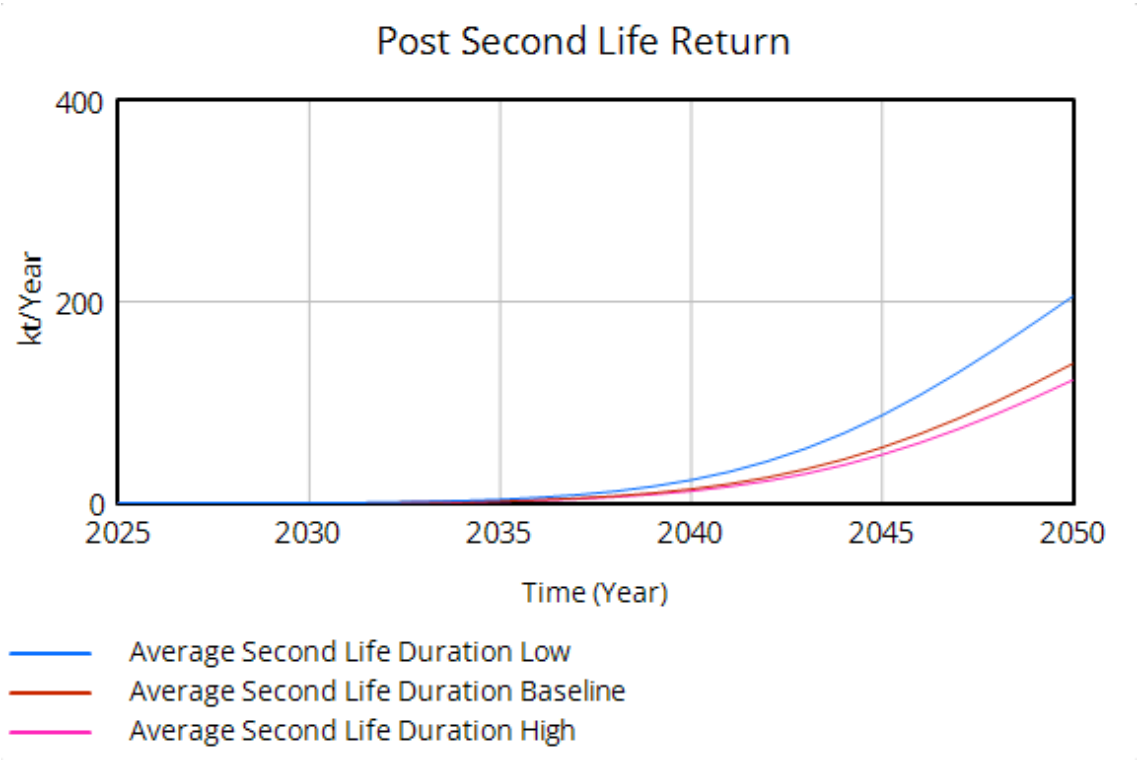


Figure 5: Post-Second-Life Return under Average Second-Life Duration Sensitivity. Source: Author's elaboration based on Vensim simulation results.

Figure 5 shows how Average Second-Life Duration changes the timing of battery returns to the recycling pathway. The 5-year case produces the highest Post-Second-Life Return toward the end of the simulation because batteries leave second life more quickly, while the 12-year case delays these returns and produces the lowest flow. The differences become more visible in the later years as the second-life stock grows.

Material Recovery Efficiency

Material Recovery Efficiency was tested under three values: 0.50 for the low case, 0.60 for the baseline, and 0.70 for the high case. The baseline follows the approximately 60% recovery of input materials reported for a typical hydrometallurgical recycling process in [33]. The lower value represents a conservative recovery case and is consistent with the 50% weight-based recycling-efficiency benchmark applied to other waste batteries under the previous European framework, which included lithium-ion batteries. The upper value reflects the 70% recycling-efficiency target established for lithium-based batteries by Regulation (EU) 2023/1542 for 2030 [24]. These regulatory values are used as reference bounds for the sensitivity analysis and are not treated as direct equivalents of the aggregated Material Recovery Efficiency implemented in the model.

Changing Material Recovery Efficiency affected only the recovered-material indicators. Cumulative Recovered Materials decreased from 1,236.56 kt in the baseline to 1,030.46 kt under the 0.50 case and increased to 1,442.65 kt under the 0.70 case. Battery Recovery Yield changed accordingly, from 26.95% in the low case to 37.73% in the high case, compared with 32.34% in the baseline.

The remaining operational indicators were unchanged across the three runs. Peak Recycling Backlog remained at 1,763.04 kt, peak Estimated Processing Delay at 6.53 years, and average Recycling Capacity Utilization at 82.50%. This is consistent with the model structure, since Material Recovery Efficiency is applied after battery processing and does not affect recycling inflow, throughput, or backlog dynamics.

KPI	Low 0.50	Baseline 0.60	High 0.70	Low vs Baseline	High vs Baseline
Peak recycling demand (kt/year)	475.70	475.70	475.70	No change	No change
Peak recycling backlog (kt)	1,763.04	1,763.04	1,763.04	No change	No change
Peak processing delay (year)	6.53	6.53	6.53	No change	No change
Avg. capacity utilization	82.50%	82.50%	82.50%	No change	No change
Cumulative recovered materials (kt)	**1,030.46**	**1,236.56**	**1,442.65**	**−16.67%**	**+16.67%**
Battery Recovery Yield	**26.95%**	**32.34%**	**37.73%**	**−5.39 pp**	**+5.39 pp**
Terminal second-life stock (kt)	1,386.67	1,386.67	1,386.67	No change	No change
Backlog burden (kt·year)	9,483.89	9,483.89	9,483.89	No change	No change
Demand-capacity gap in 2050 (kt/year)	108.70	108.70	108.70	No change	No change

Table 21: Sensitivity Analysis Results for Material Recovery Efficiency. Source: Author's elaboration based on Vensim simulation results.

Minimum Processing Time

Minimum Processing Time was tested under three values: 0.5 years for the low case, 1 year for the baseline, and 1.5 years for the high case. The baseline is a modeling assumption used to determine how quickly the available Recycling Backlog can be processed when sufficient recycling capacity is available. Since no directly compatible

empirical value was identified for this aggregated relationship, the lower and upper values were defined as ±50% analytical variations around the baseline assumption.

The effect on the main congestion indicators was limited. Reducing Minimum Processing Time to 0.5 years decreased peak Recycling Backlog from 1,763.04 to 1,755.93 kt and Backlog Burden from 9,483.89 to 9,339.25 kt·year. Increasing it to 1.5 years raised these values to 1,771.29 kt and 9,637.45 kt·year. Peak Estimated Processing Delay also changed only slightly, ranging from 6.50 to 6.57 years across the tested cases.

Average Recycling Capacity Utilization showed a more visible response, increasing to 84.54% in the 0.5-year case and decreasing to 80.47% in the 1.5-year case. A shorter processing time allows available feedstock to be processed more quickly during periods in which recycling capacity is not fully used.

Cumulative Recovered Materials changed by less than 0.5%, while peak Recycling Demand, terminal second-life stock, and the final demand-capacity gap remained unchanged. The limited overall effect shows that Minimum Processing Time mainly influences processing during periods of spare capacity. Once Recycling Capacity becomes binding, capacity determines throughput and reduces the influence of this assumption.

KPI	Low 0.5 years	Baseline 1 year	High 1.5 years	Low vs Baseline	High vs Baseline
Peak recycling demand (kt/year)	475.70	475.70	475.70	No change	No change
Peak recycling backlog (kt)	1,755.93	1,763.04	1,771.29	−0.40%	+0.47%
Peak processing delay (year)	6.50	6.53	6.57	−0.46%	+0.54%
Avg. capacity utilization	84.54%	82.50%	80.47%	+2.04 pp	−2.03 pp
Cumulative recovered materials (kt)	1,240.82	1,236.56	1,231.61	+0.34%	−0.40%
Battery Recovery Yield	32.45%	32.34%	32.21%	+0.11 pp	−0.13 pp
Terminal second-life stock (kt)	1,386.67	1,386.67	1,386.67	No change	No change

Backlog burden (kt·year)	9,339.25	9,483.89	9,637.45	−1.53%	+1.62%
Demand-capacity gap in 2050 (kt/year)	108.70	108.70	108.70	No change	No change

Table 22: Sensitivity Analysis Results for Minimum Processing Time. Source: Author's elaboration based on Vensim simulation results.

Weibull Scale Parameter

The Weibull scale parameter was tested under three values: 10 years for the low case, 12 years for the baseline, and 15 years for the high case. The baseline follows the Italy-specific parameterization adopted in [16], while the lower and upper values are analytical variations around the 12-year reference. For each case, the external vehicle-retirement and battery-flow calculations were recalculated before running the baseline System Dynamics configuration.

The Weibull scale parameter produced substantial changes in the timing and amount of battery mass reaching end of first life within the simulation horizon. With a scale parameter of 10 years, peak Recycling Backlog increased from 1,763.04 to 2,927.71 kt, peak Estimated Processing Delay increased from 6.53 to 11.79 years, and Backlog Burden reached 17,289.10 kt·year. Peak Recycling Demand also increased to 550.20 kt/year.

Increasing the scale parameter to 15 years reduced recycling pressure considerably. Peak Recycling Backlog decreased to 583.95 kt and peak Estimated Processing Delay to 2.00 years. Peak Recycling Demand fell to 364.92 kt/year, slightly below the 367 kt/year recycling capacity available in 2050.

The change in recycling pressure reflects the timing of battery retirement. A lower scale parameter brings more battery mass to end of first life earlier, while a higher value keeps more mass in automotive use for longer. Cumulative Recovered Materials therefore changed less strongly than the operational indicators, reaching 1,249.31 kt in the 10-year case and 1,179.17 kt in the 15-year case.

Battery Recovery Yield ranged from 24.94% in the low case to 46.26% in the high case. As in the previous sensitivity tests, this variation does not indicate a change in technical

recycling efficiency. It reflects the amount of battery mass entering the recycling pathway and the share that can be processed within the simulation horizon.

KPI	Low λ=10	Baseline λ=12	High λ=15	Low vs Baseline	High vs Baseline
Peak recycling demand (kt/year)	550.20	475.70	364.92	**+15.66%**	**−23.29%**
Peak recycling backlog (kt)	2,927.71	1,763.04	583.95	**+66.06%**	**−66.88%**
Peak processing delay (year)	11.79	6.53	2.00	**+80.41%**	**−69.35%**
Avg. capacity utilization	88.63%	82.50%	69.49%	**+6.13 pp**	**−13.01 pp**
Cumulative recovered materials (kt)	1,249.31	1,236.56	1,179.17	**+1.03%**	**−4.64%**
Battery Recovery Yield	24.94%	32.34%	46.26%	**−7.40 pp**	**+13.92 pp**
Terminal second-life stock (kt)	1,712.60	1,386.67	984.40	**+23.50%**	**−29.01%**
Backlog burden (kt·year)	17,289.10	9,483.89	2,925.42	**+82.30%**	**−69.15%**
Demand-capacity gap in 2050 (kt/year)	183.20	108.70	−2.08	**+68.54%**	—

Table 23: Sensitivity Analysis Results for Weibull Scale Parameter. Source: Author's elaboration based on Vensim simulation results.

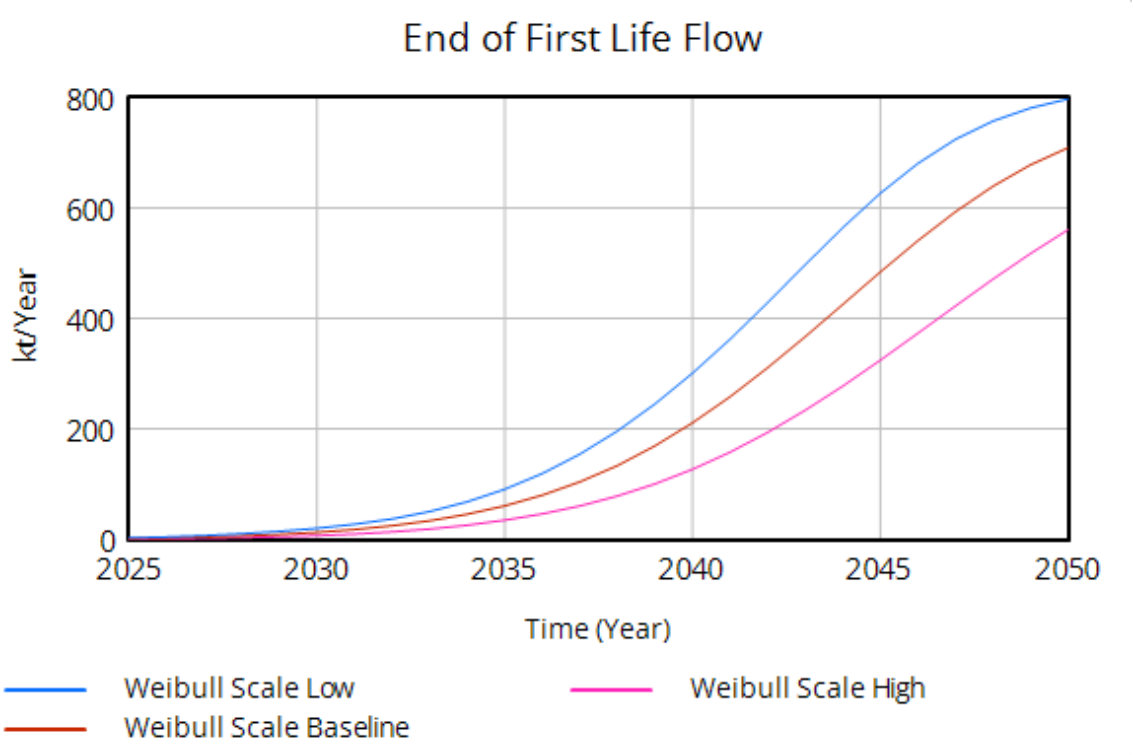


Figure 6: End-of-First-Life Flow under Weibull Scale Parameter Sensitivity. Source: Author's elaboration based on Vensim simulation results.

Figure 6 shows that the Weibull scale parameter strongly affects the timing of battery retirement. The 10-year case produces earlier and higher End-of-First-Life Flow throughout most of the simulation, while the 15-year case delays battery retirement and produces lower flows within the 2025–2050 horizon. These differences explain the stronger recycling pressure observed under the lower scale parameter.

Parameter	Tested values	Main effect observed	Observed influence within the tested range
Collection Rate	0.90 / 0.95 / 1.00	Recycling demand, backlog, processing delay, and backlog burden	Moderate
Average Second-Life Duration	5 / 10 / 12 years	Timing of post-second-life returns, backlog, delay, and terminal second-life stock	Moderate
Material Recovery Efficiency	0.50 / 0.60 / 0.70	Cumulative Recovered Materials and Battery Recovery Yield	High for material-recovery outputs; negligible for operational outputs
Minimum Processing Time	0.5 / 1 / 1.5 years	Capacity utilization and small changes in backlog-related indicators	Low
Weibull Scale Parameter	10 / 12 / 15 years	End-of-first-life timing, recycling demand, backlog, processing delay, and backlog burden	High

Table 24: Summary of Sensitivity Analysis Results for Selected Model Parameters. Source: Author's elaboration based on sensitivity-analysis results.

Overall, the sensitivity results show that the model parameters affect different parts of the system. Collection Rate and Average Second-Life Duration mainly influence the amount and timing of battery mass reaching recycling, which affects backlog and processing delay. Material Recovery Efficiency directly changes recovered-material availability but does not modify the physical recycling dynamics. Minimum Processing Time has a limited effect because Recycling Capacity becomes the main constraint during much of the baseline simulation.

Within the tested ranges, the Weibull scale parameter produced the largest variation in the operational indicators. Shorter first-life duration increased the amount of battery mass reaching end of first life within the simulation horizon and substantially increased recycling congestion, while longer first-life duration delayed these flows. These results show that the external battery-retirement assumptions are important for the magnitude

and timing of future recycling pressure. However, the influence reported here should be interpreted within the specific parameter ranges tested, since the sensitivity bounds were selected according to the available literature or the role of each assumption in the model.

4.7.7. Behavioral and External Validation

Behavioral validation was performed by comparing the main simulated relationships with the mechanisms identified in the literature. The model reproduces the expected timing effect of second-life allocation: increasing the share of batteries sent to second life reduces recycling pressure during earlier years but delays part of the battery mass reaching recycling. This behavior is consistent with Pratap et al. [7] and Bobba et al. [31], who show that second-life use postpones material recovery and shifts recyclable battery availability toward later periods.

The recycling-capacity behavior is also consistent with the reviewed literature. When recycling inflows exceed available processing capacity, unprocessed battery mass accumulates in the Recycling Backlog and processing delay increases. This follows the inventory and capacity-constraint logic represented in BattOpt [28]. When processing capacity becomes available earlier, backlog and processing delay decrease, although utilization can remain lower during periods with limited recycling feedstock. This behavior is consistent with the capacity-utilization problem discussed by Li and Srai [18].

External consistency was assessed using the comparisons presented in Section 4.7.3. The reconstructed End-of-First-Life Flow remains within a comparable order of magnitude to the Italian projections reported by Dei et al. [16], although differences occur because of the registration trajectories, cohort coverage, battery-mass assumptions, and system boundaries used in each study. The projected combined BEV and PHEV fleet also reaches 16.69 million vehicles in 2040, within the 15–17 million range reported by Terna and Snam [47].

Taken together, the verification and validation results indicate that the model preserves mass balance, behaves consistently under extreme conditions, converges as the simulation time step is reduced, and reproduces the main behavioral relationships identified in the literature. Sensitivity analysis also shows that the qualitative mechanisms remain consistent across the tested assumptions, although the magnitude of recycling pressure is

particularly sensitive to the timing of battery retirement. The model is therefore considered suitable for comparing the strategy configurations evaluated in this thesis. Its results are interpreted as conditional decision-support outcomes and not as exact predictions of future Italian battery flows.

Validation element	Evidence used	Main result
Structural behavior	Literature on second life, recycling capacity, and backlog [7,18,28,31]	Main relationships behave in the expected direction
External battery-flow plausibility	Dei et al. [16]	Comparable long-term magnitude; differences explained by assumptions and scope
Fleet plausibility	Terna and Snam [47]	2040 fleet falls within published range
Extreme-condition behavior	Tests E1–E6	All tests passed
Numerical stability	Integration-error test	Results converge as time step decreases
Parameter robustness	Sensitivity analysis	Main mechanisms remain stable; Weibull scale has the strongest effect on operational magnitude

Table 25: Summary of Model Verification and Validation Evidence. Source: Author's elaboration based on model tests and external comparisons.

The tests presented in this section were conducted on the model under baseline and extreme parameter conditions to establish confidence in its structure and behavior before it is used for strategic scenario comparison. Chapter 5 then applies the verified model to the nine second-life allocation and recycling-capacity configurations that constitute the study's scenario analysis.

5. SIMULATION AND SCENARIO ANALYSIS

The nine scenarios are presented from S1 to S9 and grouped according to the reference, anticipatory, and delayed recycling-capacity configurations. Unless otherwise stated, all scenarios use the same battery-inflow and retirement trajectories, Collection Rate, Average Second-Life Duration, Material Recovery Efficiency, Minimum Processing Time, and initial conditions.

5.1. S1 – Baseline: Reference Capacity and Reference Second-Life Allocation

The baseline combines the reference second-life allocation and recycling-capacity trajectories and provides the common comparison case for the alternative scenarios.

5.1.1. Scenario Configuration

Second-life allocation remains at zero before 2030, reaches 10% in 2030, and subsequently increases by two percentage points per year until reaching 50% in 2050 [16]. Recycling Capacity follows the reference stepwise trajectory defined in Section 4.5.5, increasing from 5 kt/year in 2025 to 367 kt/year in 2050 [33].

Model element	Baseline configuration
Second-life allocation	0% before 2030 10% in 2030 annual increase of 2 percentage points 50% in 2050
Recycling capacity	5 kt/year in 2025 10 in 2026 12 in 2029 17 in 2030 48 in 2035 111 in 2040 235 in 2045 367 in 2050

Table 26: Baseline scenario configuration

5.1.2. Simulated Behavior

The baseline initially operates with spare recycling capacity, but the system becomes capacity-constrained as recycling inflows increase. Recycling Capacity Utilization reaches 100% in 2033 and remains at this level through 2050. As a result, Recycling Backlog increases to 60.77 kt in 2035, 278.24 kt in 2040, 901.51 kt in 2045, and 1,763.04 kt in 2050.

Total Recycling Pathway Inflow reaches 475.70 kt/year in 2050, while Recycling Capacity is limited to 367 kt/year. The resulting capacity gap is 108.70 kt/year, meaning that the backlog is still increasing at the end of the simulation. Estimated Processing Delay reaches its maximum value of 6.53 years in 2049 and decreases to 4.80 years in 2050

following the final capacity expansion. This reduction results from the higher processing rate and does not indicate that the accumulated backlog has been cleared.

By 2050, 3,823.97 kt has entered the recycling pathway and 2,060.93 kt has been processed. Cumulative Recovered Materials reaches 1,236.56 kt, producing a Battery Recovery Yield of 32.34%. This means that approximately one-third of the cumulative battery mass entering the recycling pathway has become available as recovered material within the simulation horizon. The remaining unprocessed mass forms the terminal Recycling Backlog, while 1,386.67 kt remains in second-life applications.

Indicator	Baseline result
Peak Recycling Demand	475.70 kt/year in 2050
Recycling capacity in 2050	367.00 kt/year
Demand-capacity gap in 2050	108.70 kt/year
Terminal/peak recycling backlog	1,763.04 kt in 2050
Peak estimated processing delay	6.53 years in 2049
Estimated processing delay in 2050	4.80 years
First year of full capacity utilization	2033
Average capacity utilization	82.50%
Cumulative recycling-pathway inflow	3,823.97 kt
Cumulative processed batteries	2,060.93 kt
Cumulative recovered materials	1,236.56 kt
Battery Recovery Yield	32.34%
Terminal second-life stock	1,386.67 kt

Table 27: Baseline operational and material-circularity results.

5.1.3. Interpretation

The reference capacity trajectory becomes insufficient for the battery flows generated by the cohort model. Once full utilization is reached in 2033, additional recycling inflows cannot be processed immediately and accumulate in the Recycling Backlog. The final capacity addition reduces the estimated delay in 2050, but annual inflow continues to exceed processing capability.

The Battery Recovery Yield of 32.34% reflects both the amount of battery mass that remains unprocessed and the assumed material recovery efficiency. It should therefore not be interpreted as the technical efficiency of the recycling process. Instead, it represents the share of all cumulative recycling-pathway inflow that has become available as recovered material by 2050.

These results do not demonstrate that the treatment requirements reported in [33] are incorrect, since the two calculations use different vehicle trajectories, cohort coverage, battery-mass assumptions, and system boundaries. They show that the adequacy of a capacity trajectory depends on the battery-flow assumptions used for planning. The baseline therefore provides the reference case for evaluating whether changes in second-life allocation or capacity timing reduce the observed backlog and material-recovery delay.

5.2. S2 – Reference Capacity and Low Second-Life Allocation

This scenario evaluates the effect of directing a larger share of collected battery mass toward recycling immediately after automotive first life.

5.2.1. Scenario Configuration

Second-life allocation remains at zero before 2030, reaches 5% in 2030, and subsequently increases by one percentage point per year until reaching 25% in 2050. This trajectory corresponds to half of the reference allocation rate. Recycling Capacity remains equal to the baseline configuration.

Year	Reference SL allocation	Low SL allocation
2025–2029	0%	0%
2030	10%	5%
2035	20%	10%
2040	30%	15%
2045	40%	20%
2050	50%	25%

Table 28: Reference and low second-life allocation trajectories.

5.2.2. Simulated Behavior

Lower second-life allocation directs more battery mass toward recycling immediately after automotive first life. Cumulative Recycling Pathway Inflow reaches 4,517.31 kt, 693.34 kt above the baseline. The terminal second-life stock decreases by the same amount, from 1,386.67 kt to 693.34 kt.

However, the reference capacity trajectory processes almost none of this additional inflow. Cumulative Processed Batteries increase by only 1.30 kt, while Cumulative Recovered Materials increase from 1,236.56 kt to 1,237.34 kt. Most of the additional mass therefore accumulates in the Recycling Backlog.

Terminal Recycling Backlog reaches 2,455.08 kt, 39.3% above the baseline, while Backlog Burden increases to 12,676.20 kt·year. Peak Estimated Processing Delay reaches 9.07 years in 2049.

In 2050, Total Recycling Pathway Inflow reaches 574.89 kt/year, exceeding the available capacity by 207.89 kt/year. Battery Recovery Yield decreases from 32.34% to 27.39%, showing that the increase in recycling-pathway inflow does not produce a proportional increase in recovered materials.

5.2.3. Interpretation

Under the reference capacity trajectory, lower second-life allocation mainly transfers battery mass from the second-life stock to the Recycling Backlog. Although more batteries become available for recycling earlier, the system is already operating at its processing limit.

The almost unchanged recovered-material output shows that earlier recycling availability is not sufficient when processing capacity remains constrained. Most of the additional inflow accumulates as backlog, increasing both congestion and processing delay.

Low second-life allocation therefore requires earlier or greater recycling capacity. If sufficient processing capability is not available, the additional battery inflow mainly increases pressure on the recycling system and does not translate into greater material recovery.

Indicator	S1: Baseline	S2: Low SL allocation	Change
Peak recycling demand	475.70 kt/year	574.89 kt/year	+20.8%
Peak recycling backlog	1,763.04 kt	2,455.08 kt	+39.3%
Peak processing delay	6.53 years	9.07 years	+38.8%

Average capacity utilization	82.50%	82.89%	+0.39 percentage points
Cumulative recovered materials	1,236.56 kt	1,237.34 kt	+0.1%
Battery Recovery Yield	32.34%	27.39%	−4.95 percentage points
Terminal second-life stock	1,386.67 kt	693.34 kt	−50.0%
Backlog burden	9,483.89 kt·year	12,676.20 kt·year	+33.7%
Demand-capacity gap in 2050	108.70 kt/year	207.89 kt/year	+91.2%

Table 29: Performance comparison between S1 and S2.

5.3. S3 – Reference Capacity and High Second-Life Allocation

This scenario evaluates the effect of assigning a larger share of collected battery mass to second-life applications while maintaining the reference recycling-capacity trajectory.

5.3.1. Scenario Configuration

Second-life allocation remains at zero before 2030, increases to 25% in 2030, and subsequently rises by 2.5 percentage points per year until reaching 50% in 2040. It remains at 50% through 2050. Recycling Capacity follows the baseline trajectory. This configuration represents earlier development of second-life applications than under the reference scenario.

Year	Reference SL allocation	High SL allocation
2025–2029	0%	0%
2030	10%	25%
2035	20%	37.5%
2040	30%	50%
2045	40%	50%
2050	50%	50%

Table 30: Reference and high second-life allocation trajectories.

5.3.2. Simulated Behavior

Higher second-life allocation reduces the cumulative battery mass entering the recycling pathway by 254.48 kt, from 3,823.97 kt in the baseline to 3,569.49 kt. The terminal second-life stock increases by the same amount, reaching 1,641.15 kt.

The lower recycling inflow reduces terminal Recycling Backlog to 1,518.18 kt, 13.89% below the baseline. Backlog Burden decreases by 25.0% to 7,113.05 kt·year, while peak Estimated Processing Delay falls from 6.53 to 5.41 years.

Cumulative Recovered Materials decreases slightly from 1,236.56 kt to 1,230.79 kt. Battery Recovery Yield nevertheless increases from 32.34% to 34.48%, mainly because less battery mass enters the recycling pathway during the simulation period, not because more material is recovered.

Toward the end of the horizon, larger post-second-life returns increase recycling pressure. Total Recycling Pathway Inflow reaches 501.15 kt/year in 2050, exceeding the available capacity by 134.15 kt/year. This gap is larger than in the baseline, indicating that the backlog continues to increase at the end of the simulation.

5.3.3. Interpretation

Higher second-life allocation acts as a temporary buffer by retaining more battery mass outside the recycling pathway. This reduces backlog, backlog burden, and processing delay during most of the simulation, but it also delays material recovery and leaves more battery mass in second-life applications in 2050.

The higher Battery Recovery Yield should not be interpreted as a greater quantity of recovered material. Cumulative recovery is slightly lower than in the baseline, while the yield increases because its denominator—the cumulative recycling-pathway inflow—is smaller.

Second-life allocation therefore changes when recycling demand occurs, but the battery mass eventually returns to the recycling pathway. The initial operational relief is followed by greater post-second-life returns, which increase the final demand-capacity gap. Higher allocation can reduce short- and medium-term congestion, but it does not replace the need for sufficient future recycling capacity.

Indicator	S1: Baseline	S3: High SL allocation	Change

Peak recycling demand	475.70 kt/year	501.15 kt/year	+5.35%
Peak recycling backlog	1,763.04 kt	1,518.18 kt	−13.89%
Peak processing delay	6.53 years	5.41 years	−17.10%
Average capacity utilization	82.50%	81.00%	−1.50 percentage points
Cumulative recovered materials	1,236.56 kt	1,230.79 kt	−0.47%
Battery Recovery Yield	32.34%	34.48%	+2.14 percentage points
Terminal second-life stock	1,386.67 kt	1,641.15 kt	+18.35%
Backlog burden	9,483.89 kt·year	7,113.05 kt·year	−25.00%
Demand-capacity gap in 2050	108.70 kt/year	134.15 kt/year	+23.41%

Table 31: Performance comparison between the baseline and high second-life allocation scenarios

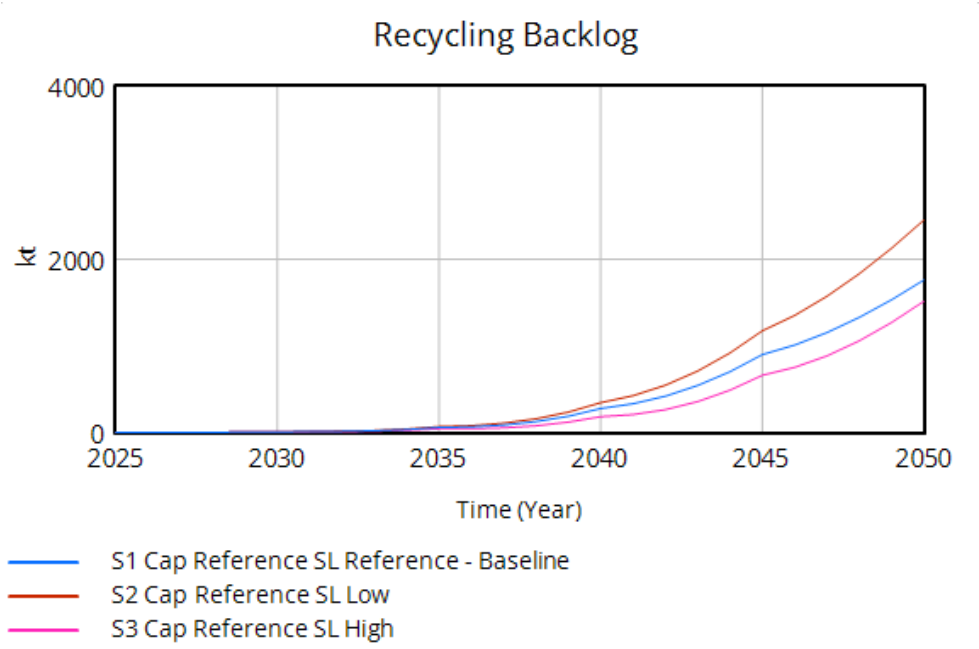


Figure 7: Recycling Backlog under Reference-Capacity Scenarios. Source: Author's elaboration based on Vensim simulation results.

The backlog trajectories in Figure 7 highlight the effect of second-life allocation under the reference-capacity pathway. Low allocation produces the highest terminal backlog, reaching 2,455.08 kt in 2050, while high allocation reduces it to 1,518.18 kt. However, backlog continues to increase in all three scenarios, indicating that the reference-capacity trajectory remains insufficient regardless of the allocation strategy.

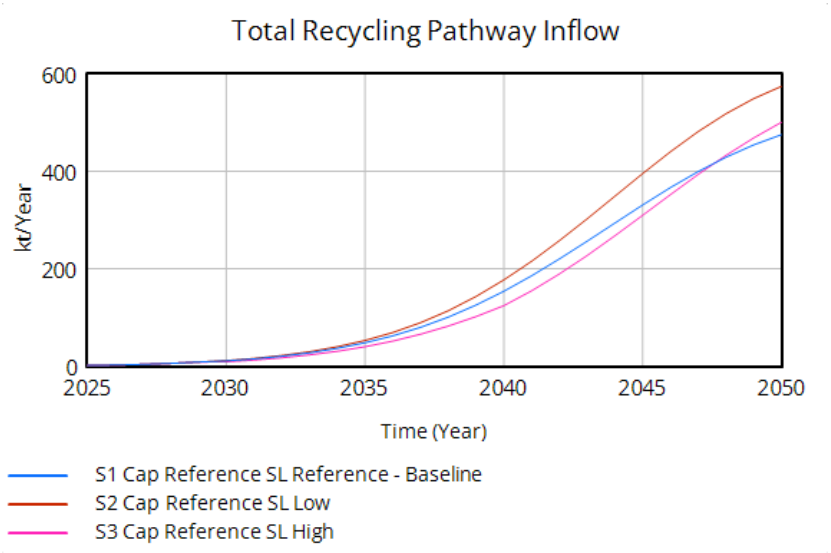


Figure 8: Total Recycling Pathway Inflow under Reference-Capacity Scenarios. Source: Author's elaboration based on Vensim simulation results.

As shown in Figure 8, low second-life allocation produces the highest recycling-pathway inflow because more battery mass is directed immediately toward recycling. High allocation reduces recycling pressure during the earlier years, but larger post-second-life returns increase inflow toward the end of the horizon. By 2050, recycling inflow exceeds the reference capacity in all three scenarios, confirming that second life changes the timing of recycling demand but does not remove the need for sufficient processing capacity.

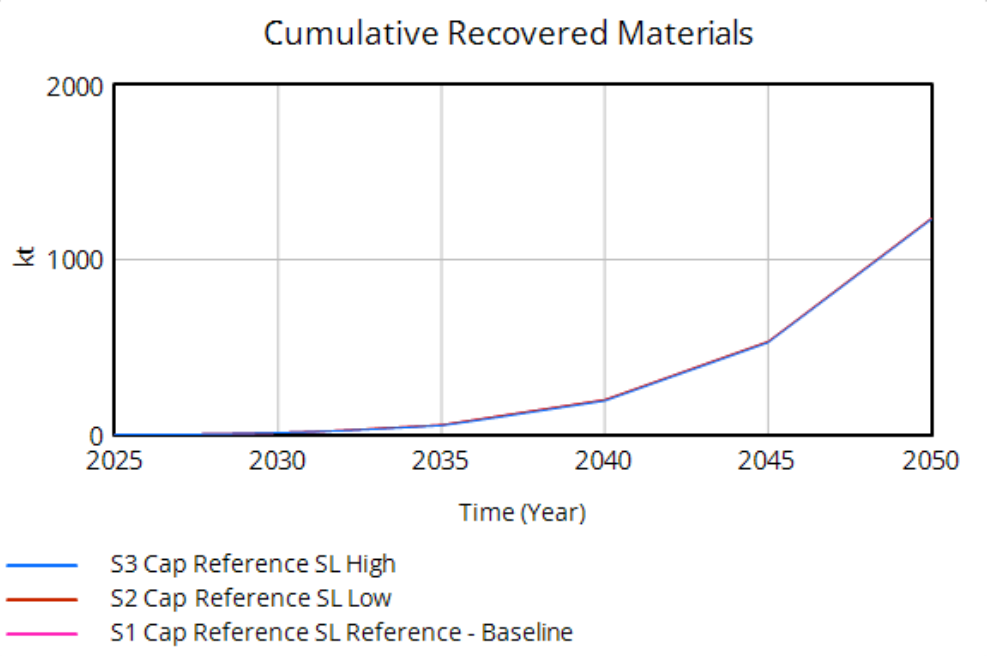


Figure 9: Cumulative Recovered Materials under Reference-Capacity Scenarios. Source: Author's elaboration based on Vensim simulation results.

The three trajectories in Figure 9 remain almost overlapping throughout the simulation. By 2050, Cumulative Recovered Materials reaches 1,236.56 kt in the baseline, 1,237.34 kt under low allocation, and 1,230.79 kt under high allocation. This small difference shows that directing more battery mass toward recycling does not substantially increase material recovery when processing capacity is already constrained.

5.4. S4 – Anticipatory Capacity and Reference Second-Life Allocation

This scenario evaluates the effect of making the main recycling-capacity additions available five years earlier while maintaining the reference second-life allocation trajectory.

5.4.1. Scenario Configuration

The initial capacity levels remain equal to the baseline through 2029. From 2030 onward, the main reference-capacity levels are introduced five years earlier. Recycling Capacity reaches 48 kt/year in 2030, 111 kt/year in 2035, 235 kt/year in 2040, and 367 kt/year in 2045. It remains at this level through 2050. The scenario therefore changes the timing of capacity availability without increasing the final capacity level.

Year	Reference capacity	Anticipatory capacity
2025	5 kt/year	5 kt/year
2026	10 kt/year	10 kt/year
2029	12 kt/year	12 kt/year
2030	17 kt/year	48 kt/year
2035	48 kt/year	111 kt/year
2040	111 kt/year	235 kt/year
2045	235 kt/year	367 kt/year
2050	367 kt/year	367 kt/year

Table 32: Reference and anticipatory recycling-capacity trajectories.

5.4.2. Simulated Behavior

Advancing the capacity additions substantially improves system performance. Terminal Recycling Backlog decreases from 1,763.04 kt in the baseline to 581.53 kt, while Backlog Burden falls from 9,483.89 to 3,544.95 kt·year.

Peak Estimated Processing Delay decreases from 6.53 to 1.58 years. In the anticipatory scenario, the peak occurs in 2050, when annual recycling inflow again exceeds the final capacity level.

Earlier processing capability increases Cumulative Recovered Materials from 1,236.56 kt to 1,945.47 kt. Battery Recovery Yield rises from 32.34% to 50.88%, showing that a much larger share of the battery mass entering the recycling pathway becomes available as recovered material within the simulation horizon.

These improvements are accompanied by lower average Recycling Capacity Utilization, which decreases from 82.50% to 61.39%. The earlier additions create periods of spare capacity before recycling inflows increase. Utilization reaches 100% in 2044, decreases after the 2045 capacity addition, and returns to full utilization from 2047 onward.

The 2050 demand-capacity gap remains 108.70 kt/year because the scenario advances the same capacity levels without increasing the final capacity magnitude. The backlog is therefore substantially smaller than in the baseline, but it is still increasing at the end of the horizon.

5.4.3. Interpretation

Earlier capacity expansion substantially reduces backlog, processing delay, and postponed material recovery. The lower average utilization reflects temporary spare capacity and should not be interpreted as poor system performance.

This result shows the main trade-off associated with anticipatory infrastructure. Installing capacity before it is fully required creates periods of underutilization, but it prevents much of the congestion that develops when expansion follows the reference timing.

However, timing alone does not solve the final capacity shortage. By 2050, recycling inflow still exceeds the available processing capacity. Anticipatory expansion reduces the backlog accumulated during the transition, but a higher long-term capacity level would still be required to match annual recycling demand.

Indicator	S1: Baseline	S4: Anticipatory capacity	Change
Peak recycling backlog	1,763.04 kt	581.53 kt	−67.0%
Peak processing delay	6.53 years	1.58 years	−75.7%
Average capacity utilization	82.50%	61.39%	−21.11 percentage points
Cumulative recovered materials	1,236.56 kt	1,945.47 kt	+57.3%
Battery Recovery Yield	32.34%	50.88%	+18.54 percentage points
Terminal second-life stock	1,386.67 kt	1,386.67 kt	No change
Backlog burden	9,483.89 kt·year	3,544.95 kt·year	−62.6%
Demand-capacity gap in 2050	108.70 kt/year	108.70 kt/year	No change

Table 33: Performance comparison between the baseline and anticipatory-capacity scenarios.

5.5. S5 – Anticipatory Capacity and Low Second-Life Allocation

This scenario combines the low second-life allocation trajectory with anticipatory recycling-capacity expansion. It evaluates whether earlier processing capacity can manage the additional recycling inflow generated when a larger share of batteries is directed to recycling immediately after automotive first life.

5.5.1. Scenario Configuration

Second-life allocation remains at zero before 2030, reaches 5% in 2030, and increases by one percentage point per year until reaching 25% in 2050. Recycling Capacity follows the anticipatory trajectory, reaching 48 kt/year in 2030, 111 kt/year in 2035, 235 kt/year in 2040, and 367 kt/year from 2045 onward.

Model element	S5 configuration
Second-life allocation before 2030	0%
Second-life allocation in 2030	5%
Second-life allocation in 2040	15%
Second-life allocation in 2050	25%
Recycling capacity in 2025	5 kt/year
Recycling capacity in 2030	48 kt/year
Recycling capacity in 2035	111 kt/year
Recycling capacity in 2040	235 kt/year
Recycling capacity from 2045 onward	367 kt/year

Table 34: Configuration of the anticipatory-capacity and low-allocation scenario

5.5.2. Simulated Behavior

Under this configuration, Cumulative Recovered Materials reaches 2,050.04 kt by 2050. This is 65.7% higher than under the same low-allocation trajectory with reference capacity in S2. Terminal Recycling Backlog decreases from 2,455.08 kt in S2 to 1,100.57 kt, while peak Estimated Processing Delay falls from 9.07 to 3.00 years.

Earlier capacity therefore processes a substantial part of the additional battery mass made available by low second-life allocation. Backlog Burden decreases by 58.0% relative to S2, and Battery Recovery Yield increases from 27.39% to 45.38%.

Compared with S4, which uses the same anticipatory capacity but reference second-life allocation, S5 recovers an additional 104.57 kt of material. However, the greater recycling inflow also increases terminal backlog from 581.53 to 1,100.57 kt and peak processing delay from 1.58 to 3.00 years. Average Capacity Utilization increases from 61.39% to 65.26%, since more recycling feedstock is available to use the anticipatory infrastructure.

In 2050, Total Recycling Pathway Inflow reaches 574.89 kt/year and exceeds capacity by 207.89 kt/year. The backlog is therefore still increasing at the end of the simulation.

5.5.3. Interpretation

Anticipatory capacity allows low second-life allocation to produce substantially more recovered material than when the same allocation strategy is combined with reference capacity. Instead of accumulating almost entirely as backlog, a larger part of the additional recycling inflow is processed within the simulation horizon.

However, the comparison with S4 shows the trade-off created by low allocation. Directing more battery mass toward recycling increases recovered-material availability and uses the installed capacity more intensively, but it also produces greater backlog and processing delay.

The scenario therefore improves performance relative to the baseline and to S2, but it does not eliminate the long-term capacity shortage. Earlier capacity reduces the

consequences of congestion, while the final capacity level remains insufficient for the recycling inflow generated by low second-life allocation.

Indicator	S1 Baseline	S2 Ref. capacity + Low SL	S4 Ant. capacity + Ref. SL	S5 Ant. capacity + Low SL
Peak recycling demand	475.70	574.89	475.70	574.89 kt/year
Peak recycling backlog	1,763.04	2,455.08	581.53	1,100.57 kt
Peak processing delay	6.53	9.07	1.58	3.00 years
Average capacity utilization	82.50%	82.89%	61.39%	65.26%
Cumulative recovered materials	1,236.56	1,237.34	1,945.47	2,050.04 kt
Battery Recovery Yield	32.34%	27.39%	50.88%	45.38%
Terminal second-life stock	1,386.67	693.34	1,386.67	693.34 kt
Backlog burden	9,483.89	12,676.20	3,544.95	5,321.50 kt·year
Demand-capacity gap in 2050	108.70	207.89	108.70	207.89 kt/year

Table 35: Performance comparison of the low-allocation and anticipatory-capacity scenario with the relevant reference configurations.

5.6. S6 – Anticipatory Capacity and High Second-Life Allocation

This scenario combines anticipatory recycling-capacity expansion with an earlier and higher second-life allocation trajectory. It evaluates whether retaining more battery mass in second-life applications can further reduce recycling pressure when processing capacity is installed in advance.

5.6.1. Scenario Configuration

Second-life allocation remains at zero before 2030, increases to 25% in 2030, and rises by 2.5 percentage points per year until reaching 50% in 2040. It remains at this level through 2050. Recycling Capacity follows the anticipatory trajectory, reaching 48 kt/year in 2030, 111 kt/year in 2035, 235 kt/year in 2040, and 367 kt/year from 2045 onward.

Model element	Scenario configuration

Second-life allocation before 2030	0%
Second-life allocation in 2030	25%
Second-life allocation in 2035	37.5%
Second-life allocation from 2040	50%
Recycling capacity in 2025	5 kt/year
Recycling capacity in 2030	48 kt/year
Recycling capacity in 2035	111 kt/year
Recycling capacity in 2040	235 kt/year
Recycling capacity from 2045	367 kt/year

Table 36: Configuration of the anticipatory-capacity and high-allocation scenario

5.6.2. Simulated Behavior

Compared with S3, which applies the same high second-life allocation under reference capacity, anticipatory capacity substantially improves operational performance. Terminal Recycling Backlog decreases from 1,518.18 kt to 592.86 kt, while peak Estimated Processing Delay falls from 5.41 to 1.62 years. Backlog Burden also decreases by 54.9%, from 7,113.05 to 3,205.60 kt·year.

Earlier capacity increases Cumulative Recovered Materials from 1,230.79 kt in S3 to 1,785.97 kt in S6. Battery Recovery Yield rises from 34.48% to 50.03%, showing that a larger proportion of the recycling-pathway inflow becomes available as recovered material within the simulation horizon.

Compared with S4, which uses the same anticipatory capacity but reference second-life allocation, S6 produces a similar terminal backlog and peak delay. However, Cumulative Recovered Materials are 159.50 kt lower, while the terminal second-life stock is 254.48 kt higher. Average Capacity Utilization also decreases from 61.39% to 55.28%, because high allocation reduces the amount of recycling feedstock available during the earlier years.

High allocation lowers cumulative congestion during most of the simulation, producing the lowest Backlog Burden among the anticipatory-capacity configurations. Toward the end of the horizon, however, larger post-second-life returns increase Total Recycling Pathway Inflow to 501.15 kt/year. This exceeds the final capacity level by 134.15 kt/year, causing the backlog to increase again by 2050.

5.6.3. Interpretation

Anticipatory capacity allows the system to manage high second-life allocation with substantially less backlog and delay than under reference capacity. The configuration benefits from both earlier processing capability and lower recycling pressure during the middle of the simulation.

However, the comparison with S4 shows that higher second-life allocation does not improve every outcome. It reduces cumulative backlog burden, but it also delays material recovery, lowers capacity utilization, and leaves more battery mass in second-life applications at the end of the horizon.

S6 therefore favors lower cumulative congestion and extended battery use, while S4 provides slightly lower terminal backlog and delay and greater recovered-material availability. High second-life allocation can postpone recycling pressure, but it cannot remove the later capacity requirement created by post-second-life returns.

Indicator	S1 Baseline	S3 Ref. capacity + High SL	S4 Ant. capacity + Ref. SL	S6 Ant. capacity + High SL
Peak recycling demand	475.70	501.15	475.70	501.15 kt/year
Peak recycling backlog	1,763.04	1,518.18	581.53	592.86 kt
Peak processing delay	6.53	5.41	1.58	1.62 years
Average capacity utilization	82.50%	81.00%	61.39%	55.28%
Cumulative recovered materials	1,236.56	1,230.79	1,945.47	1,785.97 kt
Battery Recovery Yield	32.34%	34.48%	50.88%	50.03%
Terminal second-life stock	1,386.67	1,641.15	1,386.67	1,641.15 kt
Backlog burden	9,483.89	7,113.05	3,544.95	3,205.60 kt·year
Demand-capacity gap in 2050	108.70	134.15	108.70	134.15 kt/year

Table 37: Performance comparison of the high-allocation and anticipatory-capacity scenario with the relevant reference configurations.

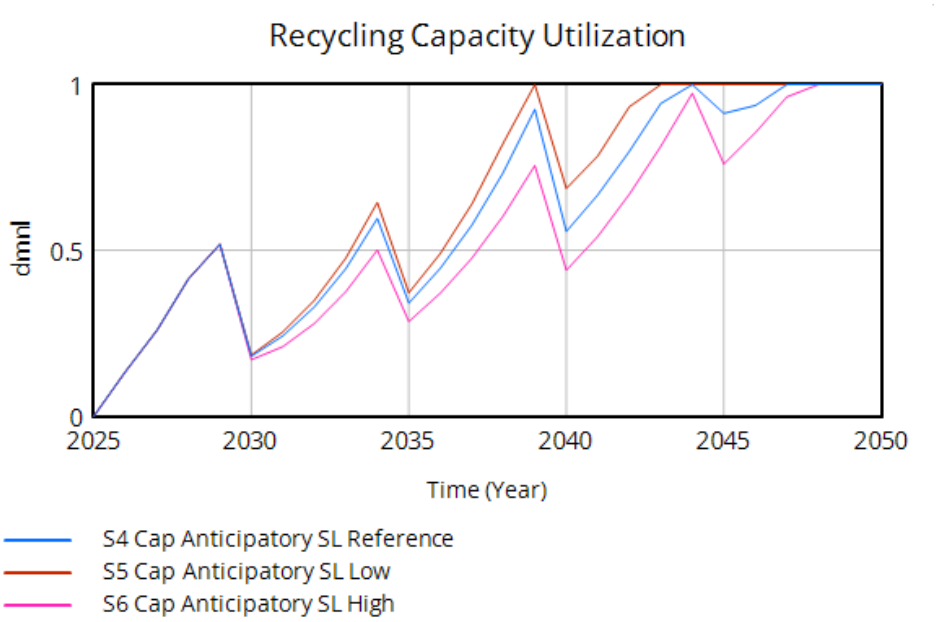


Figure 10: Recycling Capacity Utilization under Anticipatory-Capacity Scenarios. Source: Author's elaboration based on Vensim simulation results.

Figure 10 highlights the periods of spare processing capacity created by anticipatory expansion. Low second-life allocation produces the highest utilization because more battery mass reaches recycling earlier, while high allocation produces the lowest utilization by retaining more mass in second-life applications. Despite these differences, utilization returns to 100% in all three scenarios toward the end of the simulation, indicating that the final capacity level eventually becomes constrained.

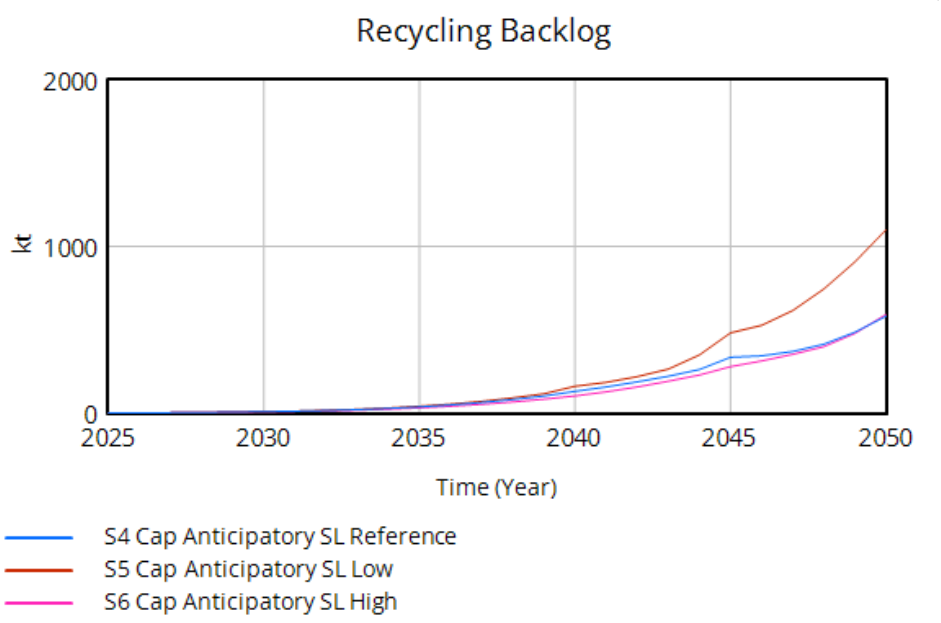


Figure 11: Recycling Backlog under Anticipatory-Capacity Scenarios. Source: Author's elaboration based on Vensim simulation results.

Under anticipatory capacity, the backlog trajectories differ mainly according to second-life allocation, as illustrated in Figure 11. Low allocation produces the highest terminal backlog, reaching 1,100.57 kt in 2050, while the reference- and high-allocation scenarios end at 581.53 and 592.86 kt, respectively. Although anticipatory expansion limits congestion compared with reference capacity, backlog increases again in all three scenarios toward the end of the horizon as recycling inflows exceed the final capacity level.

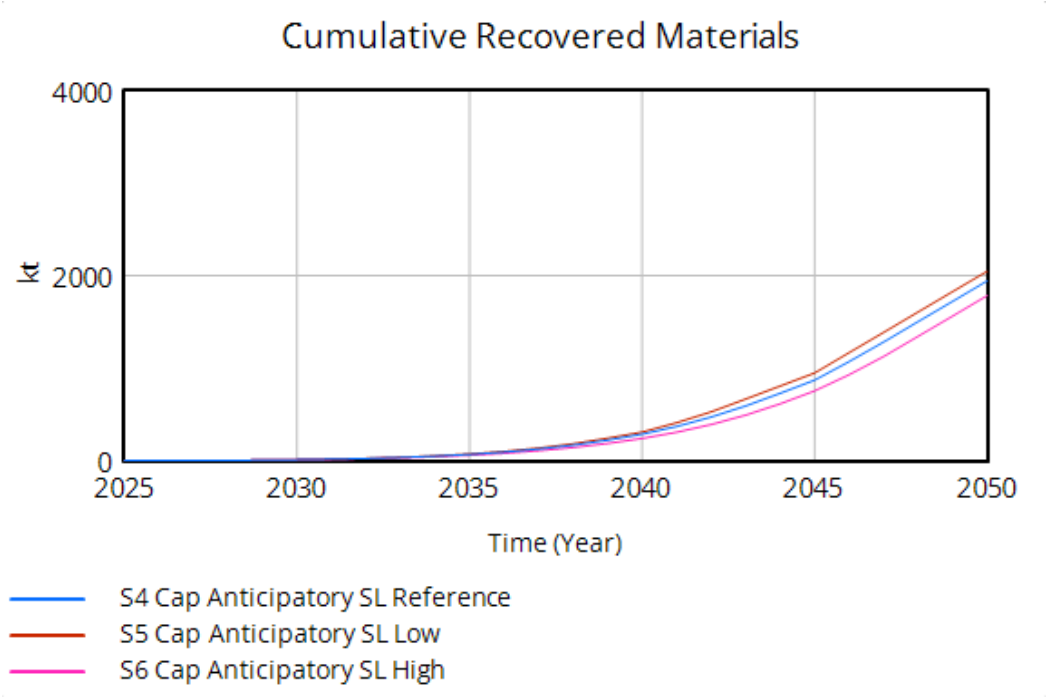


Figure 12: Cumulative Recovered Materials under Anticipatory-Capacity Scenarios. Source: Author's elaboration based on Vensim simulation results.

Recovered-material availability differs more clearly across the anticipatory scenarios in Figure 12. Low allocation produces the highest Cumulative Recovered Materials, reaching 2,050.04 kt by 2050, followed by reference allocation at 1,945.47 kt and high allocation at 1,785.97 kt. Higher allocation delays the entry of battery mass into recycling and therefore reduces the amount of material recovered within the simulation horizon.

5.7. S7 – Delayed Capacity and Reference Second-Life Allocation

This scenario shifts the main recycling-capacity additions five years later while maintaining the reference second-life allocation trajectory.

5.7.1. Scenario Configuration

Capacity remains at 12 kt/year through 2034 and subsequently reaches 17 kt/year in 2035, 48 kt/year in 2040, 111 kt/year in 2045, and 235 kt/year in 2050. The final reference-capacity level of 367 kt/year would become available in 2055 and therefore falls outside the simulation horizon.

Year	Reference capacity	Delayed capacity
2025	5 kt/year	5 kt/year

2026	10 kt/year	10 kt/year
2029	12 kt/year	12 kt/year
2030	17 kt/year	12 kt/year
2035	48 kt/year	17 kt/year
2040	111 kt/year	48 kt/year
2045	235 kt/year	111 kt/year
2050	367 kt/year	235 kt/year
2055	—	367 kt/year

Table 38: Reference and delayed recycling-capacity trajectories

Note: The 2055 capacity level lies outside the simulation horizon and does not affect the reported results.

5.7.2. Simulated Behavior

Delayed capacity causes the recycling system to reach full utilization in 2032 and remain constrained through 2050. Terminal Recycling Backlog reaches 2,868.93 kt, while peak Estimated Processing Delay rises to 23.48 years in 2044 and decreases to 12.21 years in 2050 after the final capacity expansion.

Cumulative Recovered Materials reaches 573.03 kt, less than half the baseline result, and Battery Recovery Yield falls to 14.99%. Average Capacity Utilization remains high at 84.68%.

In 2050, Total Recycling Pathway Inflow exceeds the available capacity by 240.70 kt/year. The backlog therefore continues to increase at the end of the simulation.

5.7.3. Interpretation

The delayed expansions become available only after a substantial backlog has already formed. Although each addition temporarily reduces processing delay, it does not clear the accumulated mass.

The high utilization does not indicate favorable performance. It reflects continuous capacity shortage, accompanied by larger backlog, longer delays, and substantially lower recovered-material availability than in the baseline.

Indicator	S1: Baseline	S7: Delayed capacity	Change
Peak recycling backlog	1,763.04 kt	2,868.93 kt	+62.7%
Peak processing delay	6.53 years	23.48 years	+259.6%
Year of peak processing delay	2049	2044	—
Estimated processing delay in 2050	4.80 years	12.21 years	+154.1%
Average capacity utilization	82.50%	84.68%	+2.18 percentage points
Cumulative recovered materials	1,236.56 kt	573.03 kt	−53.7%
Battery Recovery Yield	32.34%	14.99%	−17.35 percentage points
Terminal second-life stock	1,386.67 kt	1,386.67 kt	No change
Backlog burden	9,483.89 kt·year	15,459.40 kt·year	+63.0%
Recycling capacity in 2050	367.00 kt/year	235.00 kt/year	−132.00 kt/year
Demand-capacity gap in 2050	108.70 kt/year	240.70 kt/year	+132.00 kt/year

Table 39: Performance comparison between the baseline and delayed-capacity scenarios.

5.8. S8 – Delayed Capacity and Low Second-Life Allocation

This scenario combines lower second-life allocation with delayed recycling-capacity expansion. More battery mass is directed toward recycling earlier, while processing capacity becomes available later.

5.8.1. Scenario Configuration

Second-life allocation remains at zero before 2030, reaches 5% in 2030, and increases by one percentage point per year until reaching 25% in 2050. Recycling Capacity follows the delayed trajectory, remaining at 12 kt/year through 2034 and subsequently reaching 17 kt/year in 2035, 48 kt/year in 2040, 111 kt/year in 2045, and 235 kt/year in 2050.

Model element	S8 configuration
Second-life allocation before 2030	0%
Second-life allocation in 2030	5%
Second-life allocation in 2035	10%
Second-life allocation in 2040	15%

Second-life allocation in 2045	20%
Second-life allocation in 2050	25%
Recycling capacity in 2025	5 kt/year
Recycling capacity in 2030	12 kt/year
Recycling capacity in 2035	17 kt/year
Recycling capacity in 2040	48 kt/year
Recycling capacity in 2045	111 kt/year
Recycling capacity in 2050	235 kt/year

Table 40: Configuration of the delayed-capacity and low second-life allocation scenario.

The final delayed-capacity level of 367 kt/year would become available in 2055 and therefore does not affect the simulation results.

5.8.2. Simulated Behavior

Cumulative Recycling Pathway Inflow reaches 4,517.31 kt, while terminal Recycling Backlog increases to 3,561.82 kt, the highest result among the nine scenarios. Peak Estimated Processing Delay reaches 28.05 years in 2049 and remains at 15.16 years in 2050.

Cumulative Recovered Materials reaches 573.29 kt, producing a Battery Recovery Yield of 12.69%. Average Capacity Utilization remains high at 84.86%, reflecting persistent pressure on the available infrastructure.

In 2050, recycling inflow exceeds capacity by 339.89 kt/year, the largest final gap among the evaluated configurations.

5.8.3. Interpretation

Low second-life allocation makes more battery mass available for recycling earlier, but delayed capacity prevents this additional inflow from being processed. Most of the mass therefore accumulates in the Recycling Backlog.

Compared with S7, recovered materials increase by only 0.26 kt, while backlog and processing delay increase considerably. S8 is therefore the least favorable configuration for operational performance. Earlier recycling availability does not improve recovery when processing capacity becomes available too late.

Indicator	S2: Reference Capacity + Low SL	S7: Delayed Capacity + Reference SL	S8: Delayed Capacity + Low SL
Peak recycling demand	574.89 kt/year	475.70 kt/year	**574.89 kt/year**
Peak recycling backlog	2,455.08 kt	2,868.93 kt	**3,561.82 kt**
Peak processing delay	9.07 years	23.48 years	**28.05 years**
Estimated processing delay in 2050	6.69 years	12.21 years	**15.16 years**
Average capacity utilization	82.89%	84.68%	**84.86%**
Cumulative recovered materials	1,237.34 kt	573.03 kt	**573.29 kt**
Battery Recovery Yield	27.39%	14.99%	**12.69%**
Terminal second-life stock	693.34 kt	1,386.67 kt	**693.34 kt**
Backlog burden	12,676.20 kt·year	15,459.40 kt·year	**18,667.30 kt·year**
Demand-capacity gap in 2050	207.89 kt/year	240.70 kt/year	**339.89 kt/year**

Table 41: Performance comparison of S8 with the relevant low-allocation and delayed-capacity scenarios.

5.9. S9 – Delayed Capacity and High Second-Life Allocation

This scenario combines delayed recycling-capacity expansion with earlier and higher second-life allocation. It evaluates whether retaining more battery mass in second-life applications can reduce part of the pressure created by late capacity expansion.

5.9.1. Scenario Configuration

Second-life allocation remains at zero before 2030, reaches 25% in 2030, and increases by 2.5 percentage points per year until reaching 50% in 2040. It remains at this level through 2050. Recycling Capacity follows the delayed trajectory, remaining at 12 kt/year through 2034 and subsequently reaching 17 kt/year in 2035, 48 kt/year in 2040, 111 kt/year in 2045, and 235 kt/year in 2050.

Model element	S9 configuration
Second-life allocation before 2030	0%
Second-life allocation in 2030	25%
Second-life allocation in 2035	37.5%
Second-life allocation from 2040 onward	50%
Recycling capacity in 2025	5 kt/year
Recycling capacity in 2030	12 kt/year

Recycling capacity in 2035	17 kt/year
Recycling capacity in 2040	48 kt/year
Recycling capacity in 2045	111 kt/year
Recycling capacity in 2050	235 kt/year

Table 42: Configuration of the delayed-capacity and high second-life allocation scenario.

5.9.2. Simulated Behavior

Cumulative Recycling Pathway Inflow reaches 3,569.49 kt, while terminal Recycling Backlog reaches 2,616.29 kt. Peak Estimated Processing Delay rises to 20.24 years in 2049 and decreases to 11.13 years in 2050 after the final capacity expansion.

Cumulative Recovered Materials reaches 571.92 kt, and Battery Recovery Yield is 16.02%. Average Capacity Utilization remains high at 84.02%.

In 2050, Total Recycling Pathway Inflow exceeds the available capacity by 266.15 kt/year. The backlog is therefore still increasing at the end of the simulation.

5.9.3. Interpretation

High second-life allocation reduces part of the congestion created by delayed capacity. Compared with S7, backlog and processing delay are lower because more battery mass remains in second-life applications during the simulation period.

However, recovered-material availability remains almost unchanged because capacity continues to limit throughput. The higher Battery Recovery Yield results mainly from the lower cumulative recycling-pathway inflow, not from greater absolute recovery.

High allocation can therefore delay part of the pressure caused by delayed infrastructure, but it cannot compensate for insufficient recycling capacity.

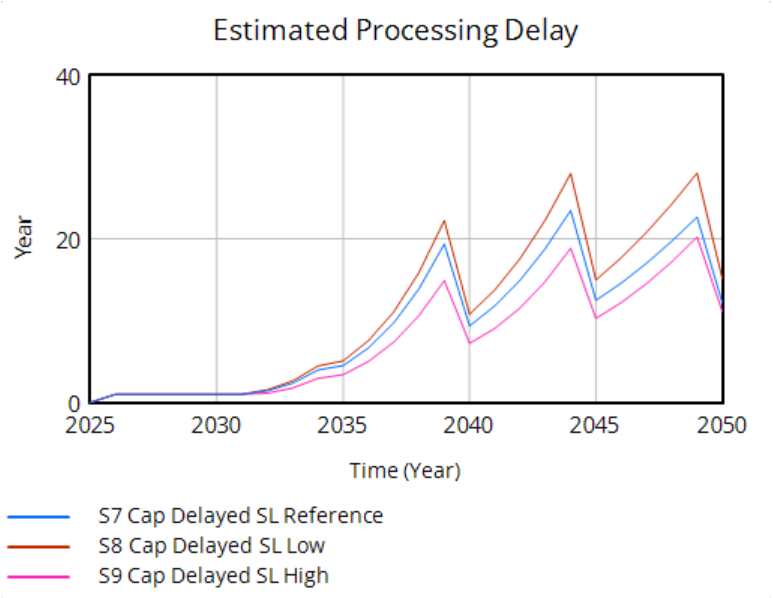


Figure 13: Estimated Processing Delay under Delayed-Capacity Scenarios. Source: Author's elaboration based on Vensim simulation results.

The processing-delay trajectories in Figure 13 show the effect of late capacity expansion across the three allocation strategies. Low second-life allocation produces the highest peak delay, reaching 28.05 years, while high allocation partially reduces it to 20.24 years. The sharp reductions following capacity additions result from higher processing rates, but they do not indicate that the accumulated backlog has been cleared.

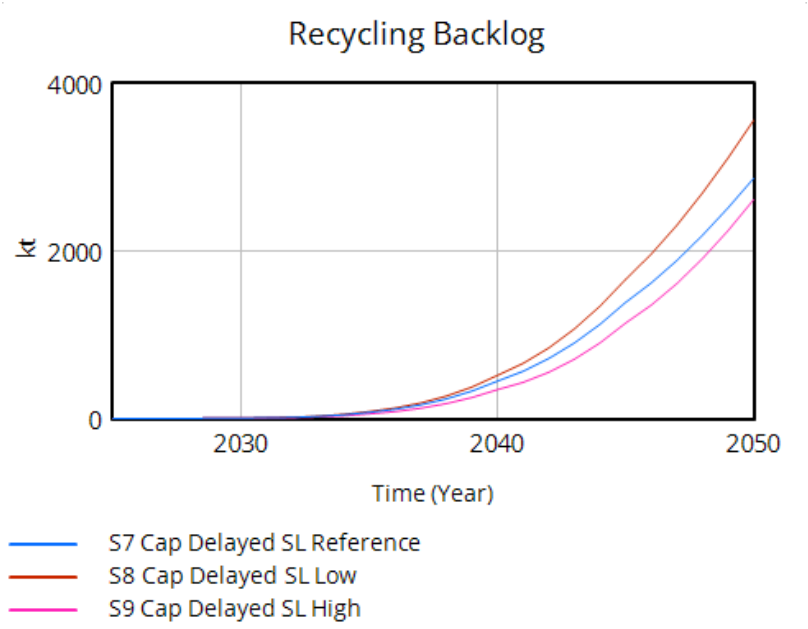


Figure 14: Recycling Backlog under Delayed-Capacity Scenarios. Source: Author's elaboration based on Vensim simulation results.

A similar pattern appears in Recycling Backlog, as shown in Figure 14. Low second-life allocation produces the highest terminal backlog, reaching 3,561.82 kt, because more

battery mass enters recycling before sufficient processing capacity is available. High allocation reduces part of this pressure, but backlog remains substantial and continues increasing through 2050.

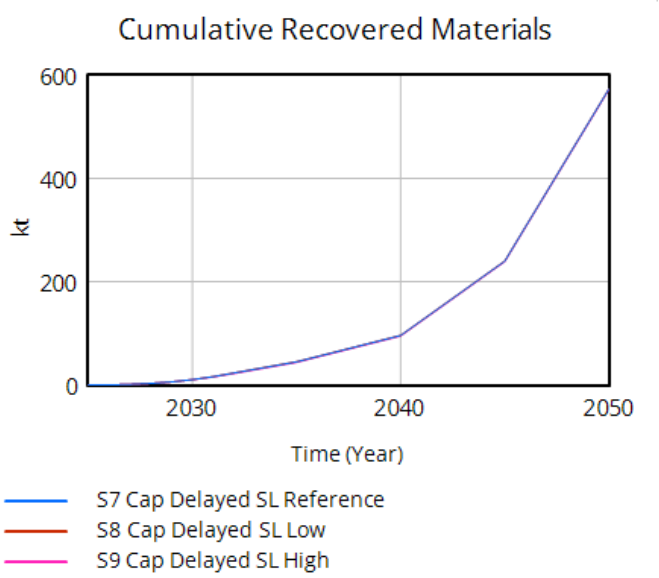


Figure 15: Cumulative Recovered Materials under Delayed-Capacity Scenarios. Source: Author's elaboration based on Vensim simulation results.

In contrast to the differences observed in backlog and processing delay, the cumulative-recovery trajectories in Figure 15 are almost identical across the delayed-capacity scenarios. By 2050, Cumulative Recovered Materials ranges only from 571.92 to 573.29 kt. This indicates that changing second-life allocation has almost no effect on material recovery when recycling throughput remains constrained by delayed capacity expansion.

5.10. Comparative Summary of Scenario Results

Table 43 summarizes the main performance indicators for the nine combinations of Second-Life Allocation Rate and Recycling Capacity timing.

KPI COMPARISON IN 9 SCENARIOS											
ID	Capacity	SL Allocation	Peak Recycling Demand	Terminal Backlog	Peak Processing Delay	Average Capacity Utilization	Cumulative Recovered materials	Battery Recovery Yield	Terminal SL Stock	Backlog Burden	2050 Demand-Capacity Gap
S1	Reference	Reference	475.70	1763.04	6.53	83%	1236.56	32%	1386.67	9483.89	108.70
S2	Reference	Low	574.89	2455.08	9.07	83%	1237.34	27%	693.34	12676.20	207.89
S3	Reference	High	501.15	1518.18	5.41	81%	1230.79	34%	1641.15	7113.05	134.15
S4	Anticipatory	Reference	475.70	581.53	1.58	61%	1945.47	51%	1386.67	3544.95	108.70
S5	Anticipatory	Low	574.89	1100.57	3.00	65%	2050.04	45%	693.34	5321.50	207.89
S6	Anticipatory	High	501.15	592.86	1.62	55%	1785.97	50%	1641.15	3205.60	134.15
S7	Delayed	Reference	475.70	2868.93	23.48	85%	573.03	15%	1386.67	15459.40	240.70
S8	Delayed	Low	574.89	3561.82	28.05	85%	573.29	13%	693.34	18667.30	339.89
S9	Delayed	High	501.15	2616.29	20.24	84%	571.92	16%	1641.15	12968.20	266.15

Table 43: Comparative performance of the nine coordination scenarios

Recycling-capacity timing produces the largest differences across the scenarios. Anticipatory capacity reduces backlog and processing delay and allows more material to be recovered by 2050. Delayed capacity produces the opposite result: persistent

congestion, long delays, and limited recovery. Its high utilization reflects continuous saturation and should not be interpreted as favorable system performance.

Second-life allocation mainly changes when battery mass reaches recycling. Low allocation increases recycling inflow and can support greater recovery when sufficient capacity is available. When capacity is constrained, however, most of the additional inflow becomes backlog. High allocation reduces pressure during earlier years but retains more battery mass in second life and increases delayed returns toward the end of the simulation.

No scenario performs best across all indicators. S5 produces the highest cumulative recovered materials, while S6 has the lowest Backlog Burden. S4 provides the most balanced result, with the lowest terminal backlog and peak processing delay, together with the highest Battery Recovery Yield. Overall, the results show that second-life allocation cannot compensate for recycling capacity that is installed too late or remains insufficient.

6. DISCUSSION

The scenario results are discussed in relation to the research hypotheses, the research question, and the engineering-design implications.

6.1. Effect of Second-Life Allocation – H1

Second-life allocation changes when battery mass reaches recycling. Lower allocation sends more batteries directly to recycling and can increase recovered-material availability within the simulation horizon when sufficient capacity is available. Under anticipatory capacity, S5 produces the highest Cumulative Recovered Materials, reaching 2,050.04 kt, but also the largest backlog and processing delay among the anticipatory scenarios. The zero-allocation extreme-condition test (E2, Section 4.7.4) confirms the routing mechanism, since the complete collected flow is directed to recycling.

Higher allocation reduces recycling pressure during earlier periods by retaining more battery mass in second life. These batteries later return through Post-Second-Life Return, so recycling demand occurs at a later stage. The full-allocation extreme-condition test (E3, Section 4.7.4) confirms the opposite routing mechanism, with the complete collected

flow passing through second life before returning to recycling. Higher allocation therefore reduces recycling pressure within the simulation horizon but also delays material recovery.

Under reference and delayed capacity, differences in recovered materials remain small because throughput is already constrained. In these cases, allocation mainly changes whether battery mass remains in second life or accumulates in the Recycling Backlog. H1 is therefore supported: higher second-life allocation delays recycling demand and recovered-material availability, although the magnitude of this effect depends on the processing capacity available when the battery mass reaches recycling.

6.2. Effect of Recycling Capacity Expansion Timing – H2 and H3

The timing of recycling capacity expansion has the strongest effect on system performance across the scenario matrix. Under anticipatory capacity, terminal backlog ranges from 581.53 to 1,100.57 kt and peak processing delay remains between 1.58 and 3.00 years. Under delayed capacity, backlog increases to between 2,616.29 and 3,561.82 kt, while peak delay reaches between 20.24 and 28.05 years.

The difference is also visible in material recovery. Anticipatory scenarios recover between 1,785.97 and 2,050.04 kt by 2050, compared with approximately 572–573 kt under delayed capacity. When capacity becomes available earlier, more of the battery mass entering recycling can be processed within the simulation horizon.

Earlier expansion also creates periods of lower utilization because capacity becomes available before demand fully develops. However, this spare capacity prevents much of the backlog and delay observed under later expansion. Even the anticipatory scenarios remain capacity-constrained by 2050, since recycling inflow exceeds the final 367 kt/year capacity level.

H2 is supported: capacity expansion that lags behind recycling inflows produces larger backlog and longer processing delays. H3 is also supported: earlier expansion reduces congestion but creates periods of lower utilization when available capacity exceeds current demand.

6.2.1. Interpretation of Capacity Utilization

Recycling Capacity Utilization should not be interpreted alone. The delayed-capacity scenarios have the highest average utilization, all above 84%, but they also produce the largest backlogs, longest processing delays, and lowest Battery Recovery Yields. In these cases, high utilization reflects persistent capacity shortage, since the available infrastructure operates close to its limit while unprocessed battery mass continues to accumulate. By contrast, average utilization in the anticipatory scenarios ranges from 55.28% to 65.26%. These lower values reflect temporary spare capacity, while the same scenarios process substantially more battery mass and maintain lower backlog and delay.

The extreme-condition tests show why utilization alone can be misleading. In the zero-capacity test (E4, Section 4.7.4), Recycling Capacity Utilization remains at 0% because no processing capacity is available, while Recycling Backlog increases to 3,823.97 kt by 2050. In the near-unconstrained-capacity test (E5), average utilization is also very low, at 1.41%, but for the opposite reason: available capacity is far above the recycling feedstock. Under this condition, terminal backlog decreases to 452.77 kt and Estimated Processing Delay remains at the 1-year minimum once recycling begins.

These results show that similar utilization values can occur under very different system conditions. Recycling Capacity Utilization should therefore be interpreted together with Recycling Backlog, Estimated Processing Delay, Recycling Throughput, Battery Recovery Yield, and recovered-material availability. High utilization may indicate system saturation, while low utilization may result from either insufficient feedstock or the absence of processing capacity.

6.3. Coordination of Second-Life Allocation and Recycling-Capacity Timing – H4

Second-life allocation determines when battery mass reaches recycling, while capacity timing determines whether that mass can be processed when it arrives. The two decisions therefore need to be evaluated together.

S8 provides the clearest example of poor timing. Low second-life allocation sends more battery mass toward recycling earlier, while delayed capacity becomes available only after backlog has already formed. The scenario produces the highest terminal backlog, at 3,561.82 kt, and the highest peak delay, at 28.05 years.

The same low-allocation trajectory under anticipatory capacity produces a very different result. S5 recovers 2,050.04 kt by 2050 and reduces peak delay to 3.00 years. This shows that the effect of second-life allocation depends strongly on when processing capacity becomes available.

High second-life allocation can reduce pressure when capacity is limited, but it mainly postpones part of the recycling demand. It cannot replace future processing capacity.

6.3.1. Comparison of the Anticipatory Scenarios

Among the anticipatory scenarios, no configuration performs best across all indicators. S5 produces the highest Cumulative Recovered Materials, reaching 2,050.04 kt, but also the largest terminal backlog and peak processing delay within this group. S6 produces the lowest Backlog Burden, although it leaves more battery mass in second-life applications and recovers less material by 2050.

S4 combines the lowest terminal Recycling Backlog and peak Estimated Processing Delay with the highest Battery Recovery Yield and the second-highest Cumulative Recovered Materials. Based on these indicators, it provides the most balanced trade-off among the evaluated configurations, without implying that it is preferable for every planning objective.

6.3.2. Evaluation of Hypothesis 4

H4 is supported. Configurations in which recycling capacity becomes available earlier produce substantially lower backlog burden and processing delay than configurations in which capacity expansion is delayed. This pattern is observed across all three second-life allocation trajectories.

Second-life allocation modifies the timing and magnitude of recycling pressure, but recycling-capacity timing determines whether those flows can be processed when they

arrive. The results therefore show that second-life allocation can reduce or postpone congestion, but it cannot compensate for recycling capacity that becomes available too late.

6.4. Answer to the Research Question

Within the evaluated scenarios, material circularity improves with lower recycling backlog and material-recovery delays when recycling capacity becomes available before large direct and post-second-life battery flows reach the recycling pathway. Anticipatory capacity provides the most favorable conditions across the three second-life allocation trajectories, with S4 offering the most balanced combination of operational and material-circularity outcomes.

No single second-life allocation level is preferable under every condition. Its effect depends on the processing capacity available when battery mass reaches recycling. Lower allocation can support earlier material recovery when sufficient capacity is available, while higher allocation can reduce recycling pressure during earlier periods by delaying part of the recycling demand. Overall, recycling-capacity timing has the stronger effect on system performance, and second-life allocation mainly changes when recycling demand and material recovery occur.

6.5. Robustness and Sensitivity Implications

The sensitivity results show that the main behavioral relationships remain consistent across the tested ranges, although the magnitude of the results depends on the model assumptions. Collection Rate and Average Second-Life Duration mainly affect the amount and timing of battery mass reaching recycling, while Material Recovery Efficiency directly affects recovered-material outputs. Minimum Processing Time has a limited influence under the baseline configuration because Recycling Capacity becomes the main constraint during much of the simulation.

The Weibull scale parameter produces the largest variation in the operational indicators within the tested sensitivity ranges. Reducing the scale parameter from 12 to 10 years brings battery retirements forward and increases peak Recycling Backlog from 1,763.04 to 2,927.71 kt and peak Estimated Processing Delay from 6.53 to 11.79 years. Increasing

it to 15 years delays battery retirement and reduces these indicators to 583.95 kt and 2.00 years, respectively. The future magnitude and timing of recycling pressure are therefore strongly dependent on the assumed first-life retirement pattern.

This result does not change the mechanism identified in the scenario analysis: when recycling inflows exceed available capacity, backlog and processing delay increase; when processing capacity becomes available earlier or battery retirements occur later, congestion is reduced. The sensitivity analysis reinforces the importance of coordinating capacity expansion with the timing of future battery returns and shows that the numerical magnitude of the results should be interpreted as conditional on the adopted retirement and technical assumptions. In particular, the strong influence of the Weibull scale parameter means that future applications of the model should update the retirement assumptions as more evidence on EV battery lifetimes becomes available.

6.6. Engineering Design Implications

The Vensim model functions as a strategic decision-support prototype for comparing second-life allocation and recycling-capacity configurations. It does not predict one exact future pathway or optimize individual facilities; instead, it shows how alternative long-term configurations affect operational performance and material recovery.

The results indicate that capacity planning should consider projected future recycling inflows in addition to current utilization levels. Waiting until available capacity is fully used allows backlog and delay to develop before additional processing capability becomes available. Earlier expansion creates periods of spare capacity but provides more flexibility as battery retirements increase.

Post-second-life returns also need to be considered when planning future capacity. Higher allocation reduces direct recycling inflow during earlier periods, but the retained batteries return later and may increase recycling pressure in subsequent years. Capacity planning should therefore account for both direct recycling inflows and delayed post-second-life returns.

The prototype can be used to compare alternative capacity timings and second-life trajectories and identify configurations that may create persistent bottlenecks. More detailed facility-level decisions would require spatial, economic, technology-specific, and stakeholder data that are outside the current model boundary.

The sensitivity results provide an additional use of the model by showing how planning needs may change under different assumptions about battery retirement, collection, second-life duration, processing, and material recovery. This is particularly relevant for long-term capacity decisions because the timing of future battery retirements remains uncertain.

7. CONCLUSION

This thesis developed a System Dynamics model to examine how second-life allocation and recycling-capacity timing interact in the Italian EV battery system over the 2025–2050 period. The model represents battery retirement, second-life use, delayed post-second-life returns, recycling backlog, capacity-constrained processing, and recovered-material availability. Its main contribution is to bring second-life allocation and recycling-capacity planning into the same decision-support model so their effects can be compared using the same operational and material-circularity indicators.

Across the nine evaluated configurations, recycling-capacity timing produced the largest differences in system performance. Under anticipatory capacity, terminal Recycling Backlog ranged from 581.53 to 1,100.57 kt and peak Estimated Processing Delay from 1.58 to 3.00 years. Under delayed capacity, these ranges increased to 2,616.29–3,561.82 kt and 20.24–28.05 years, respectively. Second-life allocation mainly changed when battery mass reached recycling and therefore modified the timing and level of recycling pressure. Among the evaluated configurations, S4 provided the most balanced combination of operational and material-circularity outcomes. The results also show that no single configuration performs best across every indicator, reinforcing the need to evaluate second-life allocation and recycling-capacity timing together.

Limitations

The model represents the Italian EV battery system at an aggregated national level and does not include facility-level, spatial, or economic detail. Its results therefore describe

system-level behavior and are not intended to support decisions for individual recycling facilities. Battery chemistries are also not modeled separately, so Battery Recovery Yield represents total recovered battery-derived material and not the recovery of individual materials such as lithium, nickel, or cobalt.

First-life retirement is represented using one Weibull distribution for both BEV and PHEV cohorts. The sensitivity analysis showed that this assumption has an important effect on the timing and magnitude of recycling pressure. The reference recycling-capacity trajectory is based on published treatment requirements, which are used as a proxy in the absence of compatible facility-level capacity data. External validation was based on comparison with published Italian projections because a compatible long-term operational dataset covering second-life and recycling flows was not identified within the scope of the study. The numerical results should therefore be interpreted as conditional scenario outcomes and not as validated forecasts of future Italian battery flows.

The model also treats second-life allocation, collection performance, processing assumptions, and recycling-capacity trajectories as exogenous inputs. Their possible responses to costs, regulation, investment decisions, and market conditions are outside the current model boundary. In addition, the simulation ends in 2050, so battery mass remaining in second-life applications or in the Recycling Backlog is not followed until final recycling.

Future Work

Future applications of the model could incorporate new operational data on Italian battery retirement, second-life activity, and recycling infrastructure as these become available. Updated evidence on battery lifetimes would be particularly useful because the sensitivity analysis showed that retirement timing strongly affects future recycling pressure. Alternative EV adoption trajectories could also be evaluated to represent uncertainty in future battery inflows.

The model could also be extended to distinguish battery chemistries, material-specific recovery rates, State of Health, and different second-life applications. Including facility location, transportation, processing technologies, investment costs, and cross-border movements would allow the framework to support more detailed recycling-capacity

planning. Extending the simulation beyond 2050 would also make it possible to follow the battery mass remaining in second life and in the Recycling Backlog at the end of the current horizon.

Overall, the study shows that improving material circularity while limiting recycling backlog and material-recovery delays depends on matching recycling-capacity expansion with the timing of future battery returns. Second-life allocation can redistribute recycling pressure over time, but it cannot compensate for processing capacity that becomes available too late. Considering both decisions together is therefore important for the long-term management of EV batteries in Italy.

8. BIBLIOGRAPHY

1. Esmaeilian, B., Xiao, Y., Goyal, G. K., Zuo, L., Chen, L., & Behdad, S. (2026). Electric vehicle batteries recycling: A review. Waste Management. https://www.sciencedirect.com/science/article/abs/pii/S0956053X25007135?via%3Dihub
2. Alamerew, Y. A., & Brissaud, D. (2020). Modelling reverse supply chain through system dynamics for realizing the transition towards the circular economy: A case study on electric vehicle batteries. Journal of Cleaner Production, 254, 120025. https://www.sciencedirect.com/science/article/abs/pii/S095965262030072X
3. Nurdiawati, A., & Agrawal, T. K. (2022). Creating a circular EV battery value chain: End-of-life strategies and future perspective. Resources, Conservation and Recycling, 185, 106484. https://www.sciencedirect.com/science/article/pii/S0921344922003275
4. Zhao, Y., Pohl, O., Bhatt, A. I., Collis, G. E., Mahon, P. J., Rüther, T., & Hollenkamp, A. F. (2021). A review on battery market trends, second-life reuse, and recycling. Sustainable Chemistry, 2(1), 167–205. https://www.mdpi.com/2673-4079/2/1/11
5. Harper, G., Sommerville, R., Kendrick, E., Driscoll, L., Slater, P., Stolkin, R., Walton, A., Christensen, P., Heidrich, O., Lambert, S., Abbott, A., Ryder, K., Gaines, L., & Anderson, P. (2019). Recycling lithium-ion batteries from electric vehicles. Nature, 575(7781), 75–86. https://www.nature.com/articles/s41586-019-1682-5
6. Meegoda, J. N., Malladi, S., & Zayas, I. C. (2022). End-of-life management of electric vehicle lithium-ion batteries in the United States. Clean Technologies, 4(4), 1162–1174. https://www.mdpi.com/2571-8797/4/4/71
7. Pratap, B., Krishna Mohan, T. V., Amit, R. K., & Venugopal, S. (2024). Evaluating circular economy strategies for raw material recovery from end-of-life lithium-ion batteries: A system dynamics model. Sustainable Production and Consumption. https://www.sciencedirect.com/science/article/pii/S2352550924002197
8. Ibarra Vega, D., & Bautista-Rodriguez, S. (2024). The impact of circular economy strategies on municipal waste management: A system dynamics approach. Cleaner Engineering and Technology, 21, 100761.

https://www.sciencedirect.com/science/article/pii/S2666790824000417?via%3Dihub

9. Safarzadeh, H., Ebrahimzadeh Sarvestani, M., Enayati, M., & Di Maria, F. (2026). Hourly energy demand impacts of battery electric vehicle adoption in Italy: A grid simulation and policy analysis. Renewable Energy Focus, 56, 100761. https://www.sciencedirect.com/science/article/pii/S1755008425000833
10. Eurostat. (2025). Passenger cars in the EU. Statistics Explained. European Commission.
11. European Automobile Manufacturers' Association. (2026). Vehicles on European roads 2026. ACEA.
12. International Energy Agency. (2025). Global EV Outlook 2025: Trends in electric car markets. IEA.
13. Motus-E, Strategy&, and Politecnico di Milano. (2023). Electric vehicle battery recycling @2050: Evolutionary scenarios and enabling technologies.
14. European Commission. (2023). New law on more sustainable, circular and safe batteries enters into force.
15. European Commission. (2025). New rules to boost recycling efficiency from waste batteries.
16. Dei, F., Brussa, G., Puricelli, S., Rigamonti, L., & Grosso, M. (2026). Forecasting waste from key energy transition technologies in Italy. Waste Management. https://www.sciencedirect.com/science/article/pii/S0956053X26001534
17. Kalchenko, O. (2026). System Dynamics Model of Electric Vehicles Battery Recycling for Europe's Circular Economy. Proceedings of the 44th International System Dynamics Conference, Delft, Netherlands. https://proceedings.systemdynamics.org/2026/abstracts/1337.html
18. Li, X., & Srai, J. S. (2026). Informal Trade in Circular EV Battery Supply Networks: Who Controls the Flow? Proceedings of the 44th International System Dynamics Conference, Delft, Netherlands. https://proceedings.systemdynamics.org/2026/abstracts/1373.html
19. Tankou, A., Bieker, G., & Hall, D. (2023). Scaling up reuse and recycling of electric vehicle batteries: Assessing challenges and policy approaches. International Council on Clean Transportation (ICCT).
20. Kamath, D., Moore, S., Arsenault, R., & Anctil, A. (2023). A system dynamics model for end-of-life management of electric vehicle batteries in the US:

Comparing the cost, carbon, and material requirements of remanufacturing and recycling. *Resources, Conservation and Recycling,* 196, 107061. https://www.sciencedirect.com/science/article/pii/S0921344923001970

21. Cobb, A., Ramirez-Meyers, K., Michalek, J., Swaminathan, S., Gasper, P., Polzin, B., & Smith, K. (2026). Electric-vehicle battery second-life and recycling pathways: How economics depend on chemistry, processing, and application. *Applied Energy*, 414, 127809. https://www.sciencedirect.com/science/article/pii/S0306261926004617
22. Zhu, J., Mathews, I., Ren, D., Li, W., Cogswell, D., Xing, B., Sedlatschek, T., Kantareddy, S. N. R., Yi, M., Gao, T., Xia, Y., Zhou, Q., Wierzbicki, T., & Bazant, M. Z. (2021). End-of-life or second-life options for retired electric vehicle batteries. *Cell Reports Physical Science*, 2(8), 100537. https://www.sciencedirect.com/science/article/pii/S2666386421002484
23. Etxandi-Santolaya, M., Canals Casals, L., & Corchero, C. (2024). Extending the electric vehicle battery first life: Performance beyond the current end of life threshold. *Heliyon,* 10(4), e26066. https://www.sciencedirect.com/science/article/pii/S2405844024020978
24. Regulation (EU) 2023/1542 of the European Parliament and of the Council of 12 July 2023 concerning batteries and waste batteries, amending Directive 2008/98/EC and Regulation (EU) 2019/1020 and repealing Directive 2006/66/EC (consolidated text), Articles 61 and 69. *Official Journal of the European Union,* L 191/1. https://eur-lex.europa.eu/eli/reg/2023/1542/2025-07-31/eng
25. Kotak, Y., Marchante Fernández, C., Canals Casals, L., Kotak, B. S., Koch, D., Geisbauer, C., Trilla, L., Gómez-Núñez, A., & Schweiger, H.-G. (2021). End of Electric Vehicle Batteries: Reuse vs. Recycle. *Energies,* 14(8), 2217. https://www.mdpi.com/1996-1073/14/8/2217
26. Gu, X., Bai, H., Cui, X., Zhu, J., Zhuang, W., Li, Z., Hu, X., & Song, Z. (2024). Challenges and opportunities for second-life batteries: Key technologies and economy. *Renewable and Sustainable Energy Reviews*, 192, 114191. https://www.sciencedirect.com/science/article/abs/pii/S1364032123010493
27. Seika, J., & Kubli, M. (2025). The Technology Valley of Death of Circular Economy Solutions: A System Dynamics Simulation of Business Strategies for the Second-Use Battery Industry. Business Strategy and the Environment, 1–17. https://onlinelibrary.wiley.com/doi/10.1002/bse.70491

28. Brun, M., & Sun, X. A. (2024). BattOpt: Optimal Facility Planning for Electric Vehicle Battery Recycling. https://arxiv.org/abs/2407.00864
29. Vaz, C. R., dos Santos, É. F. N., & Uriona Maldonado, M. (2026). Modelling future scenarios for end-of-life battery management of electric vehicles in São Paulo. *Systems Research and Behavioral Science*, 43(2), 452–469. https://onlinelibrary.wiley.com/doi/10.1002/sres.3183
30. Seika, J., & Kubli, M. (2024). Repurpose or recycle? Simulating end-of-life scenarios for electric vehicle batteries under the EU Battery Regulation. *Sustainable Production and Consumption*, 51, 644–656. https://www.sciencedirect.com/science/article/pii/S235255092400280X
31. Bobba, S., Mathieux, F., & Blengini, G. A. (2019). How will second-use of batteries affect stocks and flows in the EU? A model for traction Li-ion batteries. Resources, Conservation and Recycling, 145, 279–291. https://www.sciencedirect.com/science/article/pii/S0921344919300795
32. Kastanaki, E., & Giannis, A. (2023). Dynamic estimation of end-of-life electric vehicle batteries in the EU-27 considering reuse, remanufacturing and recycling options. *Journal of Cleaner Production*, 393, 136349. https://www.sciencedirect.com/science/article/pii/S0959652623005073
33. Motus-E, Strategy&, and Politecnico di Milano. (2023). Il riciclo delle batterie dei veicoli elettrici @2050: scenari evolutivi e tecnologie abilitanti. https://www.motus-e.org/studi_e_ricerche/il-riciclo-delle-batterie-dei-veicoli-elettrici-2050-scenari-evolutivi-e-tecnologie-abilitanti/
34. Motus-E. (2024). The implications for Italy of the new EU Battery Regulation. https://www.motus-e.org/wp-content/uploads/2024/03/The-implications-for-Italy-of-the-new-EU-battery-regulation.pdf
35. UNRAE. (2026). UNRAE Book 2025: Analisi del mercato autoveicoli in Italia. https://www.unrae.it/files/Book_UNRAE_2025_69a187fa05efd.pdf
36. Motus-E and Strategy&. (2024). Il futuro della mobilità elettrica in Italia @2035. https://www.motus-e.org/wp-content/uploads/2024/09/2024.10.01_Strategy_Motus-E_Report-IdR@2035_vFinal.pdf
37. Bielewski, M., et al. (2023). Battery Technology in the European Union: Status Report on Technology Development, Trends, Value Chains and Markets. Joint

Research Centre. https://publications.jrc.ec.europa.eu/repository/handle/JRC145289

38. Bruno, M., & Fiore, S. (2023). Material Flow Analysis of Lithium-Ion Battery Recycling in Europe: Environmental and Economic Implications. Batteries, 9, 231. https://www.mdpi.com/2313-0105/9/4/231
39. Bruno, M., & Fiore, S. (2024). Review of lithium-ion batteries' supply-chain in Europe: Material flow analysis and environmental assessment. Journal of Environmental Management, 358, 120758. https://www.sciencedirect.com/science/article/pii/S0301479724007448
40. Baradaran Kazemian, P., Gentile, C., Dino, G. A., & Baricco, M. (2025). Legislative strategies for battery management toward the circular economy: a comparative study of Germany, the Netherlands, Italy, and Armenia. *Sustainable Energy Technologies and Assessments*, 84, 104698. https://www.sciencedirect.com/science/article/pii/S2213138825005296
41. Sterman, J. D. (2000). Business Dynamics: Systems Thinking and Modeling for a Complex World. Boston: Irwin/McGraw-Hill. https://lalt.fecfau.unicamp.br/projects/wp-content/uploads/2020/livros/Sistemas%20dinamicos/John_D_Sterman_2000_EN_Business_Dynamics_-_Systems_Thinking_and_Modeling_for_a_Complex_World.pdf
42. European Alternative Fuels Observatory. (2026). Vehicles and fleet: Italy. European Commission, Directorate-General for Mobility and Transport. https://alternative-fuels-observatory.ec.europa.eu/transport-mode/road/italy/vehicles-and-fleet
43. Sanclemente Crespo, M., Van Ginkel González, M., & Talens Peiró, L. (2022). Prospects on end of life electric vehicle batteries through 2050 in Catalonia. *Resources, Conservation & Recycling*, 180, 106133. https://www.sciencedirect.com/science/article/pii/S0921344921007412
44. Wu, Y., Yang, L., Tian, X., Li, Y., & Zuo, T. (2020). Temporal and spatial analysis for end-of-life power batteries from electric vehicles in China. *Resources, Conservation & Recycling,* 155, 104651. https://www.sciencedirect.com/science/article/abs/pii/S0921344919305579
45. Shafique, M., Rafiq, M., Azam, A., & Luo, X. (2022). Material flow analysis for end-of-life lithium-ion batteries from battery electric vehicles in the USA and

China. *Resources, Conservation & Recycling, 178*, 106061. https://www.sciencedirect.com/science/article/pii/S0921344921006698

46. Rettenmeier, M., Petrik, D., Möller, M., & Sauer, A. (2025). A modeling framework and benchmark for end-of-life automotive traction battery pack forecasting. *Journal of Cleaner Production*, 491, 144752. https://www.sciencedirect.com/science/article/pii/S0959652625001027
47. Snam & Terna. (2025). Prospettive di sviluppo del sistema energetico nel settore trasporti al 2050. *Scheda tecnica*. https://download.terna.it/terna/Terna_Snam_Prospettive_Sviluppo_Sistema_Energetico_Settore_Trasporti_2050_8de0c0c2165c804.pdf
48. Bielewski, M., et al. (2022). Batteries for energy storage in the European Union: Status report on technology development, trends, value chains and markets. *European Commission, Joint Research Centre*, JRC130724. https://publications.jrc.ec.europa.eu/repository/handle/JRC130724
49. Vaccari, M., Parlanti, F., Manni, F. M., Orefice, M., Mathieux, F., Pannocchia, G., Tognotti, L., & Bertei, A. (2024). Assessing performance in lithium-ion batteries recycling processes: A quantitative modeling perspective. *Resources, Conservation and Recycling,* 206, 107643. https://www.sciencedirect.com/science/article/pii/S0921344924002374